Dissertation

submitted to the

Combined Faculties for the Natural Sciences and for Mathematics

of the Ruperto-Carola University of Heidelberg, Germany

for the degree of

Doctor of Natural Sciences

Generation of a shut-off system for Adeno-associated viral gene transfer vectors

presented by

M. Sc. Carolin Rohwedder

born in: Waren (Müritz), Germany

Dissertation

submitted to the

Combined Faculties for the Natural Sciences and for Mathematics

of the Ruperto-Carola University of Heidelberg, Germany

for the degree of

Doctor of Natural Sciences

Generation of a shut-off system for Adeno-associated viral gene transfer vectors

presented by

M. Sc. Carolin Rohwedder

born in: Waren (Müritz), Germany

Oral-examination:

Generation of a shut-off system for Adeno-associated viral gene transfer vectors

Referees:

Prof. Dr. Martin Müller

Prof. Dr. Oliver Müller

Die vorliegende Arbeit wurde in der Zeit von September 2013 bis November 2016 in der Abteilung für Kardiologie des Universitätsklinikums Heidelberg in der Arbeitsgruppe „Kardiovaskulärer Gentransfer“ unter der wissenschaftlichen Anleitung von Prof. Dr. Oliver Müller verfasst.

Gemäß § 8 (3) der Promotionsordnung erkläre ich hiermit, dass ich die vorliegende Dissertation selbst verfasst und mich dabei keiner anderen als der von mir ausdrücklich gekennzeichneten Quellen und Hilfen bedient habe.

Heidelberg, 09.01.2017

The present study has been submitted for patenting:

Deutsche Patentanmeldung Nr. 10 2016 011 106.2
"ADENO-ASSOCIATED VIRUS (AAV) BASED REGULATORY SYSTEM"

Parts of the present study have been presented at international conferences:

Rohwedder C, Zimmermann DR, Jungmann A, Mühlburger K, Jung F, Katus HA, Müller OJ. Generation of a shut-off system for AAV vectors using the Cre/loxP system. Annual Meeting of the German Society of Gene Therapy, Heidelberg, September 14-16, 2016 (**poster presentation**)

Rohwedder C, Zimmermann DR, Jungmann A, Mühlburger K, Jung F, Katus HA, Müller OJ. Towards safety for gene therapy applications: Generation of a shut-off system for AAV vectors. Annual Meeting of the European Society of Gene and Cell Therapy (ESGCT), Florence, October 18-21, 2016 (**poster presentation**)

INDEX

ABBREVIATIONS

°C	degree Celsius
µ	micro
4-OHT	(Z)-4-hydroxytamoxifen
A	adenosine
AAV	Adeno-associated virus
bp	base pairs
C	cytosine
cDNA	complementary DNA
CO_2	carbon dioxide
d	day
ddH_2O	double-distilled water
DMEM	Dulbecco's Modified Eagle Medium
DMSO	dimethyl sulfoxid
DNA	deoxyribonucleic acid
dNTP	deoxynucleoside triphosphate
E. coli	Escherichia coli
e.g.	*exempli gratia*, for example
EDTA	Ethylenediaminetetraacetic acid
eGFP	enhanced green fluorescent protein
et al.	*et alii*, and others
EtOH	ethanol
FBS	fetal bovine serum
floxed	flanked by loxP sites
g	gram
G	guanine
gDNA	genomic DNA
h	hour
H_2O	water
HEK	human embryonic kidney
HRP	horseradish peroxidase
i.p.	intraperitoneal
i.v.	intravenous
ITR	inverted terminal repeats
k	kilo
kb	kilo bases
kDa	kilo Dalton
l	liter
lacZ	gene encoding for ß-galactosidase
LB	lysogeny broth/Luria-Bertani medium

loxP	locus of cross-over in P1
m	meter
m	milli
M	molarity (mole/l)
max.	maximum
min	minute
n	nano
NaCl	sodium chloride
nt	nucleotide
oligo	oligonucleotide
PAGE	polyacrylamide gel electrophoresis
PBS	phosphate buffered saline
PCR	polymerase chain reaction
PEI	polyethylenimine
PFA	paraformaldehyde
PHO	phosphate group
qRT-PCR	quantitative real-time PCR
RNA	ribonucleic acid
RPM	rounds per minute
RT	room temperature
s	second
SV40	Simian vacuolating virus 40
T	thymine
U	unit
V	Volt
vg	viral genome copies
wt	wild type
X-Gal	5-Bromo-4-chloro-3-indoyl-ß-D-galactopyranoside

INDEX OF FIGURES

INDEX OF TABLES

SUMMARY (ENGLISH)

Systems to regulate gene expression from an Adeno-associated viral (AAV) vector are widely used. In most cases, the transgene expression has to be switched on by applying a drug. In terms of safety of gene therapy, a shut-off system for AAV vectors would be beneficial to silence gene expression in case of side-effects, ideally by destruction of the vector genome. Therefore, the aim of the present study was to develop a system for elimination of gene expression from an AAV vector after systemic injection using an inducible Cre recombinase. In presence of tamoxifen, the inducible Cre recombinase is activated which should result in excision of DNA fragments flanked by loxP sites within the vector.

Before evaluating the final shut-off system, several experiments were performed to analyze the background activity of the induced CreER^{T2} recombinase, the best suited positions of the loxP sites within the AAV genome and the influence of the loxP sites on the transgene expression. Moreover, a co-transduction of an AAV vector encoding the CreER^{T2} and a second AAV vector expressing the reporter gene flanked by loxP sites was tested.
AAV vectors of serotype 9 were used for packaging the final shut-off system consisting of the inducible CreER^{T2} recombinase, a luciferase reporter gene, and different positions of loxP sites to investigate the effect of loxP localization within the vector genome. To drive reporter gene and CreER^{T2} expression, the CMV promoter was used. All vectors were first tested *in vitro*. Afterwards, the vectors which showed a significant down-regulation of transgene expression after tamoxifen administration were also analyzed *in vivo*. Here, a significant reduction in reporter gene activity could be detected in animals receiving AAV vectors containing loxP sites one week upon tamoxifen administration. Another finding was that the insertion of loxP sites has a negative influence on the expression levels of the transgene. Thereby, the vector expressing the reporter gene flanked by loxP sites showed the lowest expression but also the highest extent of down-regulation after tamoxifen treatment. Finally, the shut-off system used was improved in terms of coding capacity of the AAV genome used. Therefore, the “self-cleaving” peptide P2A of the Porcine Teschovirus-1 was used to replace the promoter driving CreER^{T2} expression to increase the limiting coding capacity for the gene of interest. Again, these AAV9 vectors were tested *in vitro* and *in vivo*, also showing a significant reduction in reporter gene expression after tamoxifen administration.

Taken together, expression of an inducible Cre recombinase allows efficient inactivation of AAV-mediated gene expression on the expense of reduced overall expression efficiency due to insertion of loxP sites. These results contribute to the generation of a novel shut-off system for AAV-mediated gene transfer applicable for the use in combination with various promoters and AAV serotypes to target cell types or tissues of choice.

ZUSAMMENFASSUNG (DEUTSCH)

Regulationssysteme für die Genexpression von einem Adeno-assoziierten viralen (AAV) Vektor sind weit verbreitet. In den meisten Fällen wird die Transgen-Expression durch die Zugabe eines Medikamentes angeschaltet. Hinsichtlich der Sicherheit von gentherapeutischen Produkten wäre ein System, bei dem die Genexpression ausgeschaltet werden kann, von Vorteil, beispielweise wenn Nebenwirkungen auftreten. Idealerweise sollte das Vektorgenom durch ein solches System inaktiviert werden. Daher war das Ziel dieser Arbeit, ein System zur Abschaltung der Genexpression von einem AAV-Vektor zu entwickeln, welches nach der systemischen Gabe des Vektors angewendet werden kann. Dazu soll eine induzierbare Cre-Rekombinase verwendet werden. In Anwesenheit von Tamoxifen wird diese Cre-Rekombinase aktiviert, sodass ein DNA-Fragment, welches von loxP-Erkennungssequenzen flankiert ist, aus dem Vektor herausgeschnitten wird.

Bevor das finale System zum Ausschalten des AAV-Vektors evaluiert wurde, wurden einige Vorversuche durchgeführt, um die Hintergrund-Aktivität der induzierten Cre-Rekombinase, die am besten geeigneten Positionen für die loxP-Sequenzen innerhalb des AAV-Genoms und der Einfluss dieser loxP-Sequenzen auf die Expression des Transgens zu analysieren. Außerdem wurde eine Co-Transduktion getestet, bei der ein AAV-Vektor für die induzierbare CreER^{T2}-Rekombinase und ein zweiter Vektor für ein Reportergen flankiert von loxP-Sequenzen kodiert. Es wurden AAV-Vektoren des Serotyps 9 zur Verpackung des finalen Abschaltsystems eingesetzt, bestehend aus der induzierbaren CreER^{T2}-Rekombinase, einem Luciferase-Reportergen und den loxP-Sequenzen an unterschiedlichen Positionen, um den Effekt der loxP-Lokalisation innerhalb des AAV-Genoms zu untersuchen. Die Expression des Reportergens sowie der CreER^{T2}-Rekombinase wurde durch einen CMV-Promotor kontrolliert. Zunächst wurden alle Vektoren *in vitro* getestet. Die AAV-Vektoren, die zu einer signifikanten Herunterregulation des Reportergens nach Tamoxifen-Gabe geführt haben, wurden anschließend auch *in vivo* analysiert. Auch hier zeigte sich nach Behandlung mit Tamoxifen eine signifikante Reduktion der Reportergen-Aktivität. Außerdem konnte festgestellt werden, dass die Insertion der loxP-Sequenzen einen negativen Einfluss auf die Expression des Transgens hat. Dabei zeigte der Vektor, der für das Reportergen flankiert von loxP-Sequenzen kodiert, die geringste Expression, jedoch gleichzeitig die stärkste Herunterregulation nach Tamoxifen-Gabe. Schließlich wurde das Abschaltsystem in Bezug auf die verfügbare Kodierungskapazität des AAV-Genoms verbessert, indem das sogenannte „selbst-spaltende“ Peptid P2A aus dem Porcine Teschovirus-1 verwendet wurde. Dieses P2A-Peptid ersetzt den Promotor, der die Expression der CreER^{T2}-Rekombinase antreibt, wodurch die Kodierungskapazität für das Transgen erhöht wird. Auch diese AAV-Vektoren wurden sowohl *in vitro* als auch *in vivo* getestet. Hierbei zeigte sich, dass auch mit diesen Vektoren eine signifikante Reduktion der Reportergen-Expression nach Tamoxifen-Gabe erreicht werden kann.

Zusammengefasst erlaubt die Expression einer induzierbaren Cre-Rekombinase eine effiziente Inaktivierung der AAV-vermittelten Genexpression, jedoch auf Kosten einer reduzierten Expressionseffizienz durch die Insertion von loxP-Sequenzen. Diese Ergebnisse tragen zur Generierung eines neuartigen Abschaltsystems für den AAV-vermittelten Gentransfer bei, welches in Kombination mit verschiedenen Promotoren und AAV-Serotypen anwendbar ist, um die gewünschten Zelltypen oder Organe zu erreichen.

1. INTRODUCTION

1.1. GENE THERAPY

In general, gene therapy is defined as the transfer of nucleic acids (DNA or RNA) into a cell or tissue for the prevention or the treatment of a disease. According to the European Medicines Agency (EMA) the aims of gene therapy products using recombinant nucleic acids are the regulation, the repair, the replacement, the addition or the deletion of a genetic sequence. At the end, gene therapy should lead to the correction, the restoration or the modification of physiological functions in humans.

Due to ethical considerations, only somatic gene therapy is allowed to be applied in humans. There are two options for somatic gene transfer which include *ex vivo* and *in vivo* approaches. *Ex vivo* means that tissues or cells are explanted, treated with gene transfer vectors and re-implanted into the organism.

1.1.1. History and aims of gene therapy

The development of gene therapy for the application in humans has been reviewed by Wirth et al. in 2013 [1]. Briefly, the history of gene therapy started in 1961 when the inheritance of genetic mutations due to a viral infection was discovered. But at that time, strategies for the usage of recombinant DNA had not been established yet. The first human gene transfer was performed in 1968 by using the wild-type Shope papilloma virus to introduce the gene for arginase into two female patients suffering from arginase deficiency [2]. The outcome was negative which was not due to the gene transfer itself but because the desired gene was actually not encoded by the virus [3]. In 1988, the first approved trial was performed. Here, no therapeutic gene was used but a marker gene was introduced by viral gene transfer [4]. In 1995, a therapeutic gene transfer was used to treat patients suffering from ADA-SCID [5]. In the following years, further attempts to treat several diseases were performed but in most cases the treatment did not lead to the results expected. In 1999, gene therapy encountered a heavy setback when Jesse Gelsinger died of strong immune response due to a high dose adenoviral treatment [6]. At the moment, gene therapy experiences increasing interest again. Most trials conducted aim to treat cancer as well as monogenetic and cardiovascular diseases. The first gene therapy products were approved in China:

Gendicine™ (2003) for the treatment of head-and-neck squamous cell carcinoma [7] and Oncorine™ (2005) for the therapy of late-stage refractory nasopharyngeal cancer. As the first adenoviral vector that completed the clinical phase III, Cerepro® got the permission to be manufactured in the EU. Cerepro® is used for the treatment of malignant brain tumors. In 2012, the first gene therapy product was approved for the European market: Glybera® (Alipogene tiparvovec). Glybera® consists of an adeno-associated viral vector (AAV) encoding the lipoprotein lipase for the treatment of the rare disease lipoprotein lipase deficiency.

1.1.2. Vector systems used in gene therapy

For gene therapy purposes, several delivery systems for nucleic acids have been validated. Robbins and Ghivizzani summarized the most important vector systems in their review [8]. The main differentiation is made between non-viral and viral vectors. In case of non-viral delivery systems, naked plasmid DNA, liposomes, and DNA conjugates are the best-known.

Viral vectors are increasingly used due to their ability to enter cells more efficiently compared to non-viral vectors. The most prominent viral vector systems are based on Retroviruses, Lentiviruses, Adenoviruses, and Adeno-associated viruses (AAV). These various viral vector systems differ in terms of nucleic acid encoded (DNA, RNA), coding capacity, and tissue specificity. Moreover, retroviral and lentiviral vectors belong to the family of integrating vectors whereas adenoviral and AAV-based vectors integrate at much lower frequency. Another differentiation can be made by the cells that are transduced by theses vectors. Retroviral vectors require cell division for efficient integration whereas the other viral vectors are also capable of transducing non-dividing cells [9].

1.1.3. General problems of gene therapy using viral vectors

Depending on the viral vectors system which is applied, different safety aspects have to be taken into account [1, 9]. Regarding retroviral and lentiviral vectors, the biggest concern is the risk of insertional mutagenesis. In some clinical trials, patients developed leukemia after treatment due to uncontrolled integration upstream of tumor genes. Improved vectors are under investigation where an insertion at preferred locations is enabled. Another problem of viral vectors is the occurrence of immune responses against the vector. In particular, adenoviral vectors are able to cause adverse immunogenic events as seen in the case of

Jesse Gelsinger in 1999. Neutralizing antibodies against the viral vector are another challenging issue. In case of adenoviral vectors, this response is very fast which leads to a rapid clearance of the vector from the organism. Also, the efficacy of AAV-based vectors is limited by pre-existing antibodies. Off-target effects due to unspecific tissue tropism of viral vectors are another problem to address. If unwanted cells or tissues are transduced by the viral vector adverse events may occur. There are several strategies to circumvent some of these problems which will be discussed below.

Taken together, viral vector systems have to be improved in terms of immunogenicity, tissue specificity, and the ability to control expression [10]. By doing so, the risks of genotoxicity, immunogenicity and cytotoxicity can be reduced and the safety profiles of viral vectors can be improved.

1.2. AAV VECTORS FOR GENE THERAPY

The gene therapy vector system used in this study is based on Adeno-associated viruses (AAV) which will be described in more detail in the following sections.

1.2.1. Biology of AAV

Adeno-associated viruses were initially described in 1965 as a contamination in adenoviral productions [11, 12]. These viruses were assigned to the genus *Dependoparvovirus* within the family of *Parvoviridae* and the subfamily of *Parvovirinae*. The name of the genus already indicates that AAVs require a co-infection with a helper virus for a productive replication cycle. Besides Adenoviruses [11], also other DNA viruses as Herpes Simplex virus [13], human Cytomegalovirus [14], Vaccinia virus [15], and Papilloma virus [16] can serve as helper viruses. Each of these helper viruses is able to provide essential genes necessary for AAV replication upon co-infection. AAV can also undergo a latent infection cycle if the cell is not co-infected with a helper virus. In this case, the AAV genome gets integrated at a specific site (AAVS1) which is located on chromosome 19 of the host [17-20]. Besides integration, the AAV genome is also able to persist in an episomal form [21]. Upon super-infection with a helper virus, the AAV provirus is rescued from the host genome so that the productive infection can take place [22].

1.2.1.1. Serotypes and receptors

So far, 12 different serotypes of AAV were isolated from humans and primates (see table 1). All serotypes known are able to transduce different human cell lines, independent on their natural host. The best characterized serotype is AAV2, but other serotypes were shown to be even more beneficial in terms of gene therapy approaches. Due to its efficient transduction of lung, liver and muscle of rodents, AAV9 gained much interest in the field. Moreover, AAV9 is capable to cross the blood-brain-barrier and therefore plays a central role in gene therapy studies of the brain [23]. Another aspect is the strong transduction of cardiac tissue at least in rodents which makes AAV9 the serotype of choice for gene therapy of cardiovascular diseases [24-26].

The receptors and co-receptors used by different serotypes are indicated in table 1. For efficient cellular uptake, the AAV capsid has to bind to the primary receptor. The entry of the viral particles is facilitated by binding of a second receptor. Capsid binding to the receptor also defines the viral tropism as not all receptors are present on every cell.

Table 1: AAV serotypes and receptors

serotype	isolated from	primary receptor	co-receptor	references
AAV1	primate	N-linked sialic acid	unknown	[27, 28]
AAV2	human	heparan sulfate proteoglycan	fibroblast growth factor receptor, hepatocyte growth factor receptor, laminin receptor, CD9	[29-34]
AAV3	human	heparan sulfate proteoglycan	fibroblast growth factor receptor, hepatocyte growth factor receptor, laminin receptor	[33, 35-37]
AAV4	primate	O-linked sialic acid	unknown	[38]
AAV5	human	N-linked sialic acid	platelet-derived growth factor receptor	[39-41]
AAV6	human	N-linked sialic acid, heparan sulfate proteoglycan	epidermal growth factor receptor	[28, 40, 42]
AAV7	primate	unknown	unknown	[43]
AAV8	primate	unknown	laminin receptor	[33, 43]
AAV9	human	O-linked galactose	laminin receptor	[33, 44, 45]
AAV10	primate	unknown	unknown	[46]
AAV11	primate	unknown	unknown	[46]
AAV12	primate	unknown	unknown	[47]

1.2.1.2. Genomic organization

The AAV genome consists of a single-stranded DNA comprising both polarities to the same extend [29, 48]. With a genome size of about 4.7 kb, the viral genome only codes for three mRNAs from three open reading frames (ORFs).

The first ORF encodes four non-structural proteins called Rep (regulatory proteins) [49]. The transcription of Rep78 (78 kDa) and its splice variant Rep68 (68 kDa) are driven by the p5 promoter. Another promoter, p19, controls the expression of Rep52 (52 kDa) and its splice variant Rep40 (40 kDa). All Rep proteins contain a nuclear localization signal (NLS) as well as a Helicase/ATPase activity [50, 51]. The unspliced variants are also able to bind to the inverted terminal repeats (ITRs) flanking the AAV genome. The Rep proteins are involved in replication, packaging of the viral genome and integration into the host genome in the absence of a helper virus [22].

The structural or capsid proteins (VP) are encoded by the second ORF which is controlled by the p40 promoter [52, 53]. VP1 (87 kDa), VP2 (73 kDa) and VP3 (62 kDa) are generated from a single mRNA by usage of different start codons and alternative splicing [54-56]. All VP proteins share the same C-terminal domain responsible for primary and secondary receptor binding [30, 57, 58]. The N-terminal domain of VP1 contains a phospholipase A_2 activity (PLA_2) required for the release from endosomes and entry into the nucleus [59-61]. The AAV genome also harbors an alternative ORF driven by the p40 promoter which encodes the assembly-activating protein (AAP) important for assembly of the capsid proteins [62].

The only *cis*-acting elements within the AAV genome are the inverted terminal repeats (ITRs) flanking the ORFs. Each ITR has a size of 145 nt and forms a t-shaped hairpin by self-annealing of palindromic sequences [63]. These palindromic sequences also comprise Rep binding elements (RBE) and a terminal resolution site (trs) [64-66]. The so-called D sequence which is single-stranded and of about 20 nt length is required for viral replication and packaging [67-69]. The ITRs function as primers for the viral replication but also fulfill tasks in genome packaging, integration [70, 71] and rescue of the integrated provirus from the host genome [72, 73].

1.2.1.3. Structure of capsids

The AAV capsid is built up by 60 subunits of the capsid proteins VP1, VP2 and VP3 [53] that form an icosahedral viral particle with a size of about 25 nm [74]. The ratio between the single capsid proteins is 1:1:10 (VP1:VP2:VP3) with 5 copies of VP1 and VP2 and 50 copies of VP3 per particle [22]. Trimers of all three capsid proteins are arranged in 20 triangular faces in a T=1 symmetry defining the complexity of the capsid [75]. As a result, 2-fold, 3-fold and 5-fold symmetry axes are formed [76]. Electron microscopy and X-ray crystallography revealed that there is a conserved 8-stranded anti-parallel β-barrel motif within the assembled particle. There are also defined structures on the surface of the capsid which can be describes as depressions (at the 2-fold axes), spikes (at the 3-fold axes) and pores (at the 5-fold axes).

1.2.1.4. Infection and replicative cycle

After binding of AAV particles to the respective receptors (see table 1), the capsids are internalized by endocytosis. AAVs are able to use several pathways for cellular uptake like clatherin-mediated [77], RacI-mediated [78] or CLIC/GEEC-mediated (clatherin-independent carriers/GPI enriched endocytic compartment) endocytosis [79].

Upon cellular uptake, AAV virions are trafficked in vesicles along the cellular cytoskeleton (microtubule network) [78]. This step is rate-limiting for AAV infection due to the slow speed of vesicular transport within many cell types [80, 81]. A conformational change within the capsid is required for the release of AAV particles from the endosomes. Therefore, N-terminal domain of VP1 containing the PLA_2 domain is externalized [60]. The low pH inside the vesicle triggers this conformational change but also cathepsins seem to play a role [82]. The PLA_2 activity facilitates the release from the endosomes into the perinuclear compartment [60].

As intact capsids, AAVs enter the nucleus through the nuclear pore complex [78, 80] or alternative pathways [83]. First, the viral particles are transported to the nucleolus. For uncoating, the virions have to be relocated to the nucleoplasm where the second-strand synthesis can take place [84]. The conversion of the viral genome into a double-stranded DNA is required for viral replication and stability of the genome [85, 86]. For the replication mediated by the helper virus, the ITRs serve as primers [70]. As described in part 1.2.1.2., the viral Rep proteins play a crucial role by unwind double-stranded viral genomes during replication to generate the single-stranded DNA genomes. In the absence of a helper virus, the Rep proteins are required for integration into the chromosome 19 of the host genome. Also, the viral genomes are able to persist extrachromosomally as episomes [87].

The assembly of viral particles also takes place in the nucleolus where host proteins (nucleophosmin, nucleolin) as well as the viral AAP protein promote the capsid formation [88]. The viral genomes are encapsidated through the pores at the 5-fold axes which is facilitated by Rep78/68 proteins [89, 90]. The final release of the AAV virions from the cells is enabled by cell lysis which is mainly caused by the helper virus.

1.2.1.5. Immunology

The major limitation in using AAVs as a gene therapy vector is the existence of neutralizing antibodies (nAb) against the AAV capsid. Within the human population, 50-80% of adult individuals have pre-existing antibodies against AAV [91].

In general, AAVs show a low immunogenicity, but mild host immune responses to AAV infections can be detected [92, 93]. The response of the innate immune system is represented by production of pro-inflammatory cytokines/chemokines in combination with infiltration of leukocytes into the liver [94, 95]. This immune reaction is transient and very mild. Moreover, a humoral immune response is activated by Toll-like receptor (TLR) signaling and uptake of AAV particles into macrophages [96, 97]. It could be shown that memory B-cells play a crucial role in immune reactions against AAV [98]. Besides the B cells, also $CD8^+$ memory T cells specific for the capsid are activated upon infection, at least in humans [99].

To circumvent these immune responses, the engineering of AAV capsids for escaping the binding of neutralizing antibodies, is under investigation [100, 101].

1.2.2. AAV as a gene therapy vector

1.2.2.1. Advantages and limitations

Currently, adeno-associated viruses (AAV) are among the safest viral vectors for application in gene therapy. Compared to other viral vectors used for this purpose, AAV vectors show several advantages. First of all, AAV itself is not known to cause disease or symptoms in humans [102] and the induced immune response is usually very mild. Moreover, AAV vectors are able to integrate into the host genome at a specific location on chromosome 19 whereas random insertions are very rare. Because of the removal of *rep* and *cap* genes from the AAV genome, AAV vectors usually exists in episomal form within the nucleus. The episomal format of vector DNA as well as the rare random integration events leads to a very low risk for insertion mutagenesis [103], which can be a problem with retroviral vectors. In non-dividing cells, AAV vectors exhibit stable transgene expression for long time periods.

The usage of AAV as a vector system for gene therapy approaches also shows some drawbacks. The AAV genome has a size of about 4.7 kilobases which also determines the cloning capacity for therapeutic genes. Another disadvantage is the existence of neutralizing antibodies against AAV, especially against serotype 2, which limits the efficiency of viral gene

transfer. Also, the broad tropism of AAV can result in off-target effects. To circumvent these problems, the usage of other serotypes and tissue-specific promoters or engineering of viral capsids enable more specific and efficient AAV-mediated gene transfer [104].

1.2.2.2. Transductional and transcriptional targeting of AAV vectors

As described above, gene therapy approaches should be efficient and specific in terms of targeting the tissue of choice and minimizing off-target effects by transduction of unwanted tissues or cell types. A first step regarding the specificity is the selection of the best AAV serotype for gene transfer. For example, AAV2 shows high expression in the liver but has overall a more unspecific tropism [57, 105]. For transduction of heart and muscle, the serotypes 1, 6, 8, and 9 are best suited although also the liver is transduced by these serotypes [105-107]. Engineering of AAV capsids serves as an alternative option to improve specificity of the gene transfer to a tissue of choice. Therefore, short peptide motifs can be inserted into defined positions within the capsid and these modified AAV vectors are then selected on the desired tissues [108-110]. Moreover, changes in the amino acid sequence of the capsid can result in a modified tropism, as it was shown with AAV2 resulting in reduction of liver transduction and simultaneous increase in cardiac transduction efficacy [106].

Besides the choice of serotypes and capsid modifications, the selection of a tissue-specific promoter enhances the efficacy and specificity of gene transfer. The use of more unspecific promoters like the CMV promoter results in ubiquitous expression of the transgene which again could lead to unwanted off-target effects [111]. By now, there are several specific promoters for various tissues and cell types available. For example, the use of the myosine light chain promoter (MLC) coupled to the CMV enhancer leads to a highly specific expression in the heart [106]. Another cardio-specific promoter is the troponin T promoter (TnT) which results in a reduced liver expression of the transgene [112].

To further improve specificity, AAV vectors can be detargeted from distinct tissues using microRNA (miRNA) target sites. These target sites are inserted into the vector so that the corresponding miRNA can bind and enable degradation. One of the first miRNA target site used was the miRNA-122 (miR122) target site. MiR122 is expressed predominantly in the liver [113], resulting in degradation of viral transcripts from the AAV vector in the liver, whereas cardiac expression remains unaffected.

1.3. REGULATORY SYSTEMS FOR AAV GENE THERAPY VECTORS

An early aim of gene therapy was the regulation of gene expression in a spatio- and temporal-controlled manner. Therefore, various regulatory systems have been developed which are summarized in the following section.

Regulatory systems have to fulfill several characteristics to be applicable in a clinical setting [114, 115]. Most important is a low background activity in the absence of an inducer drug to avoid side effects from the regulatory system itself. The system should be switched on or off by a drug within a wide dose range to titrate gene expression towards defined levels. It would be beneficial if the system consists of mainly human components to prevent immunogenic reactions. Moreover, the system should be specific to cells or tissues of interest and should not interfere with endogenous gene expression. An ideal regulation system should be reversible and the inducing drug should be safe, orally bioavailable and penetrate all tissues. As a last criterion, the expression of the therapeutic gene needs to be up- or down-regulated by the drug in a fast and dose-dependent manner to avoid toxicities due to overexpression of the transgene.

1.3.1. Tet-ON/Tet-OFF systems

Regulatory systems which are inducible by tetracycline or doxycycline administration were developed in 1992 by Gossen and Bujard [116]. The system comprises transactivators (tTAs) which are formed by the fusion of the tet repressor protein to the viral transactivation domain (VP16). The expression of the tTAs is driven by a human cytomegalovirus promoter. Moreover, the tet operator sequence (TRE, tet responsive element) is required to control the expression of the transgene of interest. In case of the Tet-OFF system, doxycycline (Dox) prevents binding of the tTAs to the TRE which results in a lack of expression of the transgene. In the absence of Dox, the tTAs bind to the TRE so that the gene expression can take place. The Tet-ON system uses mutated tTAs (rtTAs, reverse tTAs) which can be activated by Dox so that the transgene is only expressed in the presence of Dox [114]. In general, Tet-ON systems need higher doses of Dox for activation since the mutation of tTAs also affects the Dox binding ability [117]. The main concerns about the Tet systems are the background activity in the absence of Dox (Tet-ON) and the potential of development of resistances against tetracycline or doxycycline. Moreover, Dox treatment can lead to

photosensitivity in a dose-dependent manner and humoral and cellular immune responses against the Tet system were found in non-human primates [115].

The tet system was early adapted to the usage in AAV gene therapy vectors. Thereby, the system can be placed into one AAV vector [118] or can be split to two AAV vectors which have to be co-transduced [119]. The advantage of a single AAV vector containing the whole system is that the every component is delivered into each cell. Unfortunately, this also limits the coding capacity for the transgene of interest to 2-2.5 kb. If two AAV vectors are used, almost 4 kb can be used for the transgene and/or cell-specific promoters. But both vectors have to target the same cell to deliver all components which reduces the efficacy of this approach [120]. It was also described that the promoter activity in the viral ITRs can lead to higher background expression of the transgene in the absence of the transactivator.

1.3.2. Rapamycin-inducible systems

Another regulatory system was developed by Rivera et al. in 1996. This rapamycin-inducible system has an advantage over the Tet systems because it consists only of human components [114]. Rapamycin facilitates dimerization of cellular proteins and can be used for the development of a regulation system [115] by fusing a DNA-binding domain to the immunophilin FKBP12. As a second fusion protein, an activation domain (p65) is coupled to FRAP (FKBP rapamycin-associated protein). In the presence of rapamycin, the dimerization of these two fusion proteins can take place and a transcription activator is formed which can bind to a promoter containing synthetic DNA-binding sequences and thereby drive transgene expression [8]. The advantage of this system is a low background activity and a high inducibility. The main drawbacks are that the system cannot be shut-off immediately after rapamycin withdrawal and that rapamycin itself has an immunosuppressant potential [115]. In case of an use in humans, the dose of rapamycin would be too high for clinical applications. To solve this problem, rapamycin analogs are under investigation [114].

In terms of the applicability in AAV vectors, two vectors are necessary to package all components required [120]. This, again, leads to a reduction of efficacy due to the lower probability of two vectors entering the same cell.

1.3.3. Mifepristone (RU486)-inducible systems

Analogous to the rapamycin-inducible system, another regulatory approach using RU486 (mifepristone) was developed. It is composed of a mutant progesterone receptor able to bind RU486 and thereby gets activated [8]. The receptor was mutated by fusing the RU486-binding domain to the DNA-binding domain of a yeast transcription factor (GAL4) and the viral transactivator VP16 (from Herpes Simplex virus). Binding of RU486 leads to a conformational change so that promoters containing GAL4-binding sites are activated and enable subsequent transgene expression [114]. Improvements of the system in terms of leakiness and efficacy were made by usage of the p65 activation domain and other modifications [115]. A variant of this approach called “Gene Switch” is commercially available which can be strongly induced by low RU486 doses. As a drawback, the background activity in the off-state may be quite high. RU486 is in clinical use to terminate pregnancy for a long time. To fully induce the system, lower doses of RU486 are required than to terminate pregnancy. But also this low concentrations may cause side effects [115].

The RU486-inducible system can be placed onto a single AAV vector. The coding capacity for the transgene of interest is limited to 2-2.5 kb [120]. If two AAV vectors are used, cell-specific promoters can be used to drive the expression of the mutated progesterone receptor [121].

1.3.4. Other regulatory systems

Further regulation systems for gene therapy vectors include physiologically regulatable systems and the ecdysone receptor-based system. Gene expression can be regulated in a more physiological way by using hypoxia responsive elements (HRE) and antioxidant responsive elements (ARE) [117]. These systems react to reduced oxygen levels or oxidative stress.

The ecdysone receptor (EcR) is derived from insects and plays a role in molting and metamorphosis [115]. If the natural ligand (ultraspiracle, USP) binds to the receptor, a conformational change and dissociation of a repressor lead to expression of genes controlled by the EcR. Some systems also use the mammalian analog of USP, the retinoid-X-receptor (RXR). By fusing the GAL4 DNA-binding domain to EcR and the VP16 activator to RXR, the so-called “RheoSwitch” system can be improved in terms of basal activity and inducibility. A major concern is the overexpression of RXR in mammalian cells as RXR plays a role in several

pathways and resulted in cardiomyopathy in mice if overexpressed. Moreover, ecdysteroids itself are considered to be safe but humans ingest variable amounts of these compounds by eating vegetables which can lead to undesired activation of the regulatory system. To solve this problem, many non-steroidal drugs for induction were developed [122].

1.4. CRE RECOMBINASE

Besides the components of the regulatory systems mentioned, a regulation of gene expression mediated by a recombinase is possible. The recombination system will be described in detail in the next section.

1.4.1. Structure of Cre/loxP recombination

The best known recombination system is derived from bacteriophage P1 and consists of the gene for the recombinase of the λ integrase family (cre) and two recognition sites (loxP) where recombination occurs. It was discovered in 1981 by Nat Sternberg and Daniel Hamilton [123]. The Cre recombinase (38 kDa, “causes recombination”) is the only enzyme required for recombination – no additional co-factors or host proteins are needed [124]. Each loxP (“locus of x-over of P1”) sequence comprises in total 34 bp with two inverted repeats (each 13 bp) and a spacer (8 bp) required as the recognition site for the Cre [125]. The form of the DNA substrate containing the loxP sites is not important for recombination so that supercoiled, linear or nicked-circle DNA can serve as the template. The recombination products of a DNA molecule containing two loxP sites are a linear and a closed circular DNA molecule [126]. To achieve an intra-molecular recombination, the loxP sequences have to be separated by at least 82 bp [127]. Even with a distance of 400 kb between both loxP sites, excision of the intervening DNA fragment can be performed with about 50% efficacy [128]. The orientation of the loxP sequences plays a crucial role for the outcome of recombination. If they are oriented in parallel on the same DNA molecule, the flanked DNA sequences will be excised. Intra-molecular recombination in case of anti-parallel oriented loxP sites results in inversion of the intervening DNA fragment. Moreover, inter-molecular recombination (translocation) between two DNA molecules is possible if one loxP site is located on each DNA molecule [129]. The recombination reactions are reversible

as long as two homotypic lox sites are used. The efficacy of intra-molecular recombination (excision, inversion) is higher than of inter-molecular reactions (translocation, integration) with excisions as the most stable recombination events [130]. The cleavage and the strand-exchange of the DNA molecule take place within the 8 bp spacer region of the loxP [131]. The crystal structure of Cre bound to loxP sites revealed that 4 monomers of the Cre recombinase and both loxP sequences form the recombination complex with each Cre monomer bound to one inverted repeat of the loxP [132, 133]. Therefore, the Cre tetramer brings together both loxP sites for cleavage and strand exchange [128, 134]. After recombination, the loxP sites are built up by two complementary halves of the pre-existing loxP sequences.

In the infectious cycle of bacteriophage P1, Cre-mediated recombination is crucial for circularization of the viral DNA after infection of the host and the separation of dimers emerging during replication. This step is very important during cell division of the host so that each daughter cell receives a P1 DNA copy [135].

1.4.2. Improved and inducible Cre recombinases

Since the discovery of the Cre/loxP systems, several improvements of the system have been made. On one hand, researchers wanted to enhance Cre expression and activity in mammalian cells. Therefore, the Cre gene itself was modified by usage of an eukaryotic initiation sequence for translation, insertion of amino acids and mutations of splice sites [136]. Another alteration to the Cre sequence was made by implementing the mammalian codon usage. This codon-improved Cre (iCre) sequence shows reduced epigenetic silencing in mammalian cells which leads to higher expression levels [137].

For the application of the Cre/loxP system (see next chapter), inducible Cre recombinases were developed. Therefore, fusion proteins of the Cre and the ligand-binding domain (LBD) of estrogen receptors were made. The aim was the retention of the Cre fusion protein in the cytoplasm in the absence of the respective ligand. Upon ligand binding, a conformational change leads to translocation of the Cre into the nucleus where recombination between two loxP sites can occur.

One of the first developments was the CreER which uses the LBD of the human estrogen receptor [138]. The binding of estradiol or 4-hydroxytamoxifen (4-OHT) results in the activation of the CreER whereas the absence of the stimulus did not lead to any activation.

As a next step of developing an inducible Cre recombinase, the binding of endogenous estradiol should be prevented. Therefore, the LDB of the human estrogen receptor was mutated (G521R mutation) resulting in the binding of tamoxifen but not estradiol [139]. This Cre version called $CreER^{T}$ (T for tamoxifen) showed only low background activity in the absence of tamoxifen [140]. Feil et al. further improved the inducible Cre by inserting more mutations [141]. The resulting $CreER^{T1}$ (G400V/L539A/L540A) shows improved binding to the antiestrogen ICI whereas the $CreER^{T2}$ (G400V/M543A/L540A) exhibits higher affinity to 4-OHT. Both version are still insensitive to endogenous estradiol and show 3- to 4-fold more efficient binding to their ligands compared to $CreER^{T}$. If two ER^{T2} domains were fused to both ends of the Cre recombinase ($ER^{T2}iCreER^{T2}$), the basal activity in absence of the ligand could be reduced further [142, 143].

Besides the LDB of the human estrogen receptor, also mutated versions of the murine estrogen receptor (Mer) were used [144]. The fusion of the Mer domain to the Cre results in the same inducibility by tamoxifen as seen with the human estrogen receptor. Again, this CreMer recombinase is insensitive to activation upon estradiol binding. By fusing another Mer domain to the other end of the Cre recombinase (MerCreMer), the activity of the fusion protein can be controlled even more tightly [145]. Moreover, the background levels can be reduced further.

Other induction systems for the Cre include the usage of an interferon-responsive promoter to control Cre expression [146] and the fusion of Cre recombinase to the hormone binding domain of a mutated human progesterone receptor which can be induced by the synthetic steroid RU486 [147].

1.4.3. Application of the Cre/loxP system

The first approach using the Cre/loxP system in a mammalian setting was made by Sauer et al. in 1989 [148]. They placed DNA sequences containing loxP sites into the yeast genome to disrupt the expression of neomycin driven by a SV40 promoter. Upon Cre expression in this cell line, the DNA segment flanked by loxP sites was excised and neomycin expression could be detected.

The most common usage of Cre/loxP is the generation of transgenic mouse models, e.g. to develop knock-out lines [149]. Therefore, Cre expressing mice are mated with mice containing the gene of interest flanked by loxP sites (“*floxed*”). By using an inducible Cre

recombinase and tissue-specific promoters, excision of the *floxed* sequence can be controlled in a spatial and temporal manner [150].

Mouse models expressing the inducible CreER^{T2} recombinase are widely used. Depending on the expression pattern required, the expression of the CreER^{T2} can be controlled by ubiquitous or cell-specific promoters. The most prominent mouse model is the ROSA26-CreER^{T2} which allows the constitutive expression in all cell types [151, 152]. *In vivo*, the CreER^{T2} is highly sensitive to induction with tamoxifen and do not cause any toxicities. Moreover, the basal activity in the absence of tamoxifen is very low [153]. If a more specific CreER^{T2} expression is required the use of cell- or tissue-specific promoters to drive Cre expression is beneficial. For example, the endothelial cell-specific promoter Tie2 [154] or the smooth muscle-specific SM22 promoter [155] can be used.

In cardiac research, a transgenic mouse line expressing the tamoxifen-inducible MerCreMer under the control of the cardiac-specific α-myosin heavy chain (αMHC) promoter is frequently used [156]. However, in case of studying cardiac diseases or alteration, this mouse model should be used with caution. Many studies revealed that the induction of the MerCreMer by tamoxifen resulted in transient cardiomyopathy in mice, independently whether the mouse genome contains loxP sites or not [157, 158]. It could be shown that tamoxifen itself plays a role for the adverse events and the higher the tamoxifen dosing, the more severe were the side effects in the MerCreMer expressing mouse model [159]. The induction of the MerCreMer in cardiomyocytes by tamoxifen administration seems to lead to an activation of the DNA damage response which can result in apoptosis, fibrosis and dysfunction [160] in a dose-dependent manner.

To avoid the use of Cre-expressing mouse models, the Cre recombinase can also be overexpressed in tissues of interest by viral vectors. Therefore, an adenoviral gene transfer of the Cre into a mouse model containing loxP sites was investigated to achieve recombination in many cell types [161]. In this case, Cre expression could be detected for 3 to 4 weeks until the cells were eliminated by the immune system. For long-term Cre expression, an AAV-mediated gene transfer is more advantageous [112]. This approach can be used to generate knock-out mouse models without the need for long breeding schedules.

1.4.4. Cre recombinase-based regulatory systems

The Cre recombinase has been used for the establishment of a regulatory system for gene therapy vectors in many approaches. Studies were published where Cre-dependent viral vectors were used [162, 163]. These vectors contain the so-called “Flex switch” which is composed of two pairs of lox sites (loxP and lox2272) which are antiparallel and heterotypic. As a first step during recombination, the sequence flanked by one pair of lox sites is inverted. During a second reaction, two of the lox sites are excised which avoids further recombination [164]. By inversion, the expression of the transgene can be switched on or off. The inversion of a transgene is also used in Cre-ON and Cre-OFF vectors developed by Saunders et al. [165, 166]. In case of Cre-ON vectors, recombination mediated by Cre results in the expression of the transgene. Before recombination, the *floxed* transgene is in antisense orientation. In contrast, the *floxed* transgene in Cre-OFF vectors is encoded in sense orientation to the promoter. After recombination, the transgene is inverted so that expression is eliminated. Another approach used a stop cassette flanked by loxP sites which is place between the promoter and the transgene [167]. In the absence of the Cre recombinase, expression from the vector should not take place. After Cre-mediated recombination, the stop cassette is excised and transgene expression can occur. One disadvantage of this system is the size of the *floxed* stop cassette (2.8 kb) which also limits the available cloning capacity for the promoter and the transgene. Moreover, some read-through is detectable which may result in higher background activity of the system [163]. All the described systems have in common that they require the expression of the Cre recombinase in each cell or tissue which is targeted by the gene therapy vector.

Li et al. published in 2006 the development of a Cre-based regulatory system which utilizes the co-transduction of two AAV vectors [168]. One of the vectors expresses the inducible $CreER^{T2}$ recombinase whereas the second vector encodes the transgene (tyrosine hydroxylase) flanked by loxP sites. Co-transduction of these AAV vectors and application of 4-hydroxytamoxifen (4-OHT) activating the Cre recombinase lead to the excision of the transgene. By administration of 4-OHT, the expression of the gene can be regulated in a temporal and spatial manner. The authors claim that this approach may increase safety of viral vectors due to the potential to shut-off of the transgene expression in case of adverse events seen, e.g. because of long-term overexpression of the gene. Moreover, the expression from the vector can be switched off if the treatment is terminated. As seen with

other regulatory systems placed on two AAV vectors, the efficacy of this system is limited by the requirement of two AAV vectors entering into the same cell.

1.5. AIM OF THE PRESENT STUDY

Currently, Adeno-associated viruses (AAV) serve as one of the safest viral vector systems for application in gene therapy. AAV vectors exhibit a long-term and stable transgene expression in non-dividing cells which could lead – in some cases – to undesired effects. Therefore, a shut-off system to eliminate expression from the vector in case of side effects would be beneficial.

Within this thesis, such regulatory system should be established for AAV vectors targeting the heart via regulation of gene expression by an inducible Cre recombinase. The Cre recombinase used is codon-optimized (iCre) for expression in mammalian cells and fused to a mutant estrogen receptor (ER^{T2}). After expression, the $CreER^{T2}$ remains in the cytoplasm of the cell preventing recombination events. Administration of tamoxifen results in activation of the $CreER^{T2}$ and translocates it to the nucleus where recombination between two identical loxP sites can take place. To generate a shut-off system, recombination results in excision of a defined DNA fragment flanked by loxP sites which in turn leads to the destruction of the AAV vector.

This thesis addressed the questions of background activity of the inducible Cre recombinase, the most efficient positions of the loxP sites, and the optimization of a single vector genome harboring both the target gene to be controlled as well as the $CreER^{T2}$.

2. MATERIAL AND METHODS

2.1. MATERIAL

2.1.1. Animal models

denotation	*nomenclature*	*description*	*source*
C57Bl/6	C57BL/6NRj	mouse model used for general animal experiments	Janvier Labs, Saint-Berthevin (France)
MerCreMer	B6.Cg-Tg(Myh6-cre/Esr1)1Jmk/J	C57Bl/6 background, expression cassette for inducible MerCreMer recombinase controlled by αMHC promoter	Johannes Backs (University Hospital Heidelberg)
Tomato	B6.129(Cg)-*Gt(ROSA)26Sor*$^{tm4(ACTB-tdTomato,-EGFP)Luo}$/J	C57Bl/6 background, expression cassette for fluorescent Tomato dye which is flanked by loxP sites and followed by eGFP transgene	Hermann-Josef Gröne (German Cancer Research Center, Heidelberg)

2.1.2. Eukaryotic and prokaryotic cells

2.1.2.1. Eukaryotic cells

denotation	*description*	*source*
CV-1 5B	Monkey kidney cell line, stably transfected with lacZ gene which is separated from promoter by a neomycin resistance gene (Neo) flanked by loxP sites	Rolf Sprengel (Max Planck Institute for Medical Research, Heidelberg)
HEK293T	human kidney cell line, expressing the SV40 large T antigen	ATCC, Wesel

2.1.2.2. Prokaryotic cells

denotation	*description*	*source*
DH5α	chemically competent cells that can be transformed with high efficiency	Invitrogen, Karlsruhe

2.1.3. Cell culture media and supplements

2.1.3.1. Media and supplements for eukaryotic cell cultures

denotation	*description*	*source*
DMEM	Dulbecco's Modified Eagle Medium	Gibco®, Thermo Fisher Scientific, Schwerte
FBS	Fetal bovine serum	Biochrom, Berlin
L-glutamine	200 mM	Gibco®, Thermo Fisher Scientific, Schwerte
PBS	137 mM NaCl, 2.7 mM KCl, 4.3 mM Na_2HPO_4, 1.47 mM KH_2PO_4 , pH 7.4	
Penicillin/streptomycin	10,000 U/ml penicillin, 10,000 µg/ml streptomycin	Gibco®, Thermo Fisher Scientific, Schwerte
Trypsin	2.5% trypsin solution	Thermo Fisher Scientific, Schwerte

2.1.3.2. Media and supplements for prokaryotic cell cultures

denotation	*description*
LB agar	10 g/l tryptone, 5 g/l yeast extract, 10 g/l NaCl, 15 g/l agar
LB medium	10 g/l tryptone, 5 g/l yeast extract, 10 g/l NaCl
SOC medium	2% tryptone, 0.5% yeast extract, 0.05% NaCl, 2.5 mM KCl, 10 mM $MgCl_2$, 20 mM glucose

2.1.4. Plasmids

denotation	*description*	*source*	*reference*
pSSV9	coding for single-stranded AAV2 ITRs flanking AAV2 rep gene	Dirk Grimm (Bioquant, Heidelberg)	Samulski et al. (1987)
pCreER^{T2}	coding for inducible CreER^{T2} recombinase	Pierre Chambon (University of Strasbourg, France)	Feil et al. (1997)

pDP2rs/pDP9rs	coding for AAV2 rep, AAV2/9 wild type cap and red fluorescent protein (for transfection control); used for production of wtAAV2/9 vectors	Dirk Grimm (Bioquant, Heidelberg)	Grimm et al. (2003)

2.1.5. Primer and oligonucleotides

All primers and oligonucleotides were provided by Eurofins MWG Operon (Ebersberg, Germany) and are listed in 5'-to-3' orientation.

2.1.5.1. Primers for genotyping of αMHC-MerCreMer mice

denotation	*sequence (5'-3')*
control fwd 2	CAACGCTCTACTGTTGCCTCC
control rev 2	CTGCCCTAGCCAGCCTATTTGC
αMHC-MerCreMer 4F	CGGCACTCTTAGCAAACCTC
αMHC-MerCreMer 4R	AGGCAAATTTTGGTGTACGG

2.1.5.2. General PCR primers

denotation	*sequence (5'-3')*	*description*
AflII-TnT-BsiW F	CGCGCTTAAGGTCTCAGTCCATTAG	amplification of human troponin T promoter flanked by restriction sites (Afl II, BsiW I)
AflII-TnT-BsiW R	CATGCGTACGTTCTGCCGACAGATC	
Age-PolyA-Kas F	ATGCTACCGGTCAGACATGATAAGA	amplification of SV40 Poly(A) flanked by restriction sites (Age I, Kas I)
Age-PolyA-Kas R	GATTAAGGCGCCCTTTAAAAAACCTCC	
Age-Rluc-Nsi F	CTAAATGCATGCCACCATGGCTTC	amplification of Renilla Luciferase flanked by restriction sites (Age I, Nsi I)
Age-Rluc-Nsi R	GTTAACCGGTTTACTGCTCGTTCT	
Asc-CMV-AflII F	ATGGCGCGCCTTAATAGTAATC	amplification of CMV promoter flanked by restrictions sites (Asc I, Afl II)
Asc-CMV-AflII R	GGCTAGCTTAAGTGACTGCGTT	
Bam-PolyA-Cla-Sph F	ATGCTGGATCCCAGACATGATAAGA	amplification of SV40 Poly(A) flanked by restriction sites (BamH I, Cla I, Sph I)
Bam-PolyA-Cla-Sph R	GATAGCATGCATCGATGCTTTAAAAAACC	
Kas-CMV-Sbf F	CGTCCAGGCGCCTTAATAGTAATC	amplification of CMV promoter flanked by restrictions sites (Kas I, Sbf I)
Kas-CMV-Sbf R	ATATCCTGCAGGTGACTGCGTTAGC	

2.1.5.3. Cloning oligonucleotides (with 5'-PHO modification)

denotation	*sequence (5'-3')*	*description*
MCS 1 F	CTTAAGGGGCCCCCTAGGGTC	generation of a multiple cloning site (Avr II, Apa I, Afl II) for cloning into Kpn I restriction site
MCS 1 R	CCTAGGGGGCCCCTTAAGGTC	
MCS 2 F	AGCTCGTACGGATATCTCGCA	generation of a multiple cloning site (BsiW I, EcoR V, Nru I) for cloning into Hind III restriction site
MCS 2 R	AGCTTCGCGAGATATCCGTAG	
MCS 3 F	CGTTAATTAAGGCCTACATGGCCATTTAAT	generation of a multiple cloning site (Swa I, Sfi I, Pac I) for cloning into Cla I restriction site
MCS 3 R	CGATTTAAATGGCCATCTAGGCCTTAATTA	
MCS 8 F	GAATTCTTCGAAGGCGCGCCCTTAAGACC GGTGGCGCCCCTGCAGGCCGCGGGTAC	generation of a multiple cloning site (EcoR I, BstB I, Asc I, Afl II, Age I, Kas I, Sbf I, Sac II) for cloning into Sac I and Kpn I restriction sites
MCS 8 R	CCGCGGCCTGCAGGGGCGCCACCGGTCTT AAGGGCGCGCCTTCGAAGAATTCAGCT	
SacII-lox-Kpn F	GGATAACTTCGTATAGCATACATTATACGA AGTTATGGTAC	generation of a loxP site for cloning into Sac II and Kpn I restriction sites
SacII-lox-Kpn R	CATAACTTCGTATAATGTATGCTATACGAA GTTATCCGC	
lox-Asc F	CGCGATAACTTCGTATAGCATACATTATAC GAAGTTATGG	generation of a loxP site with Asc I site for cloning into Asc I restriction site
lox-Asc R	CGCGCCATAACTTCGTATAATGTATGCTAT ACGAAGTTAT	
BamH-lox-BsiW F	GATCCATAACTTCGTATAGCATACATTATAC GAAGTTATCGTACGA	generation of a loxP site and BamH I and BsiW I sites for cloning into BamH I restriction site
BamH-lox-BsiW R	GATCTCGTACGATAACTTCGTATAATGTATG CTATACGAAGTTATG	
lox-Nhe-Cla F	CGTTATAACTTCGTATAGCATACATTATACG AAGTTATGCTAGCATCGATT	generation of a loxP site and Nhe I and Cla I sites for cloning into Cla I restriction site
lox-Nhe-Cla R	CGAATCGATGCTAGCATAACTTCGTATAATG TATGCTATACGAAGTTATAA	
AflII-lox-Nsi F	TTAAGATAACTTCGTATAGCATACATTATACG AAGTTATATGCAT	generation of a loxP site and Afl II and Nsi I sites for cloning into Afl II restriction site
AflII-lox-Nsi R	TTAAATGCATATAACTTCGTATAATGTATGCT ATACGAAGTTATC	

Age-lox-Pme F	CCGGTATAACTTCGTATAGCATACATTATACG AAGTTATGTTTAAAC	generation of a loxP site and Age I and Pme I sites for cloning into Age I restriction site
Age-lox-Pme R	CCGGGTTTAAACATAACTTCGTATAATGTATG CTATACGAAGTTATA	
BstB-lox-Asc F	CGAAATAACTTCGTATAGCATACATTATACGA AGTTATGG	generation of a loxP site for cloning into BstB I and Asc I restriction sites
BstB-lox-Asc R	CGCGCCATAACTTCGTATAATGTATGCTATAC GAAGTTATTT	
BsiW-lox-BsiW F	GTACGATAACTTCGTATAGCATACATTATACG AAGTTAT	generation of a loxP site with flanking BsiW I sites for cloning into BsiW I restriction site
BsiW-lox-BsiW R	CATGTATTGAAGCATATTACATACGATATGCT TCAATAG	
AvrII-lox-Apa F	CTAGATAACTTCGTATAGCATACATTATACGA AGTTATGGCC	generation of a loxP site for cloning into Avr II and Apa I restriction sites
AvrII-lox-Apa R	ATAACTTCGTATAATGTATGCTATACGAAGTT AT	
Pac-lox-Sfi F	ATAACTTCGTATAGCATACATTATACGAAGTT ATAT	generation of a loxP site for cloning into Pac I and Sfi I restriction sites
Pac-lox-Sfi R	ATAACTTCGTATAATGTATGCTATACGAAGTT ATAGA	

2.1.5.4. Sequencing primers

denotation	*sequence (5'-3')*
CMV_seq F	CGCTATTACCATGGTGATG
CMV_seq R	GATGTACTGCCAAGTAGG
CreERT2_seq F	GGAGTGTACACATTTCTG
CreERT2_seq R	CACAGCATTGGAGTCAG
Rluc_seq F	CCTACCTGGAGCCATTC
Rluc_seq R	GATGATGCATCTAGCCAC

2.1.5.5. Primer for qRT-PCR

name	*sequence (5'-3')*
CreERT2_qPCR F	GATCTTCGACATGCTGCTGG
CreERT2_qPCR R	TCAGGGTGCTGGACAGAAAT
hGAPDH F	CACAGCATTGGAGTCAG
hGAPDH R	CACAGCATTGGAGTCAG
mGAPDH F	ATGTTCCAGTATGACTCCACTCACG

mGAPDH R	GAAGACACCAGTAGACTCCACGACA
mIL-10 F	CAAAGGACCAGCTGGACAAC
mIL-10 R	TCATTTCCGATAAGGCTTGG
Rluc_qPCR F	CGAAGAGGGCGAGAAAATGG
Rluc_qPCR R	TCTCCTTGAATGGCTCCAGG

2.1.5.6. Primer for AAV quantification

name	*sequence (5'-3')*
CMV F	TGCCCAGTACATGACCTTATTG
CMV R	GAAATCCCCGTGAGTCAAACC
SV40 PolyA F	GCGACTCTAGATCATAATCAGCCATA
SV40 PolyA R	GCTGCAATAAACAAGTTAACAACAACA

2.1.6. Enzymes

denotation	*source*
Antarctic Phosphatase	New England Biolabs, Frankfurt (Main)
Benzonase nuclease	Sigma-Aldrich, Taufkirchen
iTaq Universal SYBR Green Supermix	Bio-Rad, Munich
Large Klenow fragment	New England Biolabs, Frankfurt (Main)
Q5 DNA polymerase	New England Biolabs, Frankfurt (Main)
Quick Ligase	New England Biolabs, Frankfurt (Main)
restriction enzymes	New England Biolabs, Frankfurt (Main)
T4 DNA Ligase	New England Biolabs, Frankfurt (Main)
Taq DNA polymerase	Qiagen, Hilden

2.1.7. Antibodies

denotation	*species*	*1./2. antibody*	*source*	*dilution*
anti-Cre	rabbit	first	Rolf Sprengel (Max Planck Institute for Medical Research, Heidelberg)	1:3000
anti-GAPDH	rabbit	first	Sigma Aldrich (G9454)	1:10000
anti-rabbit-HRP	goat	second	Santa Cruz (sc-2004)	1:5000
anti-Renilla luciferase	rabbit	first	Thermo Fisher Scientific (PA5-32210)	1:2000

2.1.8. Ready-to-use kits

denotation	*source*
DNeasy Blood and Tissue Kit	Qiagen, Hilden
Gel Extraction Kit	Qiagen, Hilden
Luciferase Assay System (Firefly Luciferase)	Promega, Mannheim
Mouse IL-10 Quantikine ELISA Kit (M1000B)	R&D Systems, Wiesbaden
PCR Purification Kit	Qiagen, Hilden
Plasmid Midi/Maxi/Giga Kit	Qiagen, Hilden
QIAprep Spin MiniPrep Kit	Qiagen, Hilden
REDExtract-N-Amp Tissue PCR Kit	Sigma-Aldrich, Taufkirchen
Renilla Luciferase Assay System	Promega, Mannheim
RNeasy Mini Kit	Qiagen, Hilden
SuperScript III First-Strand Synthesis System for RT-PCR	Invitrogen, Karlsruhe

2.1.9. Buffer and solutions

denotation	*composition*
4x loading buffer (protein)	0.25 M Tris-HCl (pH 6.8), 10% SDS, 50% glycerol, 0.5% bromphenol blue, 0.8 M 2-mercaptoethanol
5x loading buffer (DNA)	25 mM Tris-HCl (pH 8.0), 150 mM EDTA, 0.25% bromphenol blue, 25% glycerol
annealing buffer (oligo)	10 mM Tris, 150 mM NaCl in ddH_2O
anode buffer	12 g Tris, ad 1 l H_2O
benzonase buffer	50% glycerol, 20 mM Tris (pH 8.0), 2 mM $MgCl_2$, 20 mM NaCl
cathode buffer	12 g Tris, 1 g SDS, 12.5 g taurine, ad 1 l H_2O
cryo-protection solution	20% sucrose, 0.1% glutaraldehyde, 2% PFA, in PBS
fixing solution for X-Gal staining	2% formaldehyde, 0.2% glutaraldehyde, in PBS
lysis buffer for AAV productions	50 mM Tris-HCl, 150 mM NaCl, 5 mM $MgCl_2$, pH 8.5, in H_2O
PBS	137 mM NaCl, 2.7 mM KCl, 4.3 mM Na_2HPO_4, 1.47 mM KH_2PO_4 , pH 7.4
RIPA buffer	10 mM Tris-HCl (pH 7.5), 15 mM EDTA, 1% NP40, 0.5% sodium deoxycholate, 0.1% SDS, protease inhibitor (1 tablet for 10 ml), 1 M DTT
TBE buffer	2 M Tris, 1.6% boric acid, 10 mM EDTA
TBS-T buffer	500 mM Tris-HCl (pH 7.4), 1.5 M NaCl, 0.2% TWEEN 20
TE buffer	10 mM Tris-HCl (pH 7.5), 1 mM EDTA
transfer buffer	1.8 g Tris, 1.9 g taurine, ad 800 ml H_2O
X-Gal solution (100x)	100 mg X-Gal in DMSO
X-gal staining solution	5 mM $K_4Fe(CN)_6$ x $3H_2O$, 5 mM $K_3Fe(CN)_6$, 2 mM $MgCl_2$, 10% DMSO, 1x X-Gal solution, in PBS

2.1.10. Chemicals and reagents

denotation	*source*
(Z)-4-hydroxytamoxifen	Sigma-Aldrich, Taufkirchen
2-log DNA ladder	New England Biolabs, Frankfurt (Main)
2-mercaptoethanol	Sigma-Aldrich, Taufkirchen
5-bromo-4-chloro-3-indoyl-β-D-galactopyranoside (X-Gal)	Thermo Fisher Scientific, Schwerte
Agarose	Sigma-Aldrich, Taufkirchen
Ammonium persulfate (APS)	usb corporation, Cleveland (OH, USA)
Ammonium sulfate	Carl Roth, Karlsruhe
Ampicillin sodium salt	Carl Roth, Karlsruhe
Aqua ad injectionem	Braun, Melsungen
Bacto Agar	BD Biosciences, Heidelberg
Bacto tryptone	BD Biosciences, Heidelberg
Boric acid	Sigma-Aldrich, Taufkirchen
Bromphenol blue sodium salt	Sigma-Aldrich, Taufkirchen
Desoxynucleoside triphosphate (dNTP) mix	New England Biolabs, Frankfurt (Main)
Dimethyl sulfoxid (DMSO)	Merck, Darmstadt
Disodium hydrogen phosphate (Na_2HPO_4)	Sigma-Aldrich, Taufkirchen
Dithiothreitol (DTT)	Sigma-Aldrich, Taufkirchen
ECL detection solution (Pierce)	Thermo Fisher Scientific, Schwerte
Ethanol (EtOH)	Sigma-Aldrich, Taufkirchen
Ethidium bromide	Carl Roth, Karlsruhe
Ethylenediamine tetraacetic acid (EDTA)	AppliChem, Darmstadt
Formaldehyde	Merck, Darmstadt
Gel loading dye (DNA), 6x	New England Biolabs, Frankfurt (Main)
GeneJuice	Merck, Darmstadt
Glucose	Merck, Darmstadt
Glutaraldehyde	Serva, Heidelberg
Glycerol	Sigma-Aldrich, Taufkirchen
Glycine	Sigma-Aldrich, Taufkirchen
Hydrochloride acid (HCl)	Merck, Darmstadt
Iodixanol solution, OptiPrep	Fresenius Kabi Norge AS, Bad Homburg
Isoflurane CP	cp-pharma, Burgdorf
Isopropanol	Sigma-Aldrich, Taufkirchen
Magnesium chloride ($MgCl_2$)	Sigma-Aldrich, Taufkirchen
Methanol	Sigma-Aldrich, Taufkirchen
Milk powder	Carl Roth, Karlsruhe
Nonidet P-40 (NP40)	Sigma-Aldrich, Taufkirchen
OptiMEM	Gibco®, Thermo Fisher Scientific, Schwerte

PageRuler Plus, prestained	Thermo Fisher Scientific, Schwerte
Polyacrylamide (Rotiphorese Gel 30)	Carl Roth, Karlsruhe
Polyethylenimine (PEI)	Polysciences, Heidelberg
Potassium chloride (KCl)	AppliChem, Darmstadt
Potassium dihydrogen phosphate (KH_2PO_4)	AppliChem, Darmstadt
Potassium ferricyanide	Sigma-Aldrich, Taufkirchen
Potassium ferrocyanide	Sigma-Aldrich, Taufkirchen
Protease inhibitor mix G	Serva, Heidelberg
Roti Histokitt mounting medium	Carl Roth, Karlsruhe
Sodium chloride (NaCl)	Sigma-Aldrich, Taufkirchen
Sodium deoxycholate	Sigma-Aldrich, Taufkirchen
Sodium dodecyl sulphate (SDS)	Serva, Heidelberg
Sodium hydroxide (NaOH)	Sigma-Aldrich, Taufkirchen
Sucrose	Sigma-Aldrich, Taufkirchen
Tamoxifen	Sigma-Aldrich, Taufkirchen
Taurine	Carl Roth, Karlsruhe
Tetramethylethylenediamine (TEMED)	Sigma-Aldrich, Taufkirchen
Tissue-Tek O.C.T. compound	Sakura Finetek, Staufen (im Breisgau)
Tris-(hydroxymethyl)-aminomethane (Tris)	Carl Roth, Karlsruhe
Tween 20	Sigma-Aldrich, Taufkirchen
VivoGlo Luciferin	Promega, Mannheim
Yeast extract	Carl Roth, Karlsruhe

2.1.11. Disposables

denotation	*source*
Cell culture flasks (T 75 cm^2, T 175 cm^2)	Sarstedt, Nürnbrecht
Cell culture plates (6-well, 12-well, 24-well)	Greiner Bio-One, Essen
Cell stack (10 layers)	Corning, Munich
Centrifuge tubes (500 ml)	Corning, Munich
Combitips advanced (for dispenser)	Eppendorf, Hamburg
Cover glass	Knittel Gläser, Braunschweig
Cryo-preservation tubes	Greiner Bio-One, Essen
Falcon tubes (15, 50 ml)	Greiner Bio-One, Essen
Filter tips (10, 200, 1000 µl)	Sarstedt, Nürnbrecht
Hard-Shell PCR plates (96-well)	Bio-Rad, Munich
Homogenization tubes (1.5 ml)	NeoLab, Heidelberg
Immobilon transfer membrane	Merck, Darmstadt
Microseal B film	Bio-Rad, Munich
Microtome blade, MX35 Premier Disposable	Thermo Fisher Scientific, Schwerte

Needles (Microlance: 20G, 23G, 27G)	BD Biosciences, Heidelberg
Peel-A-Way tissue embedding molds	Polysciences, Heidelberg
Pipette tips (10, 200, 1000 µl)	Greiner Bio-One, Essen
Quick-Seal centrifuge tubes	Beckman Coulter, Krefeld
Reaction tubes (0.5, 1.5, 2 ml)	Sarstedt, Nürnbrecht
Serologic pipets (5, 10, 25, 50 ml)	Greiner Bio-One, Essen
Superfrost Plus coverslips	Thermo Fisher Scientific, Schwerte
Surgical disposable scalpels	Braun, Melsungen
Syringes (1, 2, 5, 10 ml)	BD Biosciences, Heidelberg
VivaSpin columns	Sartorius, Göttingen
Whatman cellulose filter paper	Sigma-Aldrich, Taufkirchen
Zeba Spin Desalting Columns	Thermo Fisher Scientific, Schwerte
Zirconium oxide beads (2.8 mm)	Precellys, Montigny le Bretonneux (France)

2.1.12. Laboratory equipment

denotation	*type*	*source*
agarose gel electrophoresis chambers	MINI/MIDI electrophoresis unit	Carl Roth, Karlsruhe
agarose gel imaging system	GelDoc™ XR+	Bio-Rad, Munich
autoclave	VX-150	Systec, Linden
biological safety cabinet	HERAsafe™ KS	Thermo Fisher Scientific, Schwerte
blotting chamber (Western blot)	Mini PROTEAN® 3 cell	Bio-Rad, Munich
cell counter	Neubauer improved	Marienfeld, Lauda-Königshofen
centrifuge	Heraeus™ Multifuge 4 KR	Thermo Fisher Scientific, Schwerte
chemiluminescence imaging system	ChemiDoc™ MP	Bio-Rad, Munich
fluorescence microscope	IX81	Olympus, Hamburg
freezer (-20°C)	various models	Liebherr, Kirchdorf an der Iller
freezer (-80°C)	MDF-U73V™	Sanyo, Moriguchi (Japan)
heating block	AccuBlock™ Digital Dry Bath	Labnet International, Edison (NJ, USA)
in vivo bioluminescence imaging system	IVIS® Lumina III	PerkinElmer, Rodgan
incubation shaker (bacteria)	Certomat® BS-1 Multitron	Sartorius Stedim Biotech, Göttingen INFORS HAT, Einsbach
incubator	HERAcell™ 240i CO_2 incubator	Thermo Fisher Scientific, Schwerte
incubator (bacteria)	Heraeus™ Function Line	Thermo Fisher Scientific, Schwerte
light microscope	AXIO Vert.A1	Carl Zeiss, Jena
luminometer	GloMax® 20/20	Promega, Mannheim
magnetic mixer	RCT basis	IKA®, Staufen

microtome	CM3050S	Leica Microsystems, Wetzlar
multi pipet (dispenser)	Multipette® Plus	Eppendorf, Hamburg
PCR cycler	Mastercycler® EP S	Eppendorf, Hamburg
pH meter	pH530	WTW, Weilheim
pipet boy	Pipetboy acu	Integra Biosciences, Zurich (Switzerland)
pipets	Eppendorf Research®	Eppendorf, Hamburg
power supply	PowerPac™ HC	Bio-Rad, Munich
real-time qRT-PCR cycler	CFX96 Real-Time System, C1000 Touch™ Thermal Cycler	Bio-Rad, Munich
refrigerator	various models	Liebherr, Kirchdorf an der Iller
scales	EW 4200-2NM ABJ 220-4NM	Kern & Sohn, Balingen
SDS-PAGE system	XCell SureLock™ Mini-Cell Electrophoresis System	Thermo Fisher Scientific, Schwerte
shaker	Duomax 1030 Shaker DRS-12	Heidolph, Schwabach NeoLab, Heidelberg
shaking water bath	GFL-1083	GFL, Burgwedel
table top centrifuges	Heraeus™ Biofuge pico™ Heraeus™ Fresco™ 17	Thermo Fisher Scientific, Schwerte
thermo shaker/mixer	TSC ThermoShaker Thermomixer® Comfort	Analytik Jena, Jena Eppendorf, Hamburg
ultra centrifuge	Sorvall™ WX Ultra Series	Thermo Fisher Scientific, Schwerte
ultrasonic water bath	Sonorex TK 30	Bandelin, Berlin
UV-Vis spectral photometer	NanoDrop™ 2000	Thermo Fisher Scientific, Schwerte
vortex	Vortex-Genie 2	Scientific Industries Inc., Bohemia (NJ, USA)
water purification system	TKA-GenPure	Thermo Fisher Scientific, Schwerte

2.1.13. Software

application	*denotation*	*source*
administration of mice breedings	T.Base 14.4	4D client
analysis of agarose gels and Western blots	Image Lab™	Bio-Rad
analysis of fluorescence images	Fiji/ImageJ	open source, NCBI
analysis of *in vivo* imaging data	Living Image® 4.5	PerkinElmer
analysis of plasmid DNA sequences	ApE – A plasmid editor	M. Wayne Davis
analysis of qRT-PCR data	CFX Manager™	Bio-Rad
illustration of data with statistical analysis	Prism 5	GraphPad
reference management	EndNote X7.3	Thomson Reuters
Word, Excel, Outlook, Powerpoint	Office 2010	Microsoft

2.2. METHODS

2.2.1. Cloning and plasmid preparation

2.2.1.1. Restriction endonucleases and DNA digestion

Restriction endonucleases (type II) are enzymes found in bacteria that cut within DNA molecules at specific locations, known as restriction sites. They are used as a tool for manipulating DNA molecules by introducing double-strand breaks at specific sites within the DNA, generating blunt ends or overhangs of the remaining DNA strands.

For general digestions of DNA by restriction enzymes, 1 µg of the respective DNA was set up with 5 units of the desired restriction enzyme, 1x reaction buffer and water at a total volume of 20 µl. The incubation took place at the optimal temperature for the respective enzyme (mainly at 37°C) for about 1 h.

2.2.1.2. General cloning techniques

The cloning of plasmids was performed using different cloning approaches. The first method was the digestion of the vector plasmid as well as the insert fragment with the same restriction endonucleases. In this thesis, mainly restriction endonucleases generating “sticky ends” (overhangs) were used. The overhangs produced by the one restriction enzyme are complementary to each other so that DNA fragments from vector and insert can be ligated to produce one circular plasmid.

Another approach is the annealing of oligonucleotides (oligos) to generate a double-stranded DNA fragment serving as an insert. In this case, two single-stranded oligos were annealed by mixing 2 µg of each nucleotide and add annealing buffer to a total volume of 40 µl. The annealing took place by incubating at 95°C for 5 min, followed by 20 min at 76°C and 20 min at 37°C. The annealed oligos were then diluted with 360 µl water to achieve a concentration of 10 ng/µl. The oligos were designed with overhangs of one desired restriction site at each end of the DNA to allow ligation with the vector fragment.

Also, the amplification of inserts by PCR was used to clone specific DNA fragments. Therefore, the desired sequence was amplified using the Q5 High-Fidelity DNA polymerase (NEB) and specific primers which also contain overhangs generating desired restriction sites at each end of the PCR product. As seen with the DNA oligos, this allowed the digestion with

the restriction enzymes and the subsequent ligation with the vector fragment. The PCR reaction was performed using 1x Q5-reaction buffer, 0.5 µM of each primer, 200 µM dNTPs, 0.02 U/µl Q5 polymerase, 1 to 10 ng template DNA and nuclease-free water added to a total volume of 20 µl. PCR products were purified using the PCR Purification Kit (Qiagen) and digested with the favored restriction enzymes.

As a last cloning technique, the removal of DNA sequences from a plasmid was performed. Here, the respective DNA plasmid was digested with restriction enzymes so that the unwanted DNA fragment was excised. To fill up the remaining overhangs and generate blunt ends, the large Klenow fragment (DNA polymerase I, NEB) was used. Therefore, 1 unit of Klenow fragment was incubated with 1 µg of the respective DNA, 1x T4 Ligase reaction buffer and 33 µM of each dNTP. Water was added to a total volume of 20 µl. After an incubation time of 15 min at 25°C, EDTA was added to a final concentration of 10 mM and the mixture was heated to 75°C for 20 min.

In case of the vector fragments generated by digestion with restriction enzymes, these fragments were dephosphorylated after digestion to avoid re-ligation of the vector. For this purpose, the Antarctic Phosphatase was used to remove 5'-PHO groups from the vector DNA. The digested vector fragment was mixed with 1x reaction buffer and 1 µl of Antarctic Phosphatase (NEB) and incubated for 15 min at 37°C. To inactivate the Antarctic Phosphatase, the sample was incubated at 70°C for 5 min.

2.2.1.3. Agarose gel electrophoresis and isolation of DNA

With the help of agarose gel electrophoresis, DNA fragments can be separated according to their size. By applying a voltage of about 100 V, the negative charged DNA migrates towards the anode, with smaller fragments moving faster than bigger DNA molecules. Agarose gel electrophoresis is an important method to verify PCR products and digestions of DNA plasmids with restriction enzymes.

The agarose gel was made using a 1% agarose solution (in TBE buffer) which was boiled up in a microwave, before adding 400 ng/l ethidium bromide (EtBr) and pouring the solution into the respective equipment. After polymerization, the gel was transferred into the electrophoresis chamber filled with TBE buffer. The DNA samples were mixed with DNA loading dye in a ratio of 1:5 and applied into the pockets of the agarose gel. As a size marker for DNA fragments, the 2-log DNA ladder (NEB) was also loaded onto the gel. The gel was

allowed to run for 30 to 60 min at a voltage of 100 V. Afterwards, the gel was analyzed using UV light at a wavelength of 254 nm which excites the intercalating EtBr, resulting in a detectable fluorescence signal.

For isolation of DNA fragments from the agarose gel, UV light of a longer wavelength (312 nm) was used to avoid double-strand breaks of the DNA molecules. The desired DNA was isolated by excising the respective gel fragment with a scalpel and extracting the DNA with the Gel Extraction Kit (Qiagen) according to manufacturer's protocol. The eluate containing the DNA was then used for further cloning.

2.2.1.4. Ligation and transformation

The ligation of vector and insert fragments (from gel extractions, PCR, annealed oligos and/or digestions) was performed using the Quick Ligation Kit (NEB) containing a highly concentrated T4 DNA Ligase. In general, vector and insert DNA fragments were ligated in a ratio of 1:3 by adding 1x reaction buffer, 1 µl of Quick T4 DNA Ligase and water to a volume of 20 µl. Ligation took place at room temperature (RT, 25°C) for 5-15 min. As a specificity control, also the vector fragment without the insert was ligated (re-ligation).

The ligated DNA was then transformed into the *E.coli* derivate DH5α which were made chemically competent for efficient uptake of plasmid DNA. For each transformation, 50 µl of competent bacteria were thaw on ice before 10 µl of the ligation products were added. This mixture was incubated for 20 min on ice. The heat shock was performed at 42°C for 45 s to achieve an uptake of the plasmid DNA into the bacteria. Afterwards the bacteria were chilled on ice for 2 min before 350 µl SOC medium (without antibiotics) were added. This suspension was shaken (800 rpm) at 37°C for 45 min. A volume of 100 µl of each transformation was plated onto an agar plate containing ampicillin (100 mg/ml) and incubated over night at 37°C.

2.2.1.5. Mini preparations of plasmid DNA

To check whether the cloning/ligations are correct, mini preparations of plasmid DNA were made. Therefore, bacteria colonies were picked from the agar plates and inoculated in 6 ml LB medium containing ampicillin (100 mg/ml). These cultures were allowed to grow over night at 37°C.

Next day, plasmid DNA was isolated using the QIAprep Spin MiniPrep Kit (Qiagen) according to manufacturer's instructions. Briefly, 2 ml of the culture were transferred to a 2 ml reaction tube and centrifuged at 13000 rpm for 2 min. The supernatant was discarded and the pellet was resuspended in 250 µl P1 buffer containing RNase A. The suspension was mixed well with 250 µl P2 buffer and incubated for 5 min at RT. After adding 350 µl N3 buffer and mixing, the mixture was centrifuged at full speed (13000 rpm) for 10 min. The supernatant containing the plasmid DNA was transferred to the column und centrifuged at 10.000 rpm for 1 min. The flow-through was discarded and 750 µl washing buffer PE was pipetted onto the column. After another centrifugation step (10.000 rpm, 1 min), the column was transferred to a new 1.5 ml reaction tube and 50 µl of water were added. To elute the plasmid DNA from the column, a last centrifugation at 10.000 rpm for 1 min was performed.
As a first validation of the plasmid DNA, the DNA concentration and purity was measured using the NanoDrop photometer. Afterwards, the plasmid DNA was checked by digestion with specific restriction enzymes and analyzed by agarose gel electrophoresis. If required, the DNA and defined primers were sent for sequencing to GATC Biotech AG (Konstanz, Germany).

2.2.1.6. Midi/Maxi/Giga preparations of plasmid DNA

To get higher amounts of plasmid DNA, e.g. for *in vitro* experiments or AAV productions, Plasmid Midi/Maxi/Giga Kits (Qiagen) were used according to manufacturer's protocol. The following table shows buffers, volumes and incubation times used for each Plasmid Kit.

Table 2: Buffers, volumes and incubation times for Plasmid Kits from Qiagen

	Midi	*Maxi*	*Giga*
culture volumes [ml]	100	500	5000
P1 buffer [ml]	4	10	125
P2 buffer [ml]	4	10	125
P3 buffer [ml]	4	10	125
incubation on ice [min]	15	20	30
QBT buffer [ml]	4	10	75
QC buffer [ml]	20	60	600
QF buffer [ml]	5	15	100
Isopropanol [ml]	3.5	10.5	70
70% EtOH [ml]	2	5	10
H_2O [µl]	200	500	3000

Before isolating plasmid DNA, the culture had to be inoculated and shaken over night at 37°C and 180 rpm. For this, an existing Mini culture or a glycerol stock was used. The culture volumes complemented with ampicillin (100 mg/ml) used are shown in the table above.
Next day, the culture was centrifuged at 4.400 rpm and 4°C for 20 min. The supernatant was discarded and the bacteria pellet was resuspended in P1 buffer. P2 buffer was added, mixed well and incubated for 5 min at RT. After adding pre-chilled P3 buffer, the lysate was incubated on ice and then centrifuged at 4.400 rpm for 30 min. After equilibrate the column with QBT buffer, the supernatant was administered onto the column through a filter. Subsequently, the column was washed with QC buffer. To elute the plasmid DNA from the column, the column was put onto a new 50 ml Falcon® tube and QF buffer was added. Plasmid DNA was precipitated using 0.7 volumes of isopropyl alcohol and centrifuging at 4.400 rpm for 30 min. The pelleted DNA was washed with 70% EtOH and centrifuged again at 4.400 rpm for 10 min. After removing as much EtOH as possible, the DNA pellet was dried and solved in water. DNA concentration was measured and plasmid DNA was checked via digestion with restriction enzymes or sequencing.

2.2.2. Cell culture techniques

2.2.2.1. General cell culture techniques

In this thesis, the cell lines HEK293T and CV-1 5B (CV-1 lacZ) were used which both were grown in DMEM medium (Gibco™, Thermo Fisher Scientific), complemented with 1% L-Glutamine, 1% penicillin/streptomycin and 10% FBS. HEK293T cells are a human kidney cell line, expressing the SV40 large T antigen, and were obtained from ATCC (clone HEK293T/17). The CV-1 5B cell line is derived from monkey kidney (*Cercopithecus aethiops*) and stably transfected with an expression cassette for the *E.coli* ß-galactosidase gene (lacZ). This lacZ gene is separated from the promoter by a neomycin resistance gene (Neo) flanked by loxP sites ("*floxed*"). Cre-mediated recombination leads to excision of the Neo cassette, resulting in lacZ expression. This cell line was obtained from Rolf Sprengel (Max Planck Institute for Medical Research, Heidelberg).
Both cell lines were cultivated in sterile 75 cm^2 or 175 cm^2 cell culture flasks which are lying horizontally in a humidified incubator with 37°C and 5% CO_2 fumigation. As soon as the monolayer of cells was confluent the cells were split into new culture flasks. Therefore, the

medium was discarded and the cell layer was washed with about 10 ml PBS. After removal of PBS, 5 ml 0.05% trypsin solution was added so that the monolayer was covered completely. The enzyme trypsin acts by cleaving the adhesion molecules of the cell which leads to loss of cellular adhesion. After a short incubation time, the cells detached from the flask bottom and this cell suspension was taken up with 10 ml of fresh medium. Components in the FBS inactivate remaining trypsin to prevent toxic effects of the trypsin on the cells. The cells were split in a 1:15 ratio, with 1 ml of cell suspension (15 ml in total) was added to 29 ml fresh medium in a new culture flask. Both cell lines were passaged every 3 to 4 days as described.

2.2.2.2. Cryopreservation of cells

For freezing of cells, the cells were resuspended in 8 ml fresh medium after the exposure to trypsin. This suspension was centrifuged for 10 min at 1500 rpm. The supernatant was discarded and the cell pellet was resuspended in 1 ml of freezing medium which consists of 90% FBS and 10% DMSO. This cell suspension was transferred into cryo-tubes, and these tubes were put into a freezing box which allows slow freezing of cells to prevent fast growing ice crystals damaging the cells. First, these tubes were frozen at -80°C for about 1-2 days. After that, the cell suspensions were stored in liquid nitrogen.

2.2.2.3. Seeding of cells

For *in vitro* experiments with either CV-1 5B or HEK293T, the cells had to be seeded into multi-well plates or cell culture flasks. The cell numbers and volumes used per well/flask are stated in the following table.

Table 3: Cell numbers and volumes for different cell culture vessels

	area per well [cm^2]	*seeding cell number per well*	*volume of medium per flask/well [ml]*
T175 cm^2 flask	175	$5.2 \cdot 10^6$	30
6-well plate	10	$1 \cdot 10^5$	3
12-well plate	4	$5 \cdot 10^4$	1
24-well plate	2	$1 \cdot 10^4$	0.5

To determine the cell number from a suspension, the Neubauer improved cell counter was used. The cells in all four major squares which consist of 16 smaller squares were counted and the average value was calculated. The cell count per ml could then be calculated with the following formula.

$$(average\ cell\ counts)\ x\ (dilution\ factor)\ x\ 10^4 = cell\ count\ per\ ml$$

The respective cell numbers were then seeded into the wells or flasks and incubated for 24 h at 37°C in an atmosphere containing with 5% CO_2. The treatment of the cells (transfection or transduction) was performed the day after seeding.

2.2.2.4. Transfection

One day after seeding of cells, plasmid DNA was introduced into the cells using the GeneJuice® transfection reagent (Novagen®, Merck Millipore). Therefore, GeneJuice® was added drop-wise to serum-free medium (OptiMEM™, Gibco™, Thermo Fisher Scientific). The mixture was vortexed and incubated at RT for 5 min. DNA was added, mixed by pipetting and incubated at RT for 15 min. The DNA/GeneJuice® mixture was added drop-wise to cells in complete growth medium. To achieve an overall distribution of the transfection mix in the wells, the plate was gently rocked. The cells were then incubated for at least 24 h at 37°C (5% CO_2). The following table shows volumes and DNA amounts used for transfection.

Table 4: Transfection reagents and volumes used for different cell culture vessels

	6-well	*12-well*	*24-well*
volume of serum-free medium (µl)	100	50	25
volume of GeneJuice® transfection reagent (µl)	3	1.5	0.75
amount of plasmid DNA (µg)	1	0.5	0.25

2.2.2.5. Transduction

As seen with transfection, the cells were transduced by AAV vectors one day after seeding. In general, AAV (serotype 2) small-scale productions (see below) and 10^4-10^5 vg/cell were used in transduction experiments. The respective AAV vector amount was added to serum-free medium (e.g. 3 ml medium per well of a 6-well plate) and mixed gently. The complete growth medium was aspirated and replaced by the serum-free, AAV containing medium. The

AAV vectors were allowed to transduce the cells for 1 h at 37°C (5% CO_2), before adding 10% FBS per well and continuing incubation at 37°C (5% CO_2) for at least 24 h.

2.2.2.6. Induction of CreER^{T2} by 4-hydroxytamoxifen

To achieve recombination, the CreER^{T2} recombinase has to be induced and thereby activated by tamoxifen. In cell culture, the active metabolite of tamoxifen, 4-hydroxytamoxifen (4-OHT, H7904, Sigma Aldrich), was used. A stock solution of 5 mM 4-OHT was generated by dissolving 5 mg in 2.5 ml 100% ethanol. The stock solution can be stored at -20°C.

The induction of the CreER^{T2} in cell culture was performed 2 days after transfection/transduction by adding 1 µM 4-OHT to each well of the cell culture plates. The growth medium of control cells which were not treated by 4-OHT was complemented with the same volume of 100% ethanol. The cells were incubated for 24 h at 37°C (5% CO_2). If the treated cells were cultivated for a longer time period than 24 h, induction with 4-OHT was performed every day using fresh medium and 1 µM 4-OHT per well.

2.2.2.7. Small-scale AAV vector productions for in vitro purposes

For *in vitro* experiments, small-scale productions of AAV serotype 2 were used. One T175 cm^2 cell culture flask with $5.2 \cdot 10^6$ cells and 30 ml medium served for one AAV small-scale production. The day after seeding, the cells were transfected using polyethylenimine (PEI), AAV helper plasmid DNA and the respective AAV genome plasmid DNA. Therefore, a mixture was applied containing 1.57 ml 300 mM NaCl, 1.21 ml H_2O, 34.7 µg helper plasmid (pDP2rs, coding for the AAV serotype 2 capsid and adenoviral genes), 8.9 µg AAV genome plasmid and 350 µl PEI. This transfection mix was vortexed and incubated for 10 min at RT. After this, the solution was applied to the cells growing in complete medium. The cells were incubated for 3 days at 37°C (5% CO_2). After this time period, the medium was aspirated and cells were washed once with PBS. Cells were then detached using 5 ml 0.05% trypsin solution and a cell suspension was generated by adding 10 ml complete medium. This cell suspension was transferred to a 50 ml Falcon® tube and centrifuged for 5 min at 2000 rpm. The supernatant was discarded and the cell pellet was washed with 5 ml PBS. After another centrifugation for 5 min at 2000 rpm, the PBS was discarded and the pellet was resuspended in 1 ml lysis buffer complemented with 1x protease inhibitor. To disrupt the cell membranes,

freeze/thaw-cycles were performed. Cell pellets were frozen in liquid nitrogen und thawed at 37°C. This cycle was repeated 3 times. To digest DNA which is not incorporated in AAV particles, a digestion with Benzonase® nuclease (50 U per ml lysis buffer) was done for 30 min at 37°C. After incubation, the AAV-containing solution was centrifuged for 5 min at 4000 rpm to pellet remaining cell debris. The supernatant was transferred to a new tube and stored at 4°C. The amount of AAV vector genomes was determined by titration (see below).

2.2.2.8. Large-scale AAV vector productions for in vivo applications

The large-scale AAV vector production was performed by the vector production unit (K. Mühlburger, A. Jungmann, F. Jung, and K. Schmidt) of the Müller group according to the following protocol. In this thesis, only AAV serotype 9 vectors were produced for *in vivo* applications.

For large-scale AAV production, cell stacks with 10 layers (6360 cm^2 growth area) were used. A total cell number of $2.3 \cdot 10^8$ cells were added to 1.052 l of complete growth medium. As a positive and a negative control, each 26 ml of this cell suspension were given into two T175 cm^2 flasks. The remaining liter of cell suspension was filled into the cell stack. The cells were incubated at 37°C (5% CO_2) for 18 h at longest.

The day after seeding, the transfection was performed in a similar way as seen with the small-scale productions. The AAV genome DNA (392 µg) was pre-mixed with 1525 µg helper plasmid (pDP9rs, coding for the AAV serotype 9 capsid and adenoviral genes), 69 ml 300 mM NaCl and 53 ml water. The transfection reagent PEI was added in a volume of 15.5 ml and mixed well. After incubation at RT for 10 min, 4 ml of the mixture was added to the cells of one T175 cm^2 flask (positive control). The remaining transfection mix was filled into the cell stack. The cells were incubated at 37°C (5% CO_2) for 2-3 days.

After 2-3 days of incubation, the negative and the positive controls were checked under the microscope. The cells of the negative control should be almost confluent whereas the cells of the positive control should be less and morphologically altered. If the controls were looking fine, the cells were harvested. Therefore, the medium from the positive control and the cell stack was transferred to 500 ml centrifugation tubes. The cells were washed with PBS whereby the PBS was also transferred to the centrifugation tubes. Cells were detached by addition of PBS/EDTA and incubation at 37°C. To stop the reaction, old medium from the

centrifugation tubes was used. The cells were harvested and also transferred to the centrifugation tubes. After a centrifugation at 4400 rpm for 5 min (4°C), the supernatant was collected in a glass bottle. The cells were washed two times with PBS, centrifuged as described above and the supernatant again was collected in the glass bottle. The cell pellet was resuspended by vortexing in 3 ml lysis buffer complemented with 1x protease inhibitor and stored at -20°C. For AAV vector purification from the supernatant collected in the glass bottle, 331 g/l ammonium sulfate was added. The mixture was incubated for at least 2 h at 4°C where it was stirred at about 1200 rpm. The supernatant was then transferred to 500 ml centrifugation tubes and centrifuged for 30 min at 4400 rpm (4°C). After discarding the supernatant, the centrifugation step was repeated. The remaining pellet was resuspended in 20 ml lysis buffer complemented with 1x protease inhibitor und stored at -20°C.

To disrupt the cell membranes, freeze/thaw-cycles were performed. Cell pellets were frozen in liquid nitrogen und thawed at 37°C. This cycle was repeated 4 times. To digest DNA which is not incorporated in AAV particles, a digestion with Benzonase® nuclease (50 U per ml lysis buffer) was done for 30 min at 37°C. After incubation, the AAV-containing solution was centrifuged for 5 min at 4000 rpm to pellet remaining cell debris. The supernatant was transferred to a new tube. This centrifugation was repeated until no pellet was left. The AAV-containing supernatant was stored at 4°C.

The next step in AAV production was the purification of vectors by applying an iodixanol gradient. First, the AAV-containing sample was filled into an ultra-centrifugation tube. With the help of a Pasteur pipette, 7 ml of the first iodixanol solution (15%) were loaded below the AAV sample. The other iodixanol solutions were applied in the following order, always below the layer before: 5 ml 25%, 4 ml 40% and 4 ml 60%. The ultra-centrifugation tubes were balanced and sealed. Centrifugation was performed for 135 min at 50000 rpm (4°C). For collection of the AAV-containing layer, the 40% iodixanol phase was removed with a syringe/needle and transferred to a new tube. The AAV vectors were stored at 4°C (for max. 2 months) or at -20°C (for longer time periods).

For quantification of AAV vector genomes, the AAV-iodixanol solutions were titrated using qRT-PCR. Therefore, 10 µl of the AAV sample were mixed with 10 µl TE buffer and 20 µl 2 M NaOH solution. The sample was then incubated at 56°C for 30 min. For neutralization, 960 µl 40 mM HCl solution was added (dilution factor = 1:35000). To be able to quantify the AAV samples, an AAV plasmid standard was used, ranging from 10^3 to 10^{10} gc/well. The qRT-PCR

was performed using the iTaq Universal SYBR Green Supermix (Bio-Rad). For the plasmid standards, a master mix for 3 replicates was pipetted as follows: 30 µl iTaq Universal SYBR Green Supermix, 1.5 µl forward primer (10 pmol/µl), 1.5 µl reverse primer (10 pmol/µl), 27 µl ddH_2O and 10 µl of the plasmid standard. The AAV samples were pipetted in 2 replicates as follows: 20 µl iTaq Universal SYBR Green Supermix, 1 µl forward primer (10 pmol/µl), 1 µl reverse primer (10 pmol/µl), 18 µl ddH_2O and 6.7 µl of the sample. The primers used for titration of AAV vectors can be found in the material's part. A volume of 20 µl of the respective master mix was pipetted into each well of a 96-well plate. Also a negative control containing ddH_2O instead of a sample or standard was applied to the plate. The qRT-PCR was performed using the following cycler program: initial denaturation for 1 min at 95°C, denaturation for 5 s at 95°C, annealing and plate reading for 30 s at 60°C. The cycle of denaturation, annealing and plate reading was repeated 40 times in total. After these cycles, a melting curve analysis was performed, ranging from 65°C to 95°C with a temperature increase of 0.5°C every 5 s. The qRT-PCR data were analyzed with the CFX manager software (Bio-Rad).

For *in vivo* applications, the iodixanol in the AAV vector samples had to be exchanged by PBS. To achieve this, Zeba Spin Desalting Columns (Thermo Fisher Scientific) were used according to manufacturer's protocol. Briefly, the bottom closure of the columns was opened, the cap was unloosened and the column was place in a 50 ml collection tube. The column was centrifuged for 2 min at 2000 rpm to remove the storage solution. The flow-through was discarded and 5 ml PBS were applied onto the column. The centrifugation and washing steps with PBS were repeated for 3 times. The column was placed on a new collection tube and the AAV sample was loaded onto the column (maximum 4 ml). After another centrifugation step, the AAV vector solution is located in the flow-through and can be used for concentration.

To achieve higher AAV vector titers, AAV samples can be concentrated by VivaSpin columns (Sartorius). Therefore, the AAV sample obtained from the Zeba Spin Desalting Columns was loaded onto the concentrator column (maximum 20 ml). A centrifugation step at 4400 rpm was performed until the desired volume of AAV vector solution was reached (AAV vectors are located in the supernatant). The sample was transferred into a new tube after centrifugation. After the concentrating, the AAV samples were titrated and quantified again by qRT-PCR.

2.2.3. Molecular biological and biochemical methods

2.2.3.1. Firefly and Renilla luciferase assays from cells or homogenized organs

To quantify expression from AAV vectors, the reporter genes of *Firefly* (from the firefly *Photinus pyralis*) and *Renilla* (from the sea pansy *Renilla reniformis*) luciferases were used. These luciferases generate light if their specific substrate and oxygen are available. This process is called bioluminescence. The substrate for the *Firefly* luciferase is beetle luciferin, the substrate for the *Renilla* luciferase is called coelenterazine. The substrates for each luciferase were obtained from Promega (Luciferase Assay System and *Renilla* Luciferase System). These luciferase assays also contain specific lysis buffers.

In case of cells, these assays were performed as follows. The growth medium was removed from the cells (e.g. from a 6-well plate) and 1 ml PBS was added. By rinsing, the cells were detached from the plate and transferred to a 1.5 ml tube placed on ice. After centrifugation at 5000 rpm for 3 min, the supernatant was discarded and 100 µl of 1x lysis buffer (Cell Culture Lysis Reagent for *Firefly*, *Renilla* Luciferase Assay Lysis Buffer for *Renilla*) were added. To mix cells with lysis buffer, the tubes were vortexed for 30 s. Cell debris were collected by centrifugation at 13000 rpm for 1 min. The supernatant was transferred to a new tube and placed on ice. Before measurements can be performed, 1x of the respective substrate was prepared. As a blank value, 100 µl of the substrate were measured in the luminometer (integration time of 10 s). For determine luciferase activity, 20 µl of the sample were added, mixed well and measured in the luminometer. The measurement was repeated for each sample. All values were noted and analyzed with Microsoft Excel and GraphPad Prism 5.

For measuring the luciferase activity from homogenized organs, frozen organs were stored on dry ice until their weight was determined. The organs were transferred to a 1.5 ml homogenization tube containing ceramic beads. Tubes were always placed on ice. To 100 mg of organ, 300 µl of pre-chilled 1x lysis buffer (Reporter Lysis Buffer for *Firefly*, *Renilla* Luciferase Assay Lysis Buffer for *Renilla*) were added. The tubes were put into the homogenizer and homogenization was performed at 5500 rpm and 4°C for 30 s. This process was repeated 3 times. To pellet cell debris and connective tissue, the samples were centrifuged at 13000 rpm and 4°C for 1 min. The supernatant was transferred to a new tube placed on ice. The measurement at the luminometer was performed at described above. Remaining samples were stored at -80°C.

2.2.3.2. β-Galactosidase staining of cells

The CV-1 5B cells can be used as a tool to determine the activity of the inducible CreER^{T2} recombinase in cell culture. As describe above, the stably transfected lacZ gene gets expressed if Cre-mediated recombination is successful. The β-Galactosidase catalyzes the hydrolysis of the X-Gal (5-Bromo-4-chloro-3-indoyl-ß-D-galactopyranoside) present in the staining buffer which generates a blue staining of the positive cells. To test whether the CreER^{T2} can be induced by applying 4-hydroxytamoxifen, the β-Galactosidase staining was performed.

The earliest time point to stain the cells for β-Galactosidase expression was 24 h after induction with 4-OHT. The growth medium was aspirated and the cells were washed once with PBS. To fixate the cells, 2 ml 1x fixing solution were added per 6-well of the plate and incubated for 10 min at RT. After that time period, the fixing solution was removed and the cells were washed with PBS twice. Then, 1 ml staining buffer was added per well and the plate was incubated over night at 4°C. Next day, the staining solution was aspirated and the cells were washed with PBS. Before determine β-Galactosidase activity under a light microscope, 1 ml PBS was added per well. After microscoping, the plates can be stored at 4°C for about 1-2 weeks.

2.2.3.3. Isolation of genomic DNA from cells

To analyze genomic DNA (gDNA) by PCR, the gDNA had first to be isolated from the cells. Therefore, the growth medium was aspirated and 1 ml PBS was added per well (e.g. of a 6-well plate). The cells were detached by rinsing and transferred to a 1.5 ml tube. For pelleting the cells, they were centrifuged at 5000 rpm for 3 min. The PBS was removed afterwards. The next steps were performed according to the manufacturer's protocol from the DNeasy Blood & Tissue Kit (Qiagen). The cell pellet was resuspended in 200 µl PBS and 20 µl proteinase K was added. To lyse the cells, 200 µl of buffer AL were added and mixed by vortexing. Ethanol (100%) was applied in a volume of 200 µl and the sample was again vortexed. The mixture was loaded onto the provided column placed in a 2 ml collection tube and centrifuged at 8000 rpm for 1 min. The column was put onto a new collection tube and 500 µl buffer AW1 were added. The centrifugation step was repeated and afterwards the collection tube was discarded. A volume of 500 µl buffer AW2 were applied onto the column placed on a new collection tube. The column was centrifuged at 13000 rpm for 3 min. After

discarding the collection tube, the column was placed in a new 1.5 ml tube. The gDNA was eluted by applying 200 µl buffer AE, incubating for 1 min at RT and centrifugation at 8000 rpm for 1 min. The amount of isolated gDNA was determined using the NanoDrop spectrometer. The gDNA was stored at -20°C until the PCR was performed.

2.2.3.4. Detection of "Mini Circles" by PCR

If recombination between two loxP sites is successful the excised DNA fragment forms a circle (also called "Mini Circle"). To detect these excised DNA circles, a PCR was performed using outwardly directed primers (see figure below).

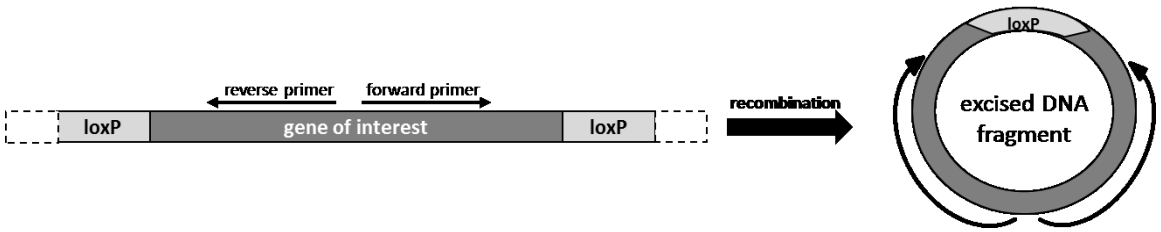

Figure 1: Detection of "Mini Circles" by PCR after Cre-mediated recombination

The PCR was performed using the Taq DNA Polymerase (Qiagen). The PCR mix consisted of 2 µl CoralLoad Buffer, 0.4 µl dNTP mix (10 µM of each), 1 µl forward primer (10 µM), 1 µl of reverse primer (10 µM), 0.1 µl Taq polymerase, 100-200 ng template DNA and water added to a total volume of 20 µl. The PCR cycler was programmed as follows: initial denaturation at 94°C for 3 min, denaturation at 94°C for 1 min, annealing at 50°C for 1 min, extension at 72°C for 4 min and final extension at 72°C for 10 min. The cycle of denaturation, annealing and extension was repeated for 35 times in total. After performing the PCR, the samples were analyzed by agarose gel electrophoresis.

2.2.3.5. Isolation of RNA, cDNA synthesis and qRT-PCR

For the analysis of vector transcripts on mRNA level, total RNA was isolated from cells and converted into cDNA. The quantification of these transcripts was performed by quantitative real-time PCR (qRT-PCR).

The RNA isolation was made with the RNeasy Mini Kit (Qiagen) according to the provided manual. The cells (e.g. from a 6-well plate) were harvested in PBS and pelleted by centrifugation at 5000 rpm for 3 min. The supernatant was discarded and 350 µl of buffer RLT complemented with 2-mercaptoethanol were added. Subsequently, 350 µl of 70% ethanol were applied to the lysate and mixed well by pipetting. A maximum volume of 700 µl of the sample was transferred to the provided column placed on a 2 ml collection tube. After centrifugation at 10000 rpm for 15 s, the flow-though was discarded and 700 µl of the buffer RW1 were applied onto the column. Again, the column was centrifuged as described above and the flow-through was removed. After adding 500 µl of buffer RPE, another centrifugation step was performed. The flow-through was discarded before 500 µl of buffer RPE were applied. This time, the centrifugation was performed for 2 min. The column was transferred to a new 1.5 ml tube and 50 µl RNase-free water were added. To elute the RNA, the column was centrifuged at 10000 rpm for 1 min. The RNA amounts were determined with the NanoDrop spectrometer. RNA was stored at -80°C until cDNA synthesis.

The first-strand cDNA synthesis was performed using the SuperScript III First-Strand Synthesis System for RT-PCR (Invitrogen). In this thesis, 500 ng of RNA were converted into cDNA. Therefore, the RNA was mixed with 1 µl of the provided oligo$(dT)_{20}$ primer, 1 µl dNTP mix (10 mM) and water to get a total volume of 10 µl. This mixture was incubated for 5 min at 65°C and then placed on ice. The cDNA synthesis mix (10 µl in total) was added which consisted of the following reagents: 2 µl 10x RT buffer, 4 µl 25 mM $MgCl_2$, 0.1 M DTT, 1 µl RNase OUT (40 U/µl) and 1 µl SuperScript III RT (200 U/µl). After incubation for 50 min at 50°C, the reaction was terminated by applying 85°C for 5 min. The samples were chilled on ice before 1 µl of RNase H was added and incubated for 20 min at 37°C. The cDNA was then stored at -20°C until qRT-PCR was performed.

As seen with the titration of AAV vectors, the qRT-PCR was executed with the iTaq Universal SYBR Green Supermix (Bio-Rad). The master mix was mixed according to the manufacturer's protocol as follows: 10 µl iTaq Universal SYBR Green Supermix, 1 µl forward primer (10 µM), 1 µl reverse primer (10 µM) and 7 µl ddH_2O. A volume of 19 µl of this master mix was

pipetted into each well of the 96-well plate. A cDNA amount of 25 ng (or water as a negative control) was added; the plate was sealed and briefly centrifuged. The qRT-PCR was performed using the following cycler program: initial denaturation for 30 s at 95°C, denaturation for 5 s at 95°C, annealing and extension for 30 s at 60°C. The cycle of denaturation, annealing and plate reading was repeated 35 times in total. After these cycles, a melting curve analysis was performed, ranging from 65°C to 95°C with a temperature increase of 0.5°C every 5 s. The qRT-PCR data were analyzed with the CFX manager software (Bio-Rad).

2.2.3.6. SDS-PAGE and Western blot analysis

The Western blot analysis was performed to detect transgenes on a protein level which are expressed by AAV vectors.

Therefore, cells (e.g. from a 6-well plate) were harvested in PBS and pelleted by centrifugation at 5000 rpm for 3 min. The supernatant was discarded and the cell pellets were stored at -20°C until the Western blot was executed. The cells were resuspended in 50-100 µl RIPA buffer complemented with protease inhibitor. To disrupt cell membranes efficiently, the lysate was frozen, thawed once and treated by ultrasound for 5 min. Then, 13-25 µl 4x loading buffer complemented with 2-mercaptoethanol were added and incubated at 95°C for 5 min.

The next step was the preparation of the polyacrylamide gels. The upper part of the gel consists of a stacking gel which concentrates the proteins. The lower part of the gel is used to separate the proteins according to their molecular weight. The composition of these gels is summarized in the following table.

Table 5: Composition of polyacrylamide gels (solutions suitable for two gels)

	10% separating gel solution	*5% stacking gel solution*
ddH_2O	7.9 ml	5.6 ml
polyacrylamide	6.7 ml	1.7 ml
Tris	5 ml of 1.5 M, pH 8.8	2.5 ml of 0.5 M, pH 6.8
20% SDS	100 µl	50 µl
10% APS	200 µl	100 µl
TEMED	20 µl	10 µl

First, the separating gel was made, filled into the chamber and overlaid with isopropyl alcohol. The gel was allowed to polymerize for about 30 min before the isopropyl alcohol was removed and the stacking gel solution was added. To form lanes for the samples, a comb was carefully inserted. The stacking gel also polymerized for 30 min before the comb could be removed. The prepared gels were put into the electrophoresis chamber which was then filled up with running buffers (anode and cathode buffers). The samples were pipetted in a volume of 20 µl into the lanes. Also, a marker to assess the molecular mass of the protein was added (PageRuler Plus, prestained). The electrophoresis was performed by applying 100 V for about 2 h. After electrophoresis, the proteins were transferred onto a nitrocellulose membrane which was first activated with methanol for 30 s. The blotting was done in a cassette containing Whatman paper, the gel and the membrane. This cassette was put into a reservoir which was filled with transfer buffer. A voltage of 70 V was applied for 1 h to transfer the proteins from the gel onto the membrane. After the transfer, the membrane was washed twice with TBS-T washing buffer and then blocked with 5% milk powder in TBS-T for 1 h at RT. By blocking unspecific binding sites for antibodies, the specificity is increased. The primary antibodies were dissolved in 10 ml 1% milk powder in TBS-T. The antibody concentration applied is given in the material's part. The membrane was incubated with the antibody solution over night at 4°C on a shaker. At the following day, the primary antibody was removed, the membrane was washed 3 times with TBS-T and the secondary antibody was added. The secondary antibody was also dissolved in 10 ml 1% milk powder in TBS-T according to the dilutions mentioned in the material's part. The membrane was incubated at RT for 1 h before the membrane was washed 3 times with TBS-T.

For detection of the proteins, the membrane was soaked with an ECL detection reagent for 1 min. ECL contains luminol which reacts with the horseradish peroxidase (HRP) coupled to the secondary antibody. Thereby, photons are emitted (chemiluminescence) which can be detected by an appropriate imaging system (Bio-Rad). The exposure time was dependent on the intensity of the chemiluminescence. After imaging, the membrane was kept in TBS-T until further use.

2.2.4. *In vivo* approaches

2.2.4.1. Breeding, husbandry and genotyping of animal models

All animal models used in this study (see material's part) were bred under standard conditions in the animal facility of the University of Heidelberg. The mice were kept in a temperature and humidity controlled room which was specified pathogen-free. A day/night cycle of 12:12 hours was applied and the animals were fed ad libitum with a complete diet of Rod 16-A (LASvendi). All animal experiments were performed according to the proposal for animal experiments, approved by the Regierungspräsidium Karlsruhe, Germany.

In case of the αMHC-MerCreMer mice, the genotype of the mice had to be verified. Therefore, a tail biopsy was taken; DNA was isolated and analyzed by PCR. DNA isolation and PCR were performed with the REDExtract-N-Amp Tissue PCR Kit (Sigma-Aldrich). Briefly, 100 µl of Extraction Solution and 25 µl of Tissue Preparation Solution were added to the mouse tail. The sample was incubated for 10 min at RT and then for 3 min at 95°C. Afterwards, 100 µl of Neutralization Solution were added and the tissue extract was transferred to a new tube and stored at 4°C. For PCR, 2 µl tissue extract were mixed with 5 µl REDExtract-N-Amp PCR Reaction Mix, 2.2 µl ddH_2O and 0.8 µl primer mix. The primer mix was generated by mixing the following primers: 10 µl αMHC-MerCreMer 4F, 10 µl αMHC-MerCreMer 4R, 2 µl control fwd 2 and 2 µl control rev 2 with 176 µl ddH_2O. The PCR was performed with the following conditions: activation of Taq polymerase at 94°C for 2 min, denaturation at 96°C for 10 s, annealing at 60°C for 15 s, extension at 72°C for 45 s and final extension 72°C for 10 min. The cycle of denaturation, annealing and extension was repeated for 35 times in total. Finally, PCR products were analyzed by agarose gel electrophoresis. If the animal contained the MerCreMer transgene, a DNA with 1200 bp should be detectable. As an internal control, also a DNA band at 297 bp should be visible.

2.2.4.2. Administration of AAV vectors by tail vein injection

For administration of AAV vectors, an amount of 10^{12} vg per mouse of the respective AAV vector was injected intravenously (i.v.) in a volume of about 100 µl. Therefore, the mouse was put into a restrainer. After warming the tail in water to 37°C, the tail vein was localized and the AAV vector (in PBS) was injected. Injections were performed by employees of the animal facility at the University of Heidelberg.

2.2.4.3. Induction of CreER^{T2} by tamoxifen

To activate the CreER^{T2} recombinase, tamoxifen dissolved in peanut oil had to be administered by intraperitoneal (i.p.) injection. In total, 1 mg tamoxifen in a volume of 100 µl was applied to each mouse daily. This process was repeated on 5 consecutive days.

The tamoxifen solution was prepared according to the protocol published by Feil et al. in 1997. Briefly, 100 mg tamoxifen (T5648, Sigma Aldrich) were dissolved in 0.5 ml EtOH before 9.5 ml peanut oil was added. The solution was mixed well by vortexing. To solve remaining tamoxifen, ultrasound was applied for 5 min at 37°C. The resulting tamoxifen stock solution had a concentration of 10 mg/ml and was stored at -20°C. Of this stock, 100 µl were injected per mouse per day (1 mg tamoxifen per day). For the control group, a vehicle solution consisting of 0.5 ml EtOH and 9.5 ml peanut oil was made of which also 100 µl were injected intraperitoneally per mouse and day.

2.2.4.4. In vivo imaging of Firefly luciferase

To image the expression of the *Firefly* luciferase from AAV vectors in the living animal, *in vivo* imaging with the IVIS Lumina III system (PerkinElmer) was performed.

As a luciferase substrate which is suitable for *in vivo* applications, the VivoGlo Luciferin (Promega) was used. According to the manufacturer's instructions, 2 mg luciferin solved in 150 µl 0.9% NaCl should be administered intraperitoneally. Therefore, 250 mg luciferin was dissolved in 18.75 ml 0.9% NaCl to achieve a concentration of 2 mg in 150 µl. This solution was stored at -20°C until further use.

Because the animals used had black fur which blocks bioluminescence measurement, they first had to be depilated with depilation cream (Veet). Afterwards, the animals were narcotized by isoflurane inhalation (2.1% flow rate) in the induction chamber. While transferring the mouse to the imaging chamber, 150 µl of the luciferin solution was administered intraperitoneally. The mouse was positioned in the inhalation mask (1.5% isoflurane flow rate) before closing the door. To check for the position of the mouse, a photograph was taken. If necessary, the mouse was re-positioned. After an incubation time of 5 min, the first image of the bioluminescence was taken. The exposure time was set to 5 s with medium binning and F/Stop = 1 (open lens). A second image was taken 7 min after luciferin administration. Usually, 3 mice were imaged at once. After termination, animals

were transferred to their cages and awakening was supervised. The bioluminescence images were analyzed using the Living Image Software from PerkinElmer.

2.2.4.5. Dissection, sample preparation and histological analyses

To terminate *in vivo* experiments, the mice had to be euthanized by CO_2 inhalation or cervical dislocation. The chest was opened; the heart was removed and washed in PBS to remove blood. For protein samples, the cardiac apex was cut and transferred to a 1.5 ml tube which was directly frozen in liquid nitrogen. The rest of the heart was put into a tube filled with cryo-protection solution to preserve fluorescent dyes (e.g. eGFP) from diffusion and bleaching. The samples were kept overnight at 4°C protected from light. Next day, the tissue samples were embedded in cryo-molds using Tissue-Tek embedding compound and frozen on dry ice until transferring the samples to -80°C. Samples from other organs (liver, skeletal muscle, kidney, spleen and brain) also were processed in similar way.

If blood sampling was required blood was taken by puncture of the heart of sedated mice. The blood was left at RT for 30 min and then centrifuged for 20 min at 2000 rpm. The plasma was transferred to a new tube and frozen at -20°C until further analysis.

The protein samples were analyzed by luciferase assays from homogenized organs (see above). The embedded organs were used for cryo-sections which were prepared using a cryostat. These cross-sections were made at 8 µm thickness and transferred onto coverslips. The sections were covered with mounting medium and a cover glass and stored at -20°C until fluorescence microscopy.

2.2.4.6. Mouse IL-10 ELISA from plasma samples

For detection of murine IL-10 levels in plasma, the ready-to-use Mouse IL-10 Quantikine ELISA Kit from R&D Systems was used. Therefore, the blood samples were prepared as described above and diluted 1:2 by mixing 70 µl of plasma with 70 µl of Calibrator Diluent RD5T. The Kit Control (positive control) and the standard were each dissolved in 1 ml H_2O. The standard (1000 pg/ml) was further diluted with Calibrator Diluent RD5T to get the following concentrations: 500, 250, 125, 62.5, 31.3, and 15.6 pg/ml. The Calibrator Diluent RD5T served as the negative control (0 pg/ml). The Kit Control was used undiluted.

First, 50 µl Assay Diluent RD1W was pipetted into each well of the 96-well plate supplied by the manufacturer. The standard, Kit Control and plasma samples were added in a volume of 50 µl per well in duplicates. The plate was sealed and incubated at RT for 2 h on an orbital shaker. Next, the liquid was removed from the plate and the wells were washed 4 times with 400 µl 1x wash buffer per well. The wash buffer was completely removed and 100 µl mIL10 Conjugate per well were added. Again, the plated was sealed and incubated at RT for 2 h on an orbital shaker. As described above, the liquid was removed and the plate was washed 4 times. After removing the wash buffer completely, 100 µl Substrate Solution (50 µl Color Reagent A + 50 µl Color Reagent B) was pipetted into each well. The plate was incubated at RT for 30 min under light protection before 100 µl Stop Solution per well were added. The measurement was performed within 30 min in a spectral photometer at wavelength of 450 nm and 570 nm (for correction). After all values were corrected for the measurement at 570 nm, the amount of IL-10 in plasma samples (in pg/ml) was calculated by generating a standard curve normalized to the negative control.

3. RESULTS

To generate a shut-off system encoded by one AAV vector, several pre-experiments were necessary. Part 1 comprised the cloning and testing of the inducible Cre recombinase ($CreER^{T2}$) in an AAV context. In part 2, the functionality and localization of loxP sites within an AAV vector were tested. The next step was the combination of the former parts where both AAV vector were co-transduced (part 3). In the last part, the $CreER^{T2}$ and the loxP sites were put onto one AAV vector so that the final shut-off system was generated.

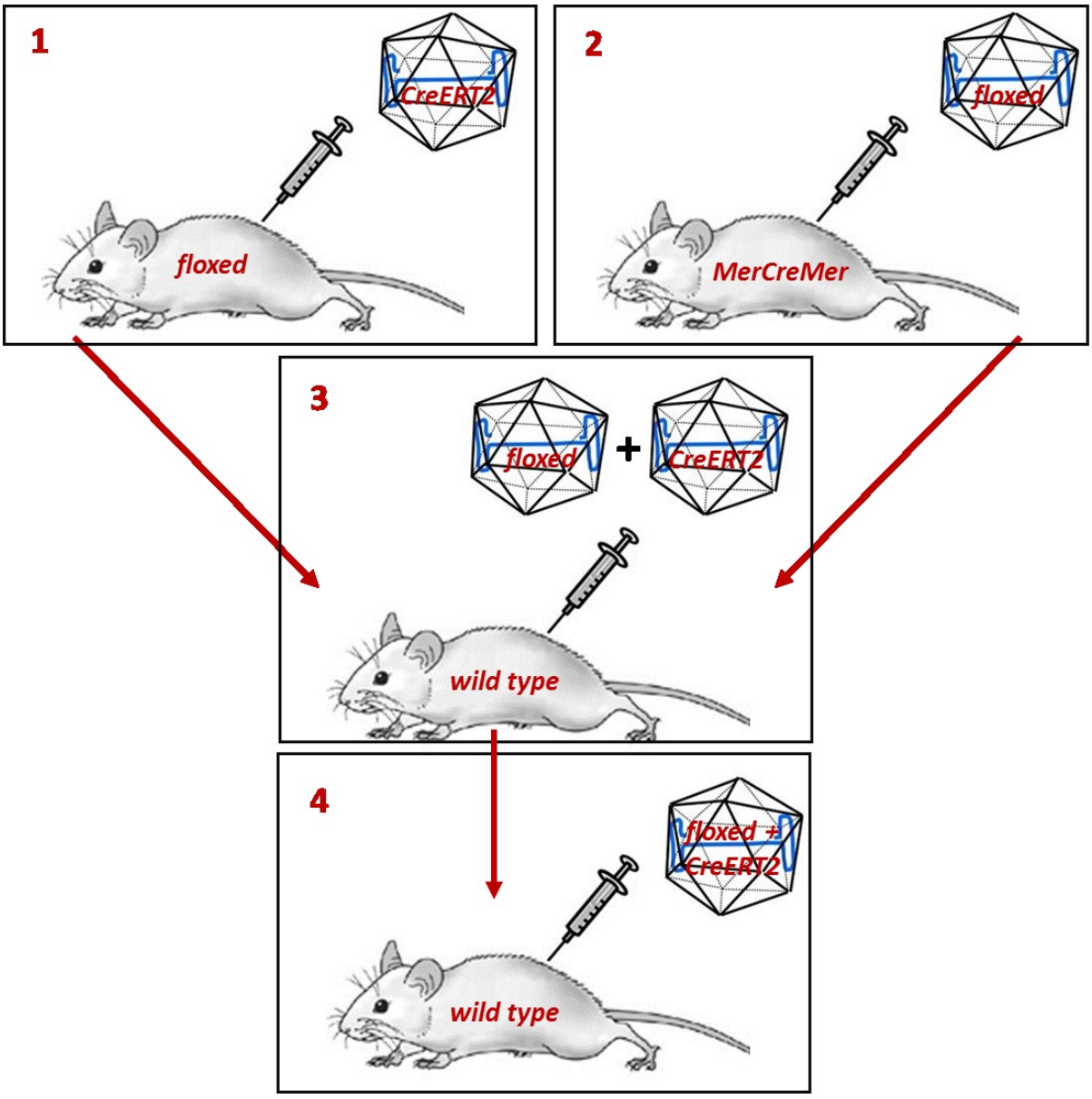

Figure 2: Experimental set-up to generate a shut-off system for AAV vectors
The crucial parts that have to be encoded by the AAV vector and/or the animal model are indicated. AAV vectors are shown as icosahedral capsids containing the AAV genome.

3.1. Part 1 – Induction of the inducible Cre recombinase from an AAV vector

3.1.1. Generation of an AAV vector encoding the CreER^{T2}

The CMV promoter and the SV40 polyA signal were subcloned with *Kas I/Sbf I* and *BamH I/Cla I*, respectively, into the CreER^{T2}-containing plasmid. The whole expression cassette was then cloned with *EcoR I/Cla I* into the single-stranded AAV2 genome plasmid (pSSV9). Primers used can be found in the material's part.

Figure 3: Scheme of AAV vector genomes generated for the first part of experiments
Promoters and transgenes were cloned into a single-stranded AAV background (pSSV9).

3.1.2. In vitro induction of the CreER^{T2} in cell culture

First, the induction of the inducible Cre recombinase was tested *in vitro*. Therefore, CV-1 5B cells were transduced by AAV2 vectors containing the CreER^{T2} gene (figure 3). The recombination events could be visualized by X-gal staining performed at different time points after the initial induction (figure 4). After the CreER^{T2} is expressed and activated by 4-OHT, the repressor flanked by loxP sites is removed so that expression of the β-galactosidase can take place. Cells positive for β-galactosidase turn blue after X-Gal staining. Therefore, it could be shown that the CreER^{T2} encoded on an AAV vector can be successfully induced by 4-OHT *in vitro*. In case of non-transduced cells, no β-galactosidase positive cells were detectable.

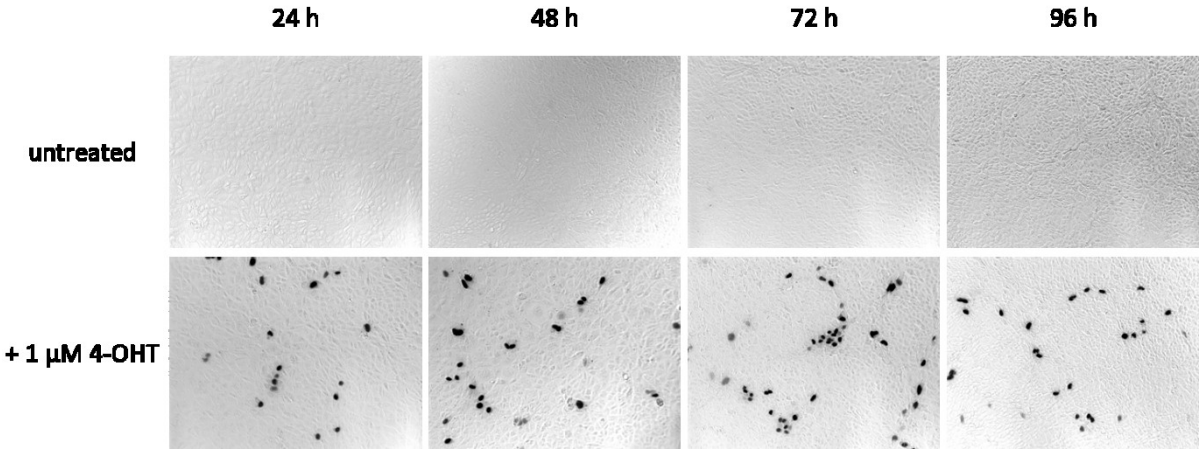

Figure 4: X-Gal staining of CV-1 5B cells transduced with AAV2-ss-CMV-CreERT2
Cells were transduced with 10^4 vg/cell. Induction with 1 µM 4-OHT was performed 2 days after transduction. Time points of X-Gal staining are indicated by hours after induction. Images were taken with 10-fold magnification.

3.1.3. In vivo induction of the CreER^{T2} in Tomato mice

After successful *in vitro* experiments, the AAV vector containing the CreER^{T2} should be tested *in vivo*. Therefore, AAV serotype 9 vectors were used to achieve a high expression of the transgene in the heart. Mice which were not treated with AAV vectors served as negative control. The positive controls were mice treated with AAV9-ds-CMV-Cre where an induction with tamoxifen was not required. In animals treated with AAV9-ss-CMV-CreER^{T2}, the recombinase was induced by tamoxifen 4 weeks after AAV administration. Animals receiving vehicle solution instead of tamoxifen were used as further controls.

Successful recombination events in Tomato mice are displayed by a conversion of the red fluorescent signal to a green fluorescent signal (figure 5). The active Cre recombinase excises the red Tomato gene from the mouse genome so that the eGFP reporter gene gets under the control of the promoter and can be expressed. In control animals which not received any AAV vector, this conversion was not observed. The switch from red to green fluorescence could be seen in animals which were treated with AAV9-ds-CMV-Cre. Most of the cardiomyocytes from these mice were transduced by the AAV vector indicated by the green fluorescent signal. In animals receiving the CreER^{T2}-expressing vector and the vehicle solution (negative control), almost no transition from red to green fluorescence was detectable. In contrast, cross-sections of mice treated with the same vector and tamoxifen showed a strong green fluorescent signal.

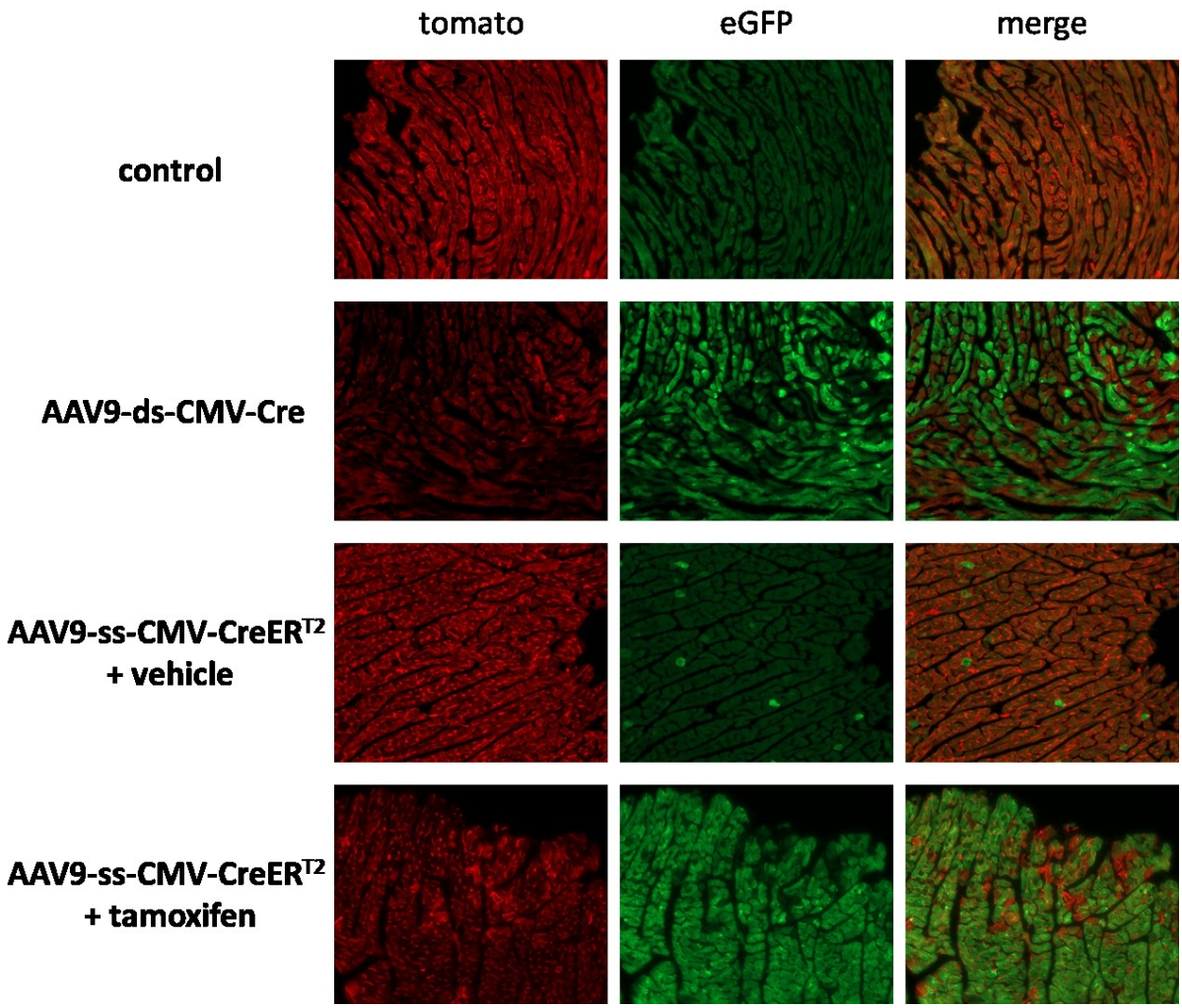

Figure 5: Cryo-sections of heart samples from Tomato mice treated with different AAV9 vectors

Mice were treated with 10^{12} vg/mouse via tail vein injection. Induction with vehicle/tamoxifen took place 4 weeks after AAV administration (1 mg/mouse/day, 5 consecutive days). The animals were sacrificed 1 week after the last vehicle/tamoxifen administration. Images of cross-sections from heart of Tomato mice taken in red fluorescent channel (for Tomato dye) and green fluorescent channel (for eGFP dye) are shown. The third column shows the images of merged channels. Images were taken with 10-fold magnification.

3.2. Part 2 - Localization and functionality of loxP sites within an AAV vector

3.2.1. Generation of an AAV vector containing loxP sequences

In this part, a cardiac-specific promoter – the human troponin T promoter (TnT) - was used. To analyze the functionality of the loxP sequences, the *Firefly* luciferase reporter gene (Fluc) or the promoter was flanked by loxP sites. The whole expression cassette was cloned into the single-stranded AAV2 genome plasmid (pSSV9). The vector genome without loxP sequences served as a control. Primers used can be found in the material's part.

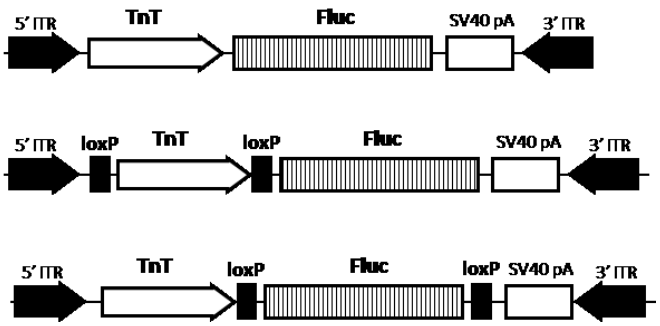

Figure 6: Scheme of AAV vector genomes generated for the second part of experiments
Promoters, transgenes and loxP sequences (in parallel orientation) were cloned into a single-stranded AAV background (pSSV9). The vector without loxP sites served as a control.

3.2.2. In vitro analysis of the loxP sequence functionality

To test the loxP sequences in cell culture, the AAV genomes (figure 6) were packaged into capsids from AAV serotype 2. These vectors were co-transduced with an AAV2-ss-CMV-CreER^{T2} vector. The *Firefly* luciferase expression was analyzed after induction of the CreER^{T2} by 4-OHT. If loxP sequences are functional the luciferase expression should be reduced after 4-OHT administration.

In figure 7, a generic *Firefly* luciferase assay is shown. In this experiment, cells treated with the control vector (without loxP sites) and 4-OHT showed significantly higher luciferase expression levels than vehicle-treated cells. If the TnT promoter (*floxed* TnT) or the *Firefly* luciferase (*floxed* Fluc) were flanked by loxP sequences the Fluc expression could be reduced significantly by applying 4-OHT to the cells. In general, the Fluc expression level was higher in the control vector without loxP sequences compared to the *floxed* vectors.

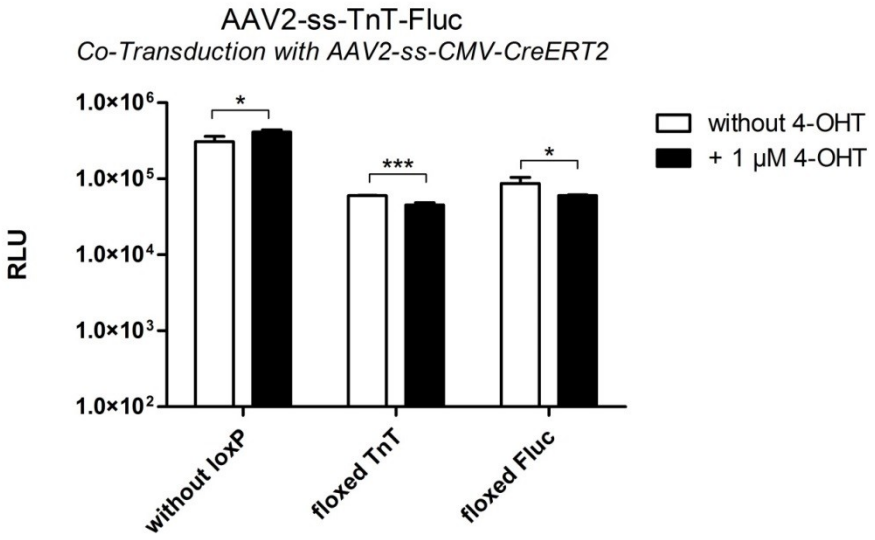

Figure 7: Generic *Firefly* luciferase assay for testing the functionality of loxP sites in cell culture

AAV vectors without and with loxP sequences at different positions were co-transduced with a $CreER^{T2}$-bearing vector (10^4 vg/cell/vector). Induction with 4-OHT (black bars) was performed 2 days after transduction. The luciferase assay was carried out 3 days after initial induction. Mean values of relative light units (RLU) with 4 replicates per group are shown. The standard deviation is indicated with error bars. Statistical analysis was made with Student's t-test (*$p<0.05$; ***$p<0.001$).

The experiment displayed in figure 7 was performed at different time points after initial induction for at least 3 times. To summarize the data from these independent experiments, the fold changes between the relative light units of vehicle and 4-OHT treated cells were calculated for all applied AAV vectors at the time points analyzed (figure 8). Compared to the control vector without loxP sites, the *Firefly* luciferase expression is significantly down-regulated in both vectors containing loxP sequences after 4-OHT administration at all time points analyzed.

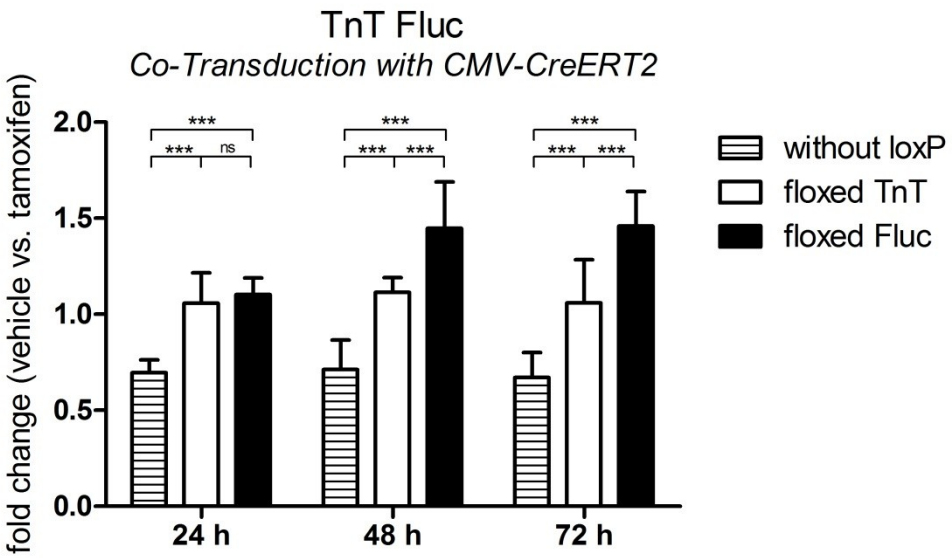

Figure 8: Analysis of fold changes between relative light units of vehicle and 4-OHT treated cells transduced with *floxed* AAV2-ss-TnT-Fluc vectors

The summary of 3 independent experiments which were performed as seen in figure 7 is shown. Fold changes between the RLUs of vehicle and tamoxifen treated cells at different time points after initial induction were calculated. The standard deviation is indicated with error bars. Statistical analysis was made with One-way ANOVA and Tukey post-test (***p<0.001; ns = not significant).

3.2.3. In vivo analysis of the loxP sequence functionality in MerCreMer mice

To verify the data from the *in vitro* experiments, the generated AAV genomes packaged in capsids from serotype 9 were analyzed in the MerCreMer mouse model. These animals express an inducible Cre recombinase (MerCreMer) under the control of a cardio-specific promoter (αMHC). The AAV vector without loxP sites served as the control. The induction with tamoxifen was performed 4 weeks after AAV administration.

First, the AAV vector containing the *floxed Firefly* luciferase gene was analyzed by *in vivo* Imaging (figure 9). Therefore, sedated mice were imaged 4 weeks after AAV administration and before tamoxifen application. In all animals analyzed, *Firefly* luciferase expression could be detected in the thorax area without any difference between the treatment groups. The next imaging analyses were performed 1 week and 3 weeks after vehicle/tamoxifen administration. In the tamoxifen-treated animals, no luciferase expression could be detected whereas the vehicle-treated mice showed a clear signal.

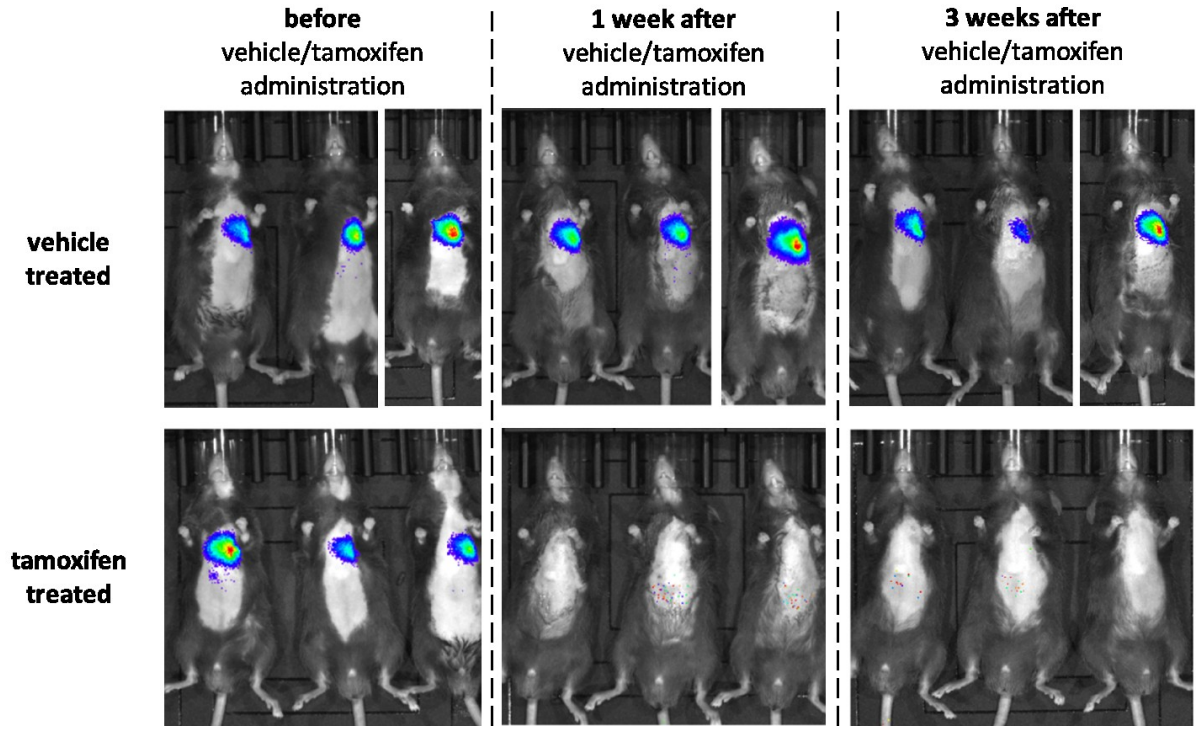

Figure 9: *In vivo* Imaging of *Firefly* luciferase expression in MerCreMer mice treated with AAV9-ss-TnT-lox-Fluc-lox

Exemplary animals of vehicle- and tamoxifen-treated mice are shown. The imaging was carried out at 3 different time points. The signal ranged from high luciferase expression levels (red) to low expression (dark blue).

With the help of a software from PerkinElmer, the signal could be analyzed by counting the photons per second (figure 10). This so-called total flux revealed that there was no difference in luciferase expression between the groups before tamoxifen was applied. In case of the vehicle-treated animals, the signal intensity increased from the first measurement to the second whereas it dropped at the third imaging to the level of the initial measurement. In the tamoxifen-treated group, a significant reduction of the total flux could be detected after tamoxifen was administered. This reduction stayed stable until the third measurement.

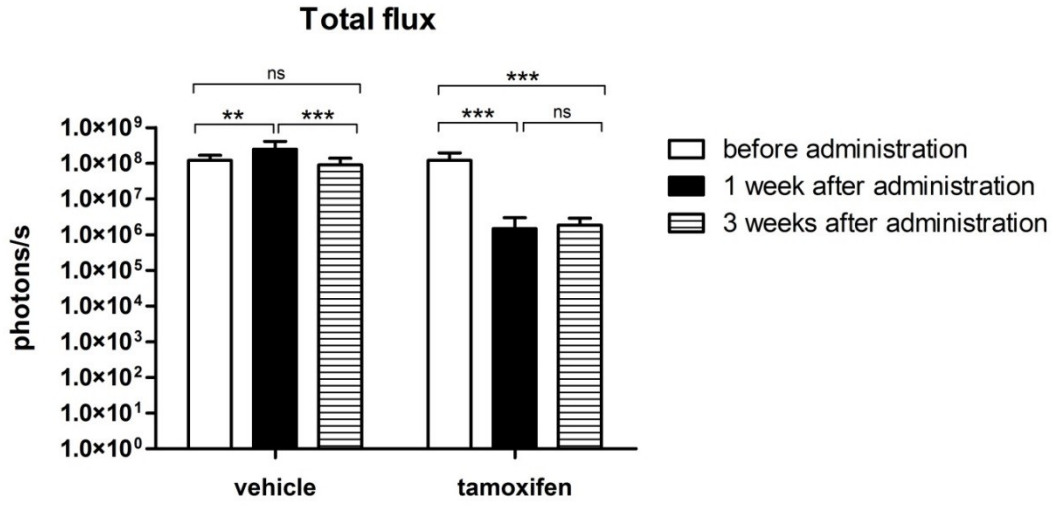

Figure 10: Total flux measured by *in vivo* Imaging of animals treated with AAV9-ss-TnT-lox-Fluc-lox

The photons that are emitted per second in vehicle- and tamoxifen-treated animals at 3 different time points (10 animals per group) are shown. The standard deviation is indicated with error bars. Statistical analysis was made with One-way ANOVA and Tukey post-test (**p<0.01; ***p<0.001; ns = not significant).

After dissection, organs from animals analyzed by *in vivo* imaging as well as animals treated with control vector or *floxed* TnT vector were homogenized and luciferase expression was measured. As displayed in figures 11 and 12, there was no difference in *Firefly* luciferase expression between vehicle and tamoxifen treated animals which received the *non-floxed* control vector. In case of the AAV vector with *floxed* TnT promoter, there was a significant reduction in luciferase expression after tamoxifen administration which was only seen in the heart samples. The heart and muscle samples of animals receiving the vector with *floxed Firefly* luciferase also showed a significant down-regulation of luciferase expression levels if tamoxifen was applied. In the liver, tamoxifen administration did not alter expression levels between vehicle and tamoxifen treated mice regardless of which vector was applied.

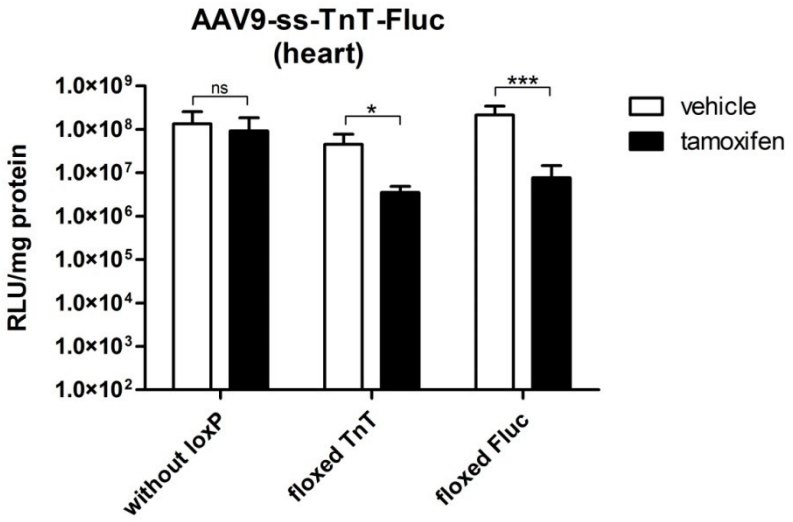

Figure 11: *Firefly* luciferase assays from homogenized heart samples of mice treated with *floxed* AAV9-ss-TnT-Fluc vectors

The rate of relative light units (RLU) to protein amount (in mg) measured is shown. White bars show animals treated with vehicle solution, black bars are tamoxifen-treated mice (5 animals per group). The standard deviation is indicated with error bars. Statistical analysis was made with Student's t-test (*p<0.05; ***p<0.001; ns = not significant).

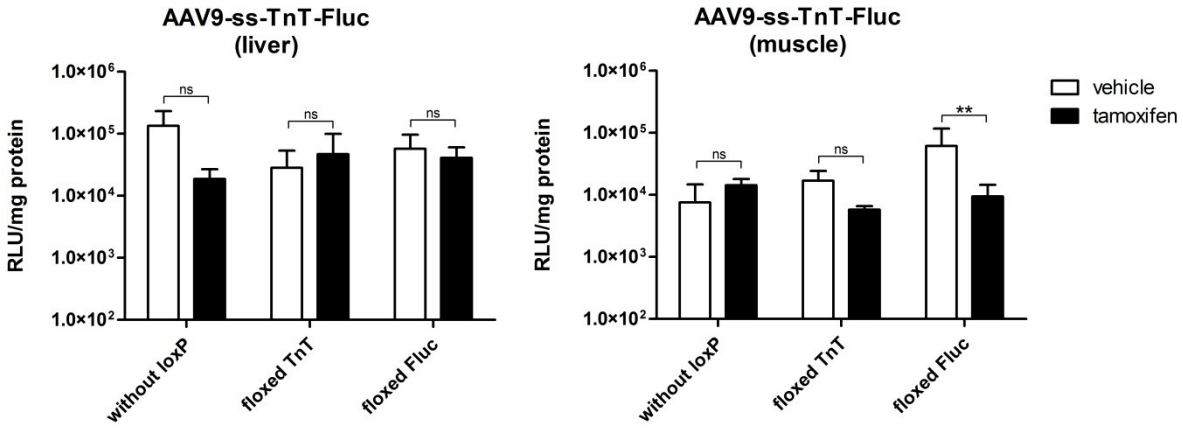

Figure 12: *Firefly* luciferase assays from homogenized liver and muscle samples of mice treated with *floxed* AAV9-ss-TnT-Fluc vectors

The rate of relative light units (RLU) to protein amount (in mg) measured is shown. White bars show animals treated with vehicle solution, black bars are tamoxifen-treated mice (5 animals per group). The standard deviation is indicated with error bars. Statistical analysis was made with Student's t-test (**p<0.01; ns = not significant).

To determine the extent of down-regulation after tamoxifen administration, the ratio between vehicle- and tamoxifen-treated animals was calculated (figure 13). In case of the AAV vector containing the *floxed* TnT promoter, luciferase expression could be down-regulated about 16-fold after tamoxifen administration. The vector expressing the *floxed* Fluc showed a 43-fold reduction in luciferase activity in the presence of tamoxifen. Due to high variations within the groups, only the fold change of the control vector compared with the *floxed* Fluc vector was significantly different.

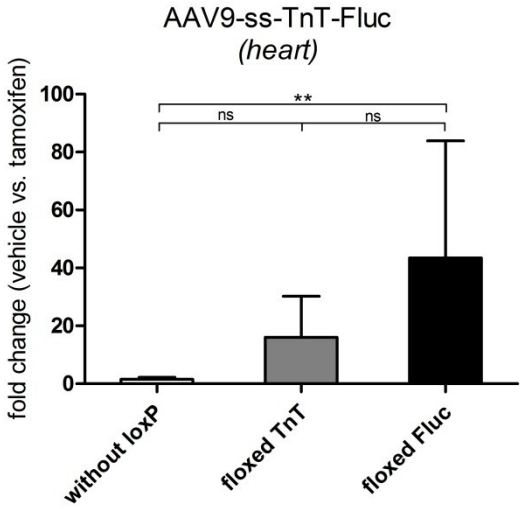

Figure 13: Extent of *Firefly* luciferase down-regulation after tamoxifen administration in heart samples from mice treated with AAV9 vectors containing a *floxed* Fluc reporter gene
The fold changes between the RLU/mg protein of vehicle- and tamoxifen-treated animals receiving different AAV9 vectors are shown. The standard deviation is indicated with error bars. Statistical analysis was made with One-way ANOVA and Tukey post-test (**$p<0.01$; ns = not significant).

3.3. Part 3 – Co-transduction of CreER^{T2}- and loxP-bearing AAV vectors

3.3.1. Generation of AAV vectors containing loxP sites at different positions

Similar to the cloning steps described for part 2, another AAV vector set containing loxP sequences at different positions was generated. For these experiments, the *Renilla* luciferase reporter gene (Rluc) under the control of the CMV promoter was used in order to allow a detailed analysis of also non-cardiac tissues. The whole expression cassette was cloned into the single-stranded AAV2 genome plasmid (pSSV9). The vector genome without loxP sequences served as a control. Primers used can be found in the material's part.

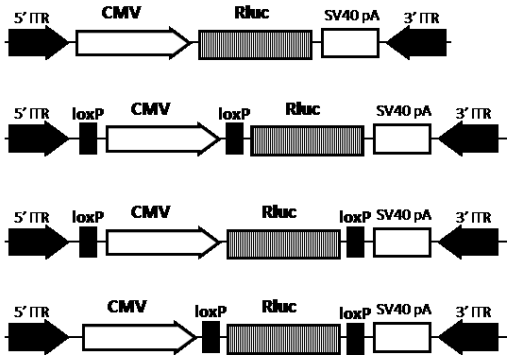

Figure 14: Scheme of AAV vector genomes generated for the third part of experiments
Promoters, transgenes and loxP sequences (in parallel orientation) were cloned into a single-stranded AAV background (pSSV9). The vector without loxP sites served as a control.

3.3.2. Co-transduction of CreER^{T2}- and loxP-bearing AAV vectors in vitro

To test the AAV vectors in cell culture, the AAV genomes (figure 14) were packaged into capsids from AAV serotype 2. These vectors were co-transduced with an AAV2-ss-CMV-CreER^{T2} vector. The *Renilla* luciferase expression was analyzed after induction of the CreER^{T2} by 4-OHT. If the co-transduction of two AAV vectors and the induction by 4-OHT were successful the luciferase expression should be reduced after 4-OHT administration.

In figure 15, a generic *Renilla* luciferase assay is shown. Here, even the control vector (without loxP sites) showed a significantly lower luciferase expression if 4-OHT was applied to the cells. In case of the AAV vectors with loxP sites at different position, there was also a reduction in luciferase expression after 4-OHT administration.

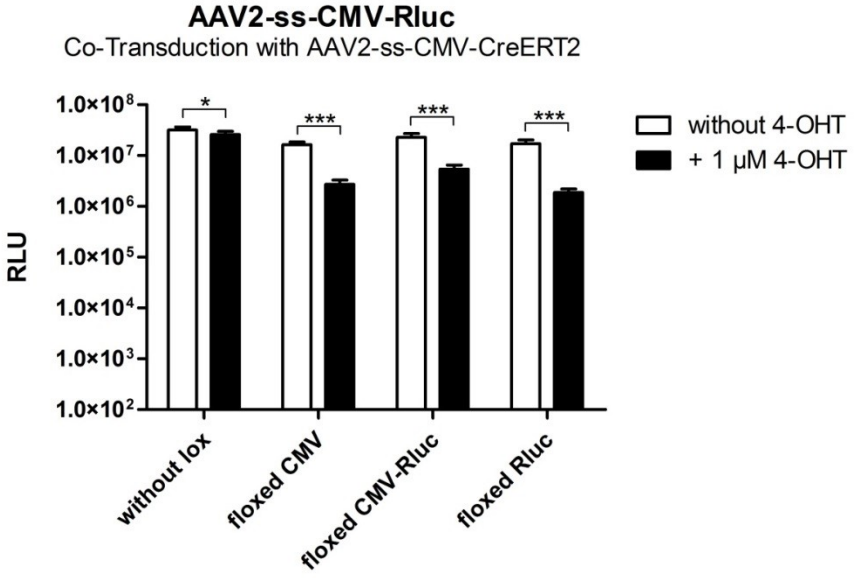

Figure 15: Generic *Renilla* luciferase assay for testing the co-transduction of CreERT2- and loxP-bearing AAV vectors *in vitro*

AAV2 vectors without and with loxP sequences at different positions were co-transduced with a $CreER^{T2}$-bearing vector (10^4 vg/cell/vector). Induction with 4-OHT (black bars) was performed 2 days after transduction. The luciferase assay was carried out 3 days after initial induction. Mean values of relative light units (RLU) with 4 replicates per group are shown. The standard deviation is indicated with error bars. Statistical analysis was made with Student's t-test (*$p<0.05$; ***$p<0.001$).

The luciferase activities shown in figure 15 were measured at different time points after initial induction. To summarize the data, the fold changes between the relative light units measured of vehicle- and 4-OHT-treated cells were calculated for all applied AAV vectors (figure 16). Statistical analysis was performed with the One-way ANOVA and the Tukey post-test. To summarize the statistical data, it could be shown that the fold changes of the single AAV vectors within each time point were significantly different compared to other AAV vectors at the same time point. The only exception from this observation was the fold change between the *floxed* CMV and the *floxed* Rluc vectors at the time points of 24 h and 48 h after induction. The highest down-regulation of luciferase expression was achieved by the *floxed* Rluc vector at the time point of 72 h after initial induction, reaching a 9-fold reduction in luciferase activity.

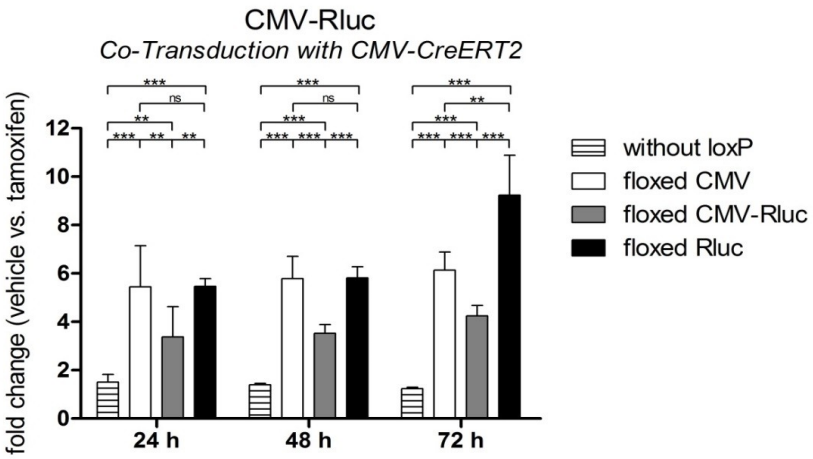

Figure 16: Analysis of fold changes between relative light units of vehicle and 4-OHT treated cells transduced with *floxed* AAV2-ss-CMV-Rluc and AAV2-CMV-CreER^{T2} vectors
Data from 3 independent experiments which were performed as seen in figure 15 are shown. Fold changes between RLUs of vehicle- and tamoxifen-treated cells at different time points after initial induction were calculated. The standard deviation is indicated with error bars. Statistical analysis was made with One-way ANOVA and Tukey post-test (**p<0.01; ***p<0.001; ns = not significant).

3.3.3. In vivo co-transduction of CreER^{T2}- and loxP-bearing AAV vectors

After identifying the AAV vector with the *floxed* Rluc reporter gene as most appropriate *in vitro*, this vector was tested in 8-weeks old male C57Bl/6 wild-type mice. For this purpose, the AAV vector genomes (with and without loxP sites) packaged into serotype 9 were administered via tail vein injection (10^{12} vg/vector/mouse) and induced with tamoxifen 4 weeks after AAV injection.

After another two weeks, samples from different organs (heart, liver, muscle, kidney, spleen) were homogenized and the *Renilla* luciferase assays were performed (figures 17 and 18). In the heart, there was no significant difference in *Renilla* luciferase expression between vehicle- and tamoxifen-treated animals which received the *non-floxed* control vector. Also, the expression levels were similar in the vehicle-treated groups, independent of which vector the animals received. In case of the AAV vector with *floxed* Rluc, there was a significant reduction in luciferase expression in the heart after tamoxifen administration which was also detectable in the liver samples. In all other organ samples, no significant down-regulation of luciferase expression after tamoxifen administration could be shown although there was a trend towards decreased luciferase activities in animals treated with the *floxed* AAV vector.

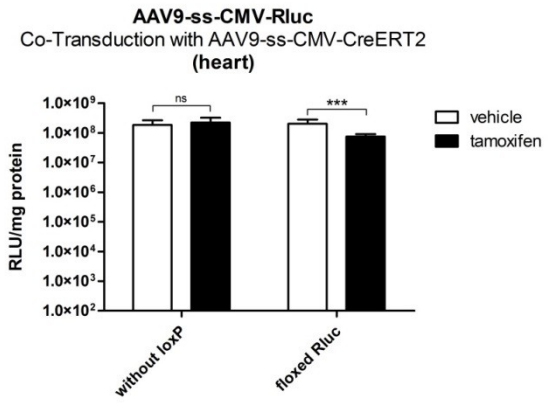

Figure 17: *Renilla* luciferase assay from homogenized heart samples of mice co-transduced with CreERT2- and loxP-bearing AAV vectors

The rate of relative light units (RLU) to protein amount (in mg) was measured. White bars show animals treated with vehicle solution, black bars represent tamoxifen-treated mice (4 animals per group). The standard deviation is indicated with error bars. Statistical analysis was made with Student's t-test (***p<0.001; ns = not significant).

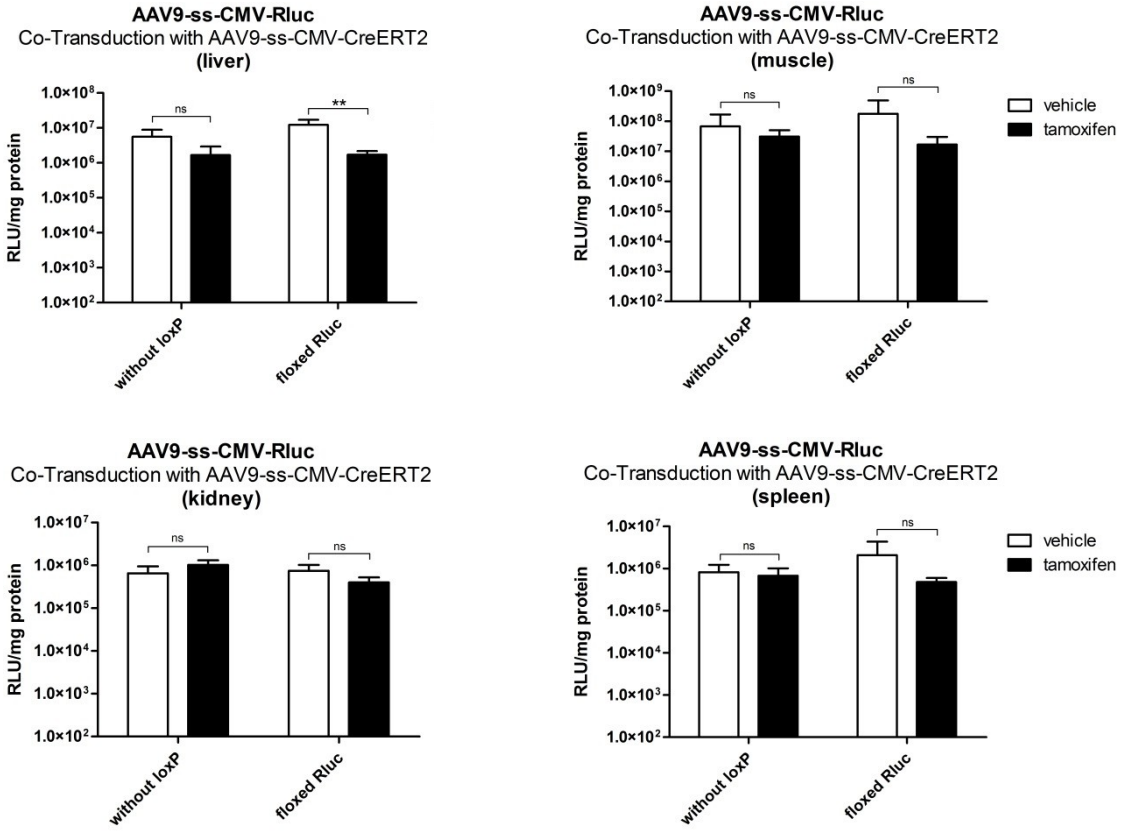

Figure 18: *Renilla* luciferase assay from homogenized organ samples of mice co-transduced with CreERT2- and loxP-bearing AAV vectors

The rate of relative light units (RLU) to protein amount (in mg) was measured. White bars show animals treated with vehicle solution, black bars represent tamoxifen-treated mice (4 animals per group). The standard deviation is indicated with error bars. Statistical analysis was made with Student's t-test (**p<0.01; ns = not significant).

3.4. Part 4 – Generation of the shut-off system encoded on a single AAV vector

3.4.1. Generation of AAV vectors containing the shut-off system

To establish the shut-off system for AAV vectors, the inducible CreER^{T2} recombinase as well as the loxP sequences had to be encoded by a single vector. Therefore, the AAV genomes seen in figure 19 were cloned and packaged in AAV serotype 2 for *in vitro* analysis.

Due to the limited coding capacity of AAV genomes, the *Renilla* luciferase was used as reporter gene. The luciferase gene as well as the gene for the CreER^{T2} each had their own CMV promoter and polyA signal. As seen in the former part of experiments, the loxP sites were positioned at different locations within the vector. The overall genome size of these AAV vectors was about 5.2 kb which is slightly exceeding the packaging limit of AAV (4.8-5.0 kb).

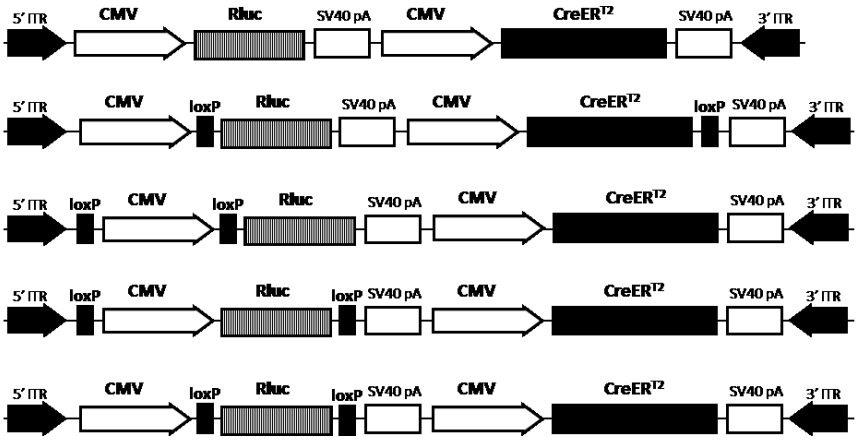

Figure 19: Scheme of AAV vector genomes generated for the fourth part of experiments
Promoters, transgenes and loxP sequences (in parallel orientation) were cloned into a single-stranded AAV background (pSSV9). The vector without loxP sites served as a control.

3.4.2. In vitro analysis of the AAV vectors containing the shut-off system

All AAV vectors generated (figure 19) were packaged into AAV serotype 2 for *in vitro* analysis. Therefore, HEK293T cells were transduced by these vectors and *Renilla* luciferase assays were performed at different time points after induction with 4-OHT. An exemplary experiment is shown in figure 20 which displays the luciferase expression 72 h after induction. In general, the treatment of cells with the control vector (without loxP sites) resulted in a higher luciferase expression than seen in cells which received any *floxed* AAV

vector. If the control vector-treated cells were induced with 4-OHT the luciferase level increased significantly. Except for the AAV vector with *floxed* Rluc-…CreER^{T2}, the administration of 4-OHT led to a significant reduction in Rluc expression in the *floxed* AAV vectors.

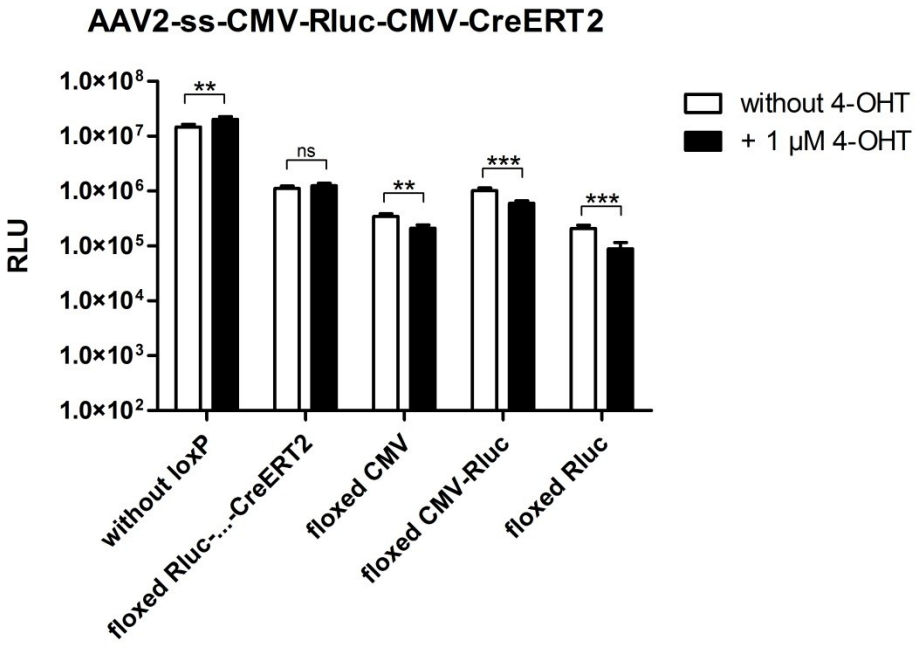

Figure 20: Generic *Renilla* luciferase assay for testing the shut-off system for AAV vectors *in vitro*

HEK293T cells were transduced with AAV vectors without and with loxP sequences at different positions (10^5 vg/cell). Induction with 4-OHT (black bars) was performed 2 days after transduction. The luciferase assay was carried out 3 days after initial induction. Mean values of relative light units (RLU) with 4 replicates per group are shown. The standard deviation is indicated with error bars. Statistical analysis was made with Student's t-test (**p<0.01; ***p<0.001; ns = not significant).

The results from three independent experiments are shown in figure 20, by calculating the extent of reduction (in fold changes) between vehicle- and tamoxifen-treated cells (figure 21). The only AAV vector which was significantly more down-regulated than all other vectors at all time points was the one containing the *floxed* Rluc (3- to 4-fold reduction). Compared to the control vector without loxP sites, the fold change of the vector with floxed Rluc-…-CreER^{T2} was not significantly reduced after tamoxifen administration at any time point analyzed.

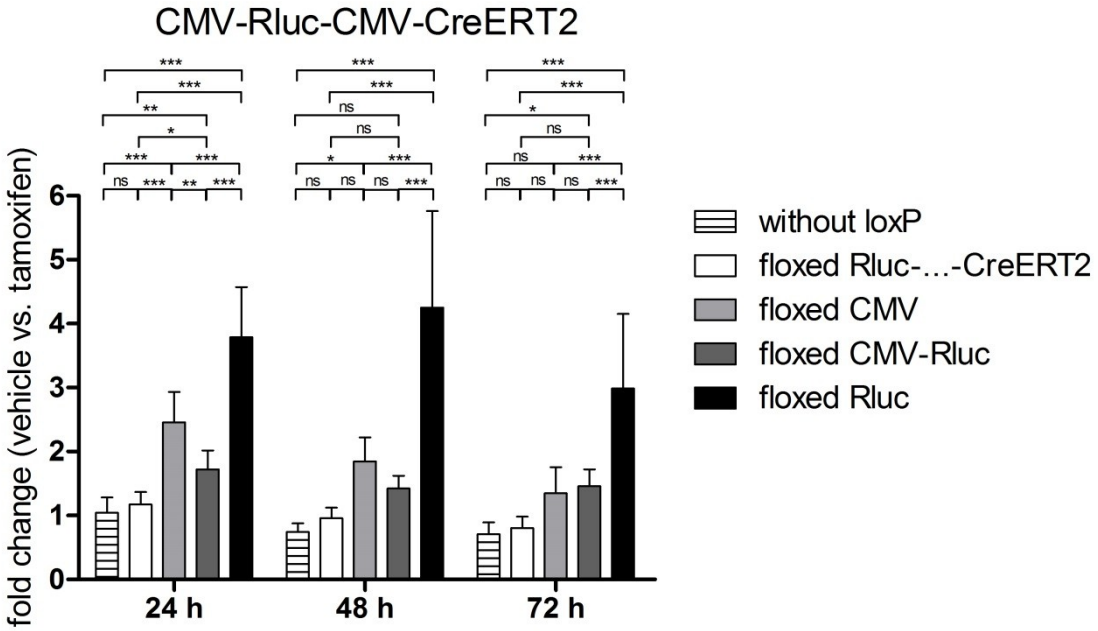

Figure 21: Analysis of fold changes between relative light units of vehicle and 4-OHT treated cells transduced with *floxed* AAV2-ss-CMV-Rluc-CMV-CreERT2 vectors

The summary of 3 independent experiments which were performed as seen in figure 20 is shown. Fold changes between RLUs of vehicle and tamoxifen treated cells at different time points after initial induction were calculated. The standard deviation is indicated with error bars. Statistical analysis was made with One-way ANOVA and Tukey post-test (*p<0.05; **p<0.01; ***p<0.001; ns = not significant).

To visualize the activity of the inducible CreER^{T2}, X-gal stainings were performed after transduction with the respective AAV vectors and induction with 4-OHT of CV-1 5B cells (figure 22). If the CreER^{T2} was active and recombination was successful, the cells are stained blue. As expected, the CreER^{T2} could be induced from any of the AAV vectors used.

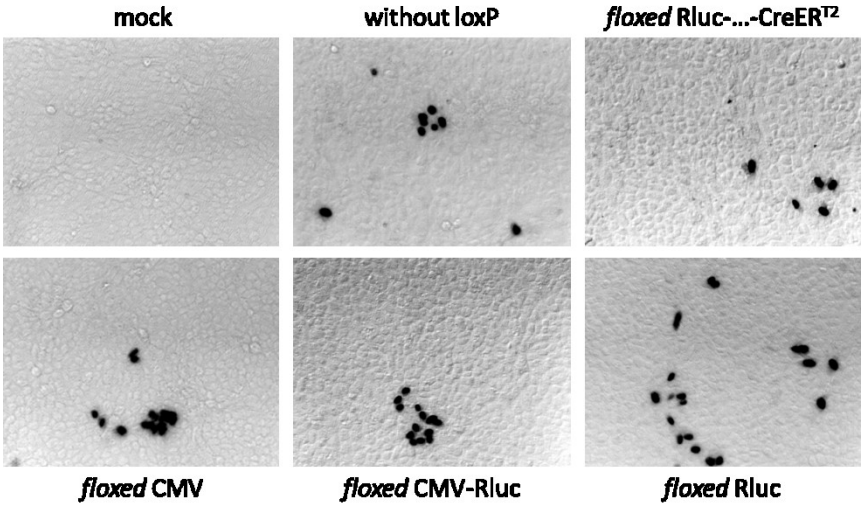

Figure 22: X-Gal staining of CV-1 5B cells transduced with *floxed* AAV2-ss-CMV-Rluc-CMV-CreERT2

Cells were transduced with 10^5 vg/cell. Induction with 1 µM 4-OHT was performed 2 days after transduction. Cells were stained for β-galactosidase expression 72 hours after induction. Images were taken with 10-fold magnification.

Another analysis for recombination events was the amplification of DNA fragments which were excised from the vector. This was done on the level of genomic DNA by the so-called "mini circle" PCR (see method's part). In case of mock-transduced cells, there were no distinct bands detectable (figure 23, A). If the cells were transduced by a *non-floxed* AAV vector only unspecific band were amplified (figure 23, B). A PCR fragment with a size of about 3500 bp but also unspecific bands could be detected in case of the *floxed* Rluc-…-CreER^{T2} vector (figure 23, C). Cells treated with the *floxed* CMV-Rluc vector showed a clear band at 1200 bp (figure 23, D) whereas the excised DNA fragment of the *floxed* Rluc vector displayed a band with 600 bp in size (figure 23, E). Besides some unspecific bands, the vector with the *floxed* CMV promoter revealed a DNA fragment of 650 bp (figure 23, F).

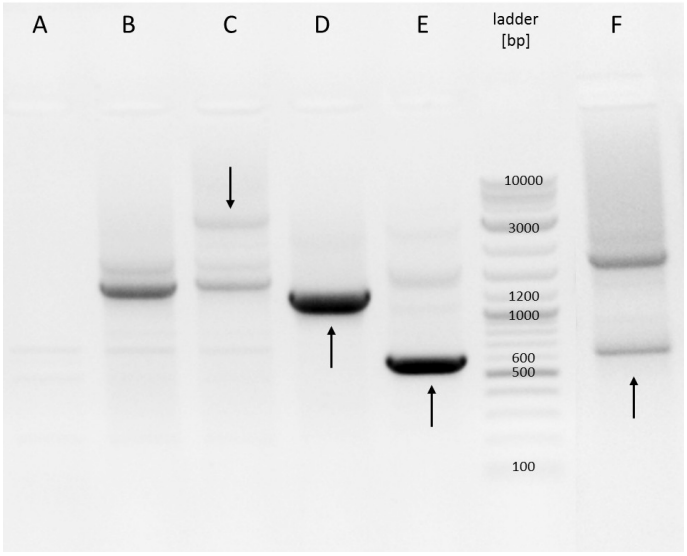

Figure 23: "Mini circle" PCR for detection of excised DNA fragments after recombination
Cells were transduced with 10^5 vg/cell and induced with 1 µM 4-OHT 2 days after transduction. Harvesting and genomic DNA isolation was performed 24 hours after induction. DNA fragments generated by "mini circle" PCR. A) mock-transduced cells are shown. B) AAV vector without loxP sites. C) *floxed* Rluc-…-CreER^{T2} vector. D) *floxed* CMV-Rluc vector. E) *floxed* Rluc vector. F) *floxed* CMV vector. Bands of excised DNA fragments are indicated with arrows.

3.4.3. Analysis of the AAV vectors containing the shut-off system in vivo

To analyze the expression of the inducible CreER^{T2} *in vivo*, the control vector without loxP sites was injected into 8-weeks old male Tomato mice. Mice were treated with vehicle solution or tamoxifen 4 weeks after AAV administration. Successful recombination events by the tamoxifen-induced CreER^{T2} were visualized by the conversion of red to green fluorescence signals (figure 24). In vehicle-treated animals, only few eGFP-positive cells were detectable. Cryo-sections from mice receiving tamoxifen showed a conversion of red to green fluorescence in nearly half of the cells. Compared to the AAV9-ss-CMV-CreER^{T2} vector (part 1), the transition from red to green fluorescence took part to a lower extend if the AAV9-ss-CMV-Rluc-CMV-CreER^{T2} vector was applied.

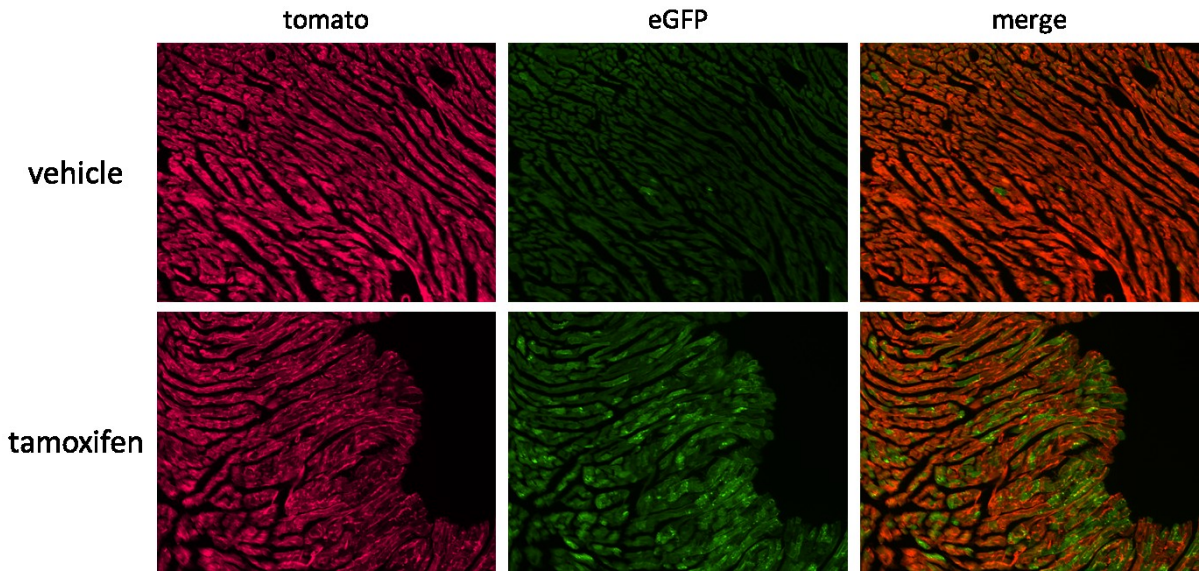

Figure 24: Cryo-sections of heart samples from Tomato mice treated with AAV9-ss-CMV-Rluc-CMV-CreERT2

Mice were treated with 10^{12} vg/mouse by tail vein injection. Induction with vehicle/tamoxifen took place 4 weeks after AAV administration (1 mg/mouse/day, 5 consecutive days). The animals were sacrificed 1 week after the last vehicle/tamoxifen administration. Images of cross-sections of hearts of Tomato mice taken in red fluorescent channel (for Tomato dye) and green fluorescent channel (for eGFP dye) are shown. The third column shows the images of merged channels. Images were taken with 10-fold magnification.

Renilla Luciferase expression from the control as well as *floxed* AAV vectors was analyzed in homogenized organ samples from C57Bl/6 mice treated with vehicle or tamoxifen. In heart samples, there was no difference in luciferase expression in mice treated with the control vector, independently of the treatment (vehicle/tamoxifen). If tamoxifen was applied, the luciferase levels in heart samples from the *floxed* CMV-Rluc vector could be reduced significantly. The same was observed for the AAV vector containing the *floxed Renilla* luciferase. In general, heart samples from animals treated with the control vector yielded higher luciferase expression levels than the *floxed* AAV vector. The vector containing the *floxed Renilla* luciferase showed the lowest luciferase expression.

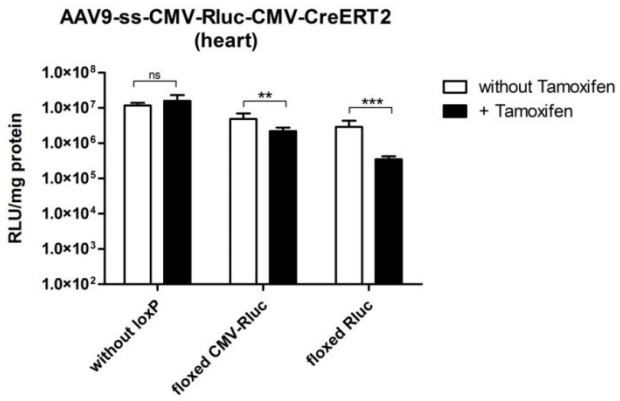

Figure 25: *Renilla* luciferase assay from homogenized heart samples of mice treated with AAV9 vectors containing the shut-off system

The rate of relative light units (RLU) to protein amount (in mg) was measured. White bars show animals treated with vehicle solution, black bars are tamoxifen-treated mice (4 animals per group). The standard deviation is indicated with error bars. Statistical analysis was made with Student's t-test (**p<0.01; ***p<0.001; ns = not significant).

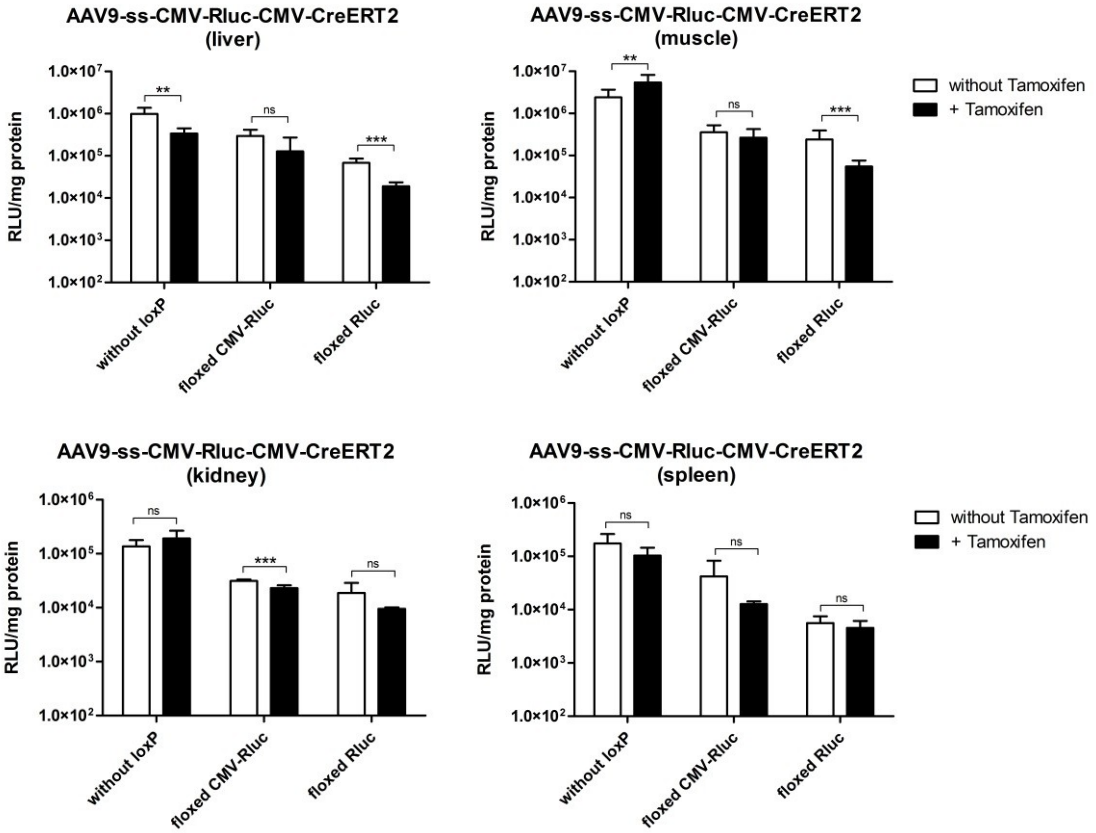

Figure 26: *Renilla* luciferase assay from homogenized organ samples of mice treated with AAV9 vectors containing the shut-off system

The rate of relative light units (RLU) to protein amount (in mg) was measured. White bars show animals treated with vehicle solution, black bars are tamoxifen-treated mice (4 animals per group). The standard deviation is indicated with error bars. Statistical analysis was made with Student's t-test (**p<0.01; ***p<0.001; ns = not significant).

In other organs than heart, luciferase expression was also higher in mice treated with the control vector compared to the *floxed* AAV vectors. In case of the control vector, luciferase activities in the liver were surprisingly decreased significantly after tamoxifen administration but not in the other organs (muscle, kidney, spleen). Regarding the *floxed* CMV-Rluc vector, a significant down-regulation of luciferase expression in tamoxifen-treated mice was only detectable in the kidney although there was a tendency towards reduction of expression levels in other organs. The decrease of *Renilla* expression in samples receiving the *floxed* Rluc vector and tamoxifen was significant in liver and muscle samples but not in kidney and spleen.

3.4.4. Repeated tamoxifen dosing to enhance efficacy of the shut-off system

To enhance the down-regulation in luciferase expression, a repeated tamoxifen administration was tested. Therefore, three groups of 8-weeks old male mice (C57Bl/6) were treated with AAV9-ss-CMV-lox-Rluc-lox-CMV-CreER^{T2}. After 4 weeks, vehicle solution was applied to the first group whereas the other groups received tamoxifen. One of the tamoxifen-treated groups got another tamoxifen treatment two weeks after the first treatment whereas the other groups received vehicle solution.

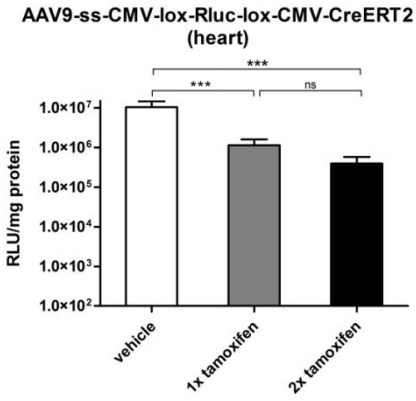

Figure 27: Effects of repeated tamoxifen dosing in heart samples from mice treated with AAV9 vectors containing a *floxed* Rluc reporter gene

Renilla luciferase assay was performed from homogenized heart samples. The rate of relative light units (RLU) to protein amount (in mg) was measured. White bars represent animals treated with vehicle solution, black bars indicate tamoxifen-treated mice (4 animals per group). The standard deviation is displayed with error bars. Statistical analysis was made with One-way ANOVA and Tukey post-test (***p<0.001; ns = not significant).

Again, luciferase expression was determined in homogenized organs. In heart samples, the expression could be significantly reduced after the first tamoxifen administration. If a second tamoxifen dosing was applied the luciferase expression could be further decreased which was not statistically significant. In the other organs analyzed, the repeated tamoxifen administration also did not yield in a further significant reduction of luciferase expression.

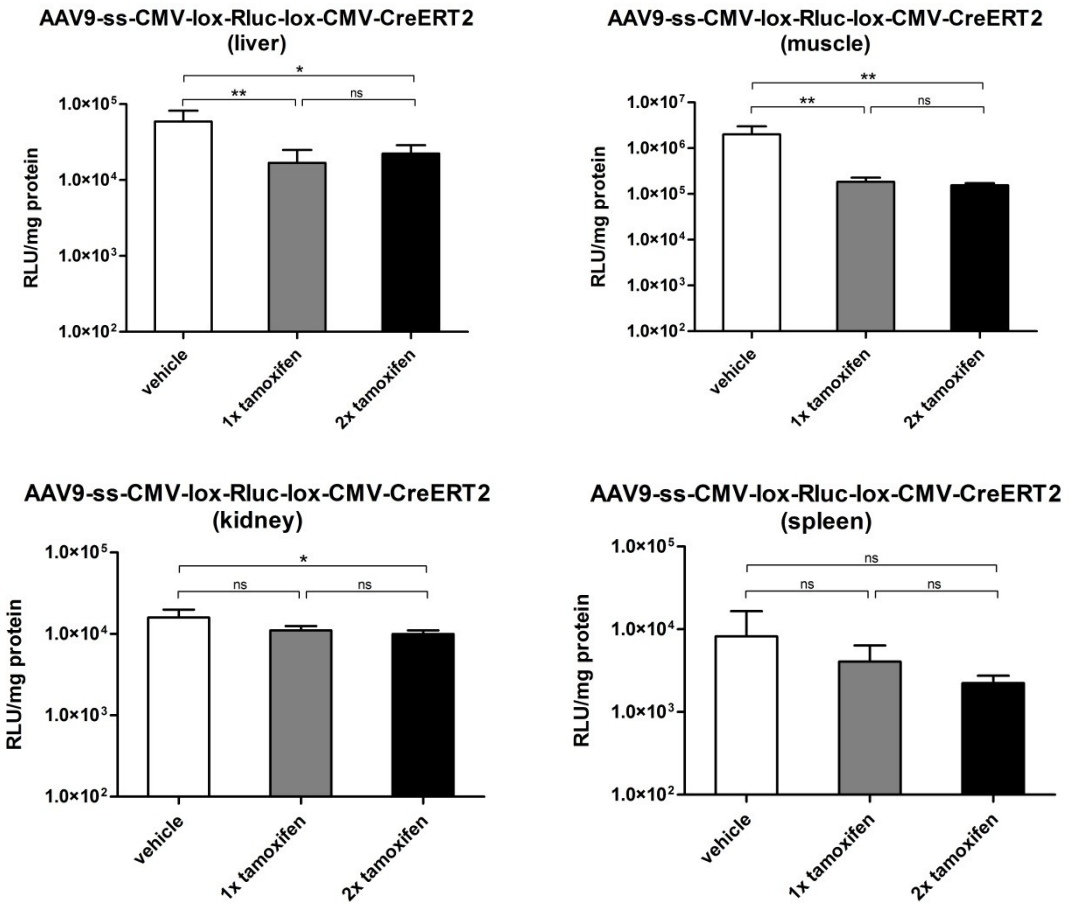

Figure 28: Effects of repeated tamoxifen dosing in organ samples from mice treated with AAV9 vectors containing a *floxed* Rluc reporter gene

Renilla luciferase assay was performed from homogenized organ samples. The rate of relative light units (RLU) to protein amount (in mg) was measured. White bars indicate animals treated with vehicle solution, grey and black bars represent tamoxifen-treated mice (4 animals per group). The standard deviation is shown with error bars. Statistical analysis was made with One-way ANOVA and Tukey post-test (*$p<0.05$; **$p<0.01$; ns = not significant).

To determine the extent of down-regulation after tamoxifen administration, the ratio between vehicle- and tamoxifen-treated animals was calculated (figure 29). Compared to the control vector without loxP sites, the *floxed* CMV-Rluc AAV vector did not show a significantly higher extent of down-regulation if tamoxifen was applied. However, the *floxed* Rluc vector yielded in a significantly reduction in luciferase activity compared to both the control vector and the *floxed* CMV-Rluc vector. To put these findings into numbers, the control vector achieved a fold change of about 0.85 whereas the *floxed* CMV-Rluc vector was down-regulated about 2.5-fold. The AAV containing the *floxed* Rluc showed a reduction of luciferase activities of about 9.1-fold if a single tamoxifen dosing was administered. If a second tamoxifen dosing was applied a significantly higher decrease of Rluc was detectable, achieving a fold change of about 26-fold.

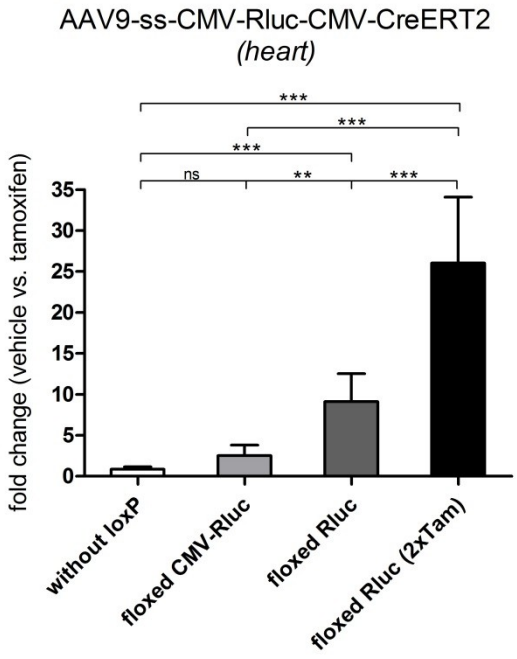

Figure 29: Extent of *Renilla* luciferase down-regulation after tamoxifen administration in heart samples from mice treated with AAV9 vectors containing a *floxed* Rluc reporter gene
The fold changes between RLU/mg protein of vehicle- and tamoxifen-treated animals receiving different AAV9 vectors and/or repeated tamoxifen dosing are shown. The standard deviation is indicated with error bars. Statistical analysis was made with One-way ANOVA and Tukey post-test (**p<0.01; ***p<0.001; ns = not significant).

3.5. Part 5 – Efficacy of the shut-off system in a vector potentially causing side effects

3.5.1. Generation of a floxed AAV vector coding for murine interleukin-10

To evaluate the efficacy of the shut-off system with a therapeutic gene, the reporter gene (*Renilla* luciferase, part 4) was substituted by the murine interleukin-10 cDNA (mIL-10). The whole expression cassette was cloned into the single-stranded AAV2 genome plasmid (pSSV9).

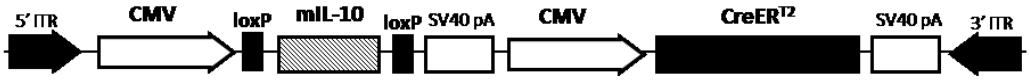

Figure 30: Scheme of AAV vector genome coding for the murine interleukin 10 gene
Promoters, transgenes and loxP sequences (in parallel orientation) were cloned into a single-stranded AAV background (pSSV9).

3.5.2. Shut-off of a side effect-causing AAV vector in vivo

The AAV vector containing the *floxed* mIL-10 gene was injected into 8-weeks old male C57Bl/6 mice. Therefore, one group received a low vector dose of $1 \cdot 10^{11}$ vg/mouse whereas the animals in the high dose group received $1 \cdot 10^{12}$ vg/mouse. Mice which did not receive any vector served as the control. The body weight was monitored 3 times per week.

After 5 weeks (day 37), some of the animals were dissected to evaluate the expression levels of the vector. To that date, the body weights of the different groups were quite similar with the high dose group showing the lowest body weight.

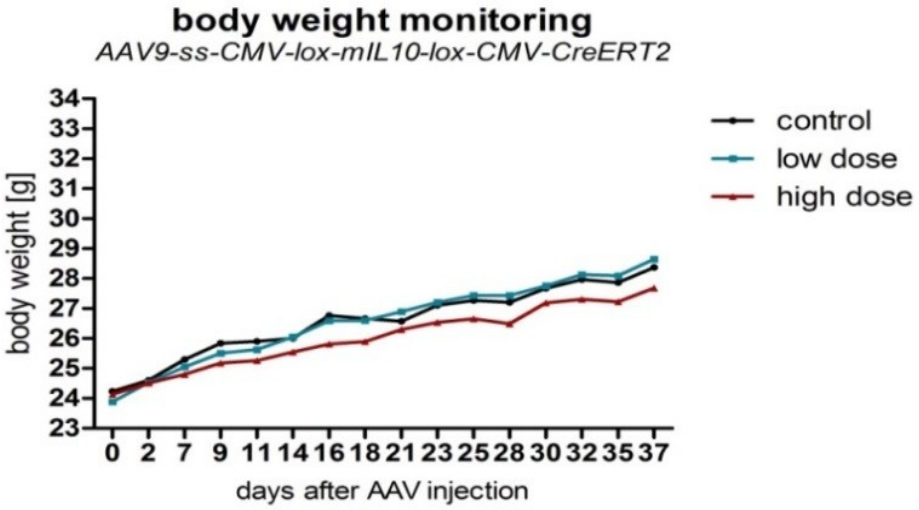

Figure 31: Body weight monitoring from day 0 to 37 of mice injected with *floxed* mIL-10-containing AAV vector

On day 0, the mice were injected with the AAV vector in different dosages. Body weight was noted 3 times per week. The control group (n=6) which did not receive any AAV vector is depicted with a black line, the low dose group (n=9) in blue and the high dose group (n=9) in red.

Out of each group, 3 mice were dissected and the body weight, the heart weight, the spleen weight and the tibia length were measured. The following ratios were calculated and analyzed (figure 32): heart weight vs body weight, heart weight vs tibia length, spleen weight vs body weight, and spleen weight vs tibia length. There were no significant differences between the groups detectable.

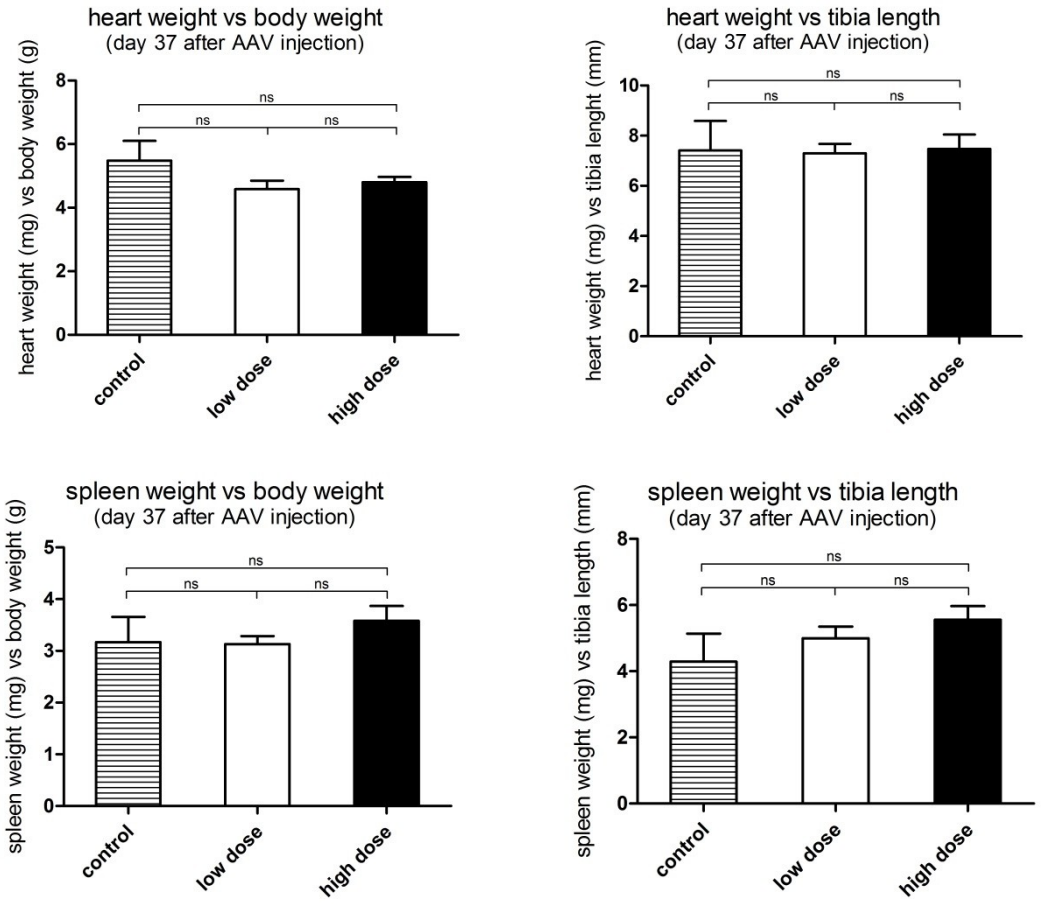

Figure 32: Morphometrical data of mice dissected on day 37 after *floxed* AAV-mIL-10 injection

The ratios between heart weight/body weight, heart weight/tibia length, spleen weight/body weight, and spleen weight/tibia length are shown. The standard deviation (n=3 per group) is indicated with error bars. Statistical analysis was made with One-way ANOVA and Tukey post-test (ns = not significant).

Furthermore, the expression of mIL-10 was analyzed in the heart and in the liver by qRT-PCR (figure 33). In the heart, there was no significant difference between the mIL-10 expression levels of the groups but there was a slightly higher expression seen in the high dose group. This higher expression of mIL-10 in animals treated with the high dose AAV vector was also seen in the liver. Here, a 77-fold overexpression of mIL-10 could be detected in the high dose group whereas the low dose group showed a 15-fold overexpression.

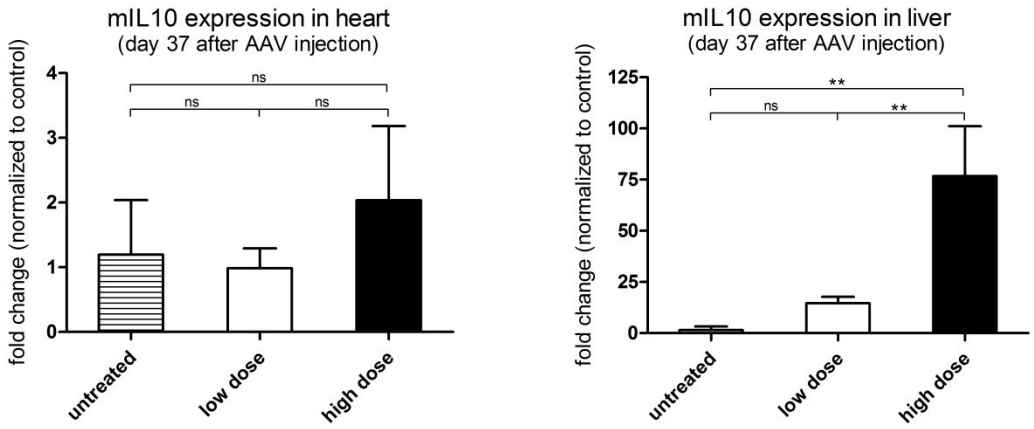

Figure 33: Expression levels of mIL-10 in heart and liver samples 37 days after AAV injection analyzed by qRT-PCR

Expression levels are shown as fold changes normalized to the untreated control group. The standard deviation (n=3 per group) is indicated with error bars. Statistical analysis was made with One-way ANOVA and Tukey post-test (**p<0.01; ns = not significant).

Also, an ELISA detecting mIL-10 in the plasma was performed (figure 34). Here, only the high dose group showed significant higher mIL-10 levels in the plasma compared to the control and the low dose groups. In the untreated control and the low dose groups, almost no mIL-10 could be detected (about 1 pg/ml) whereas the high dose group showed mIL-10 levels of about 8.5 pg/ml.

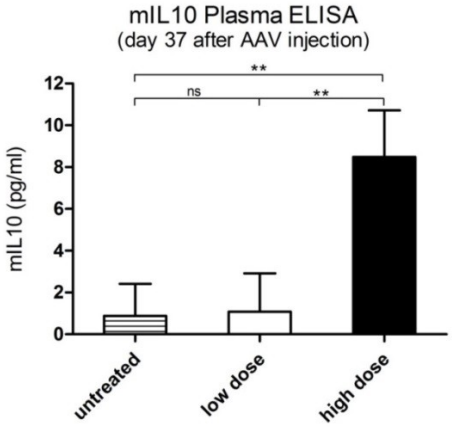

Figure 34: mIL-10 levels in the plasma 37 days after AAV injection analyzed by ELISA

The mIL-10 levels detected in plasma samples are shown in pg/ml. The standard deviation (n=3 per group) is indicated with error bars. Statistical analysis was made with One-way ANOVA and Tukey post-test (**p<0.01; ns = not significant).

Until day 91 after AAV injection, the body weight of the remaining animals was monitored 3 times per weeks (figure 35). It could be detected that the animals receiving the highest vector dose showed the lowest body weight at day 91 whereas the untreated control group gained the most body weight. Therefore, it was decided to apply vehicle or tamoxifen to the AAV-treated animals after day 91 for 5 consecutive days.

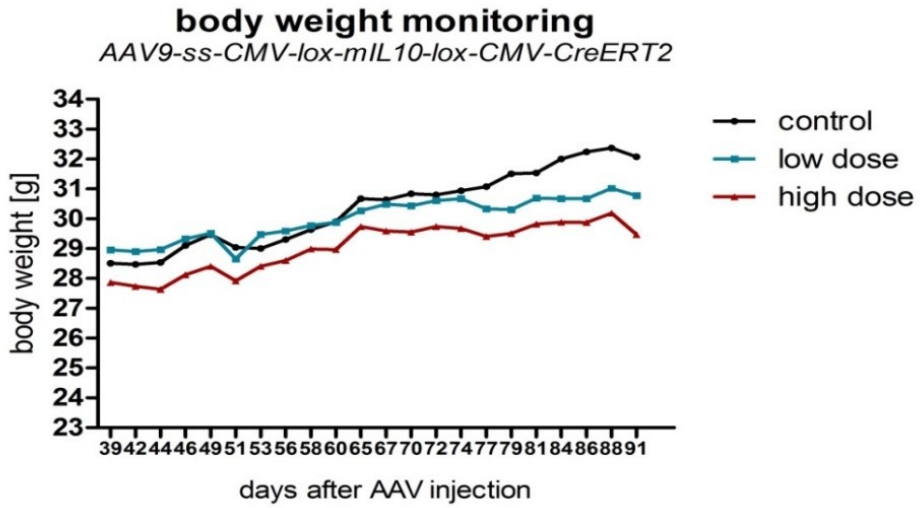

Figure 35: Body weight monitoring from day 39 to 91 of mice injected with *floxed* mIL-10-containing AAV vector
Body weight was measured 3 times per week. The control group (n=3) which did not receive any AAV vector is depicted with a black line, the low dose group (n=6) in blue and the high dose group (n=6) in red.

The administration of vehicle or tamoxifen was started on day 92 after AAV injection. Already on day 93, the groups receiving tamoxifen showed a gain in body weight. Except for the high dose group receiving vehicle solution, all groups displayed a similar body weight at the end of the experiment on day 102 (figure 36).

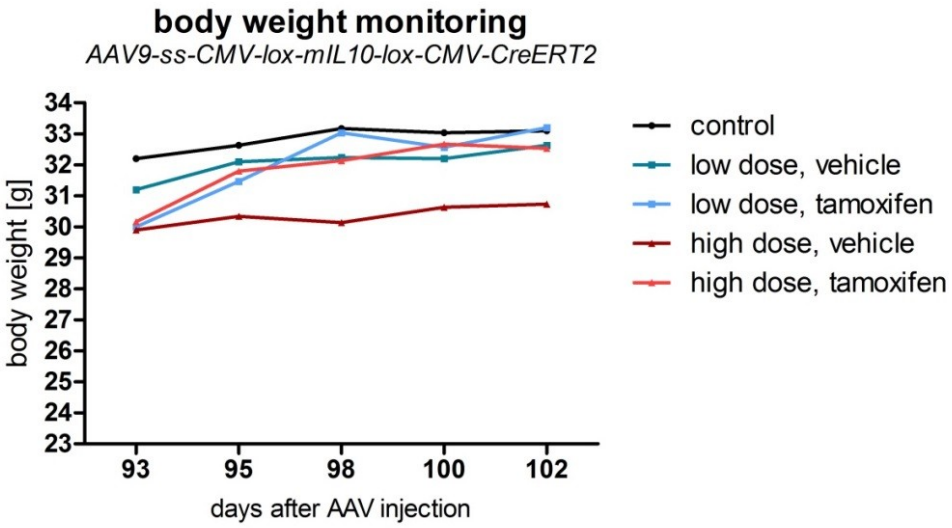

Figure 36: Body weight monitoring from day 93 to 102 of mice injected with *floxed* mIL-10-containing AAV vector

Body weight was measured 3 times per week. The control group (n=3) which did not receive any AAV vector is depicted with a black line. The low dose group treated with vehicle solution (n=3) is indicated with a dark blue line, the tamoxifen-treated low dose group (n=3) in light blue. The vehicle-treated high dose group (n=3) is displayed in dark red whereas the tamoxifen-treated high dose group (n=3) in indicated with a light red line.

After dissection of the animals, body weight, heart weight, spleen weight and tibia length were analyzed. The same ratios as seen in figure 37 were calculated. In case of heart weight/body weight and heart weight/tibia length, there were no significant differences detectable. Animals treated with tamoxifen showed a significant increase in spleen weight compared to the vehicle-treated mice.

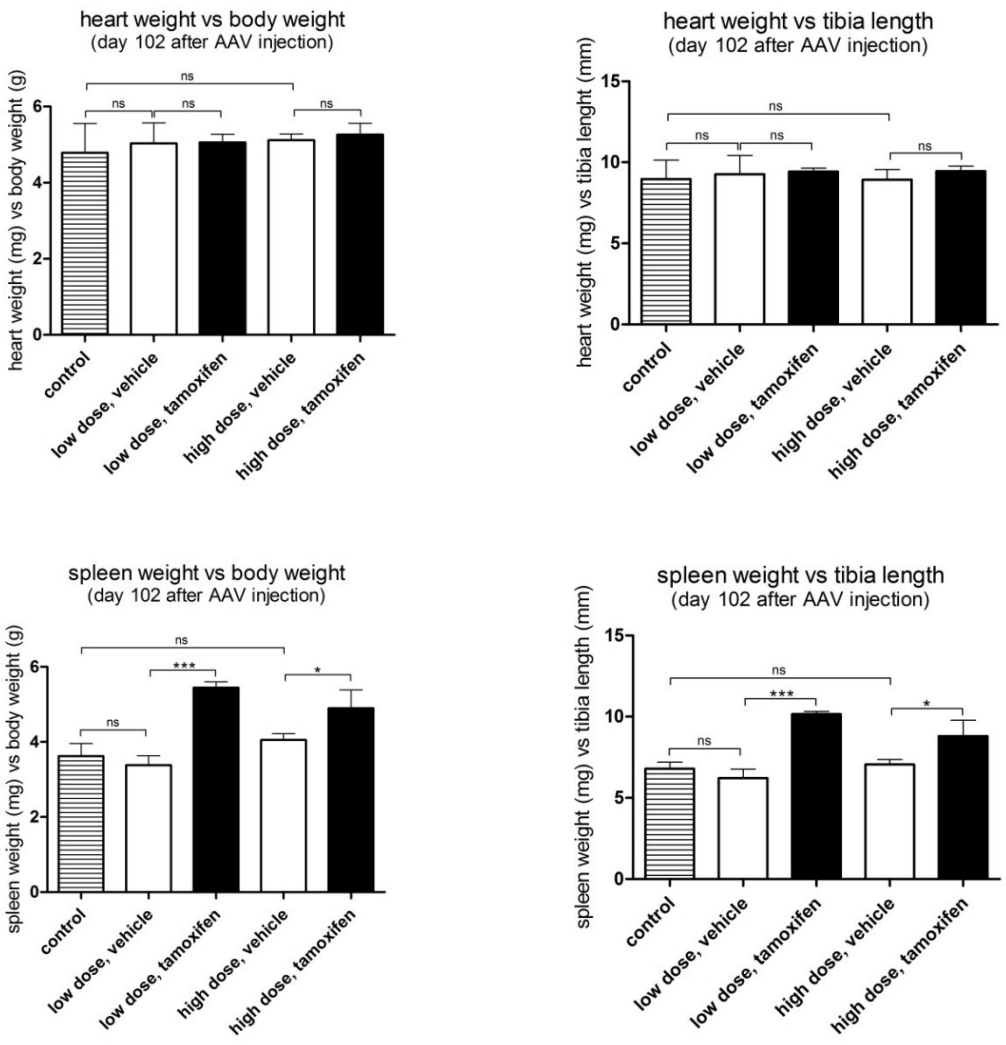

Figure 37: Morphometrical data of mice dissected on day 102 after *floxed* AAV-mIL-10 injection

The ratios between heart weight/body weight, heart weight/tibia length, spleen weight/body weight, and spleen weight/tibia length are shown. The standard deviation (n=3 per group) is indicated with error bars. Statistical analysis was made with One-way ANOVA and Tukey post-test (*p<0.05; ***p<0.001; ns = not significant).

Again, the expression of mIL-10 was analyzed in heart and liver samples by qRT-PCR (figure 38). As seen on day 37 after AAV injection, the mIL-10 expression in the heart did not yield significant differences between the groups. If tamoxifen was applied, there was a slight decrease in mIL-10 levels which also was not significant. In the liver, there were no significant differences in mIL-10 expression levels between the control group and the low dose groups detectable. The high dose group treated with vehicle solution showed a 15-fold overexpression of mIL-10 whereas this overexpression was reduced to about 4-fold upon tamoxifen administration.

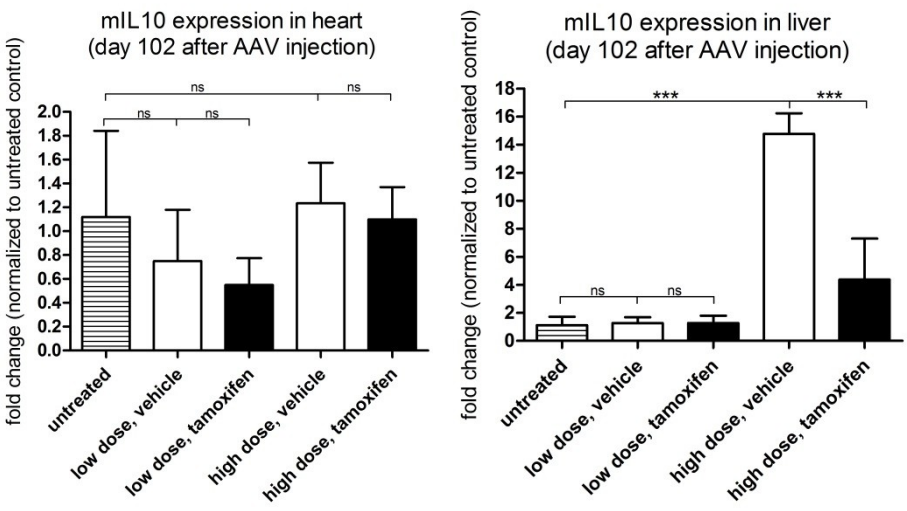

Figure 38: Expression levels of mIL-10 in heart and liver samples 102 days after AAV injection analyzed by qRT-PCR

The expression levels are shown as fold changes normalized to the untreated control group. The standard deviation (n=3 per group) is indicated with error bars. Statistical analysis was made with One-way ANOVA and Tukey post-test (***p<0.001; ns = not significant).

Furthermore, an ELISA measuring mIL-10 in plasma samples was performed as displayed in figure 39. Here, the animals treated with tamoxifen surprisingly showed significant higher mIL-10 levels compared to the untreated control and vehicle-treated animals. In case of the control group, a mIL-10 plasma level of about 9 pg/ml could be detected. This was comparable to the vehicle-treated animals. Animals from the low dose group treated with tamoxifen had mIL-10 plasma levels of about 18 pg/ml whereas the high dose group reached levels of about 21 pg/ml.

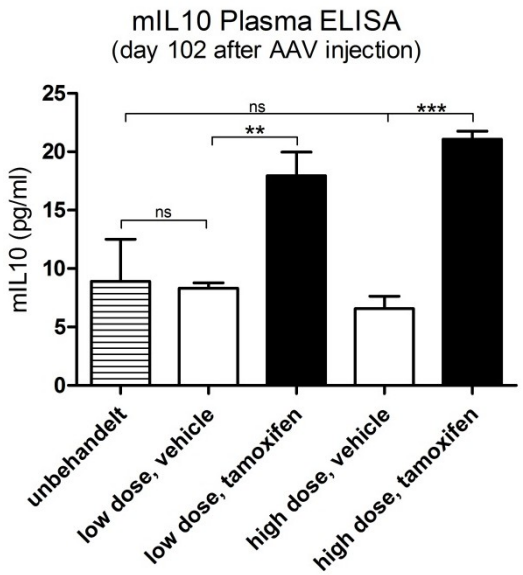

Figure 39: mIL-10 levels in the plasma 102 days after AAV injection analyzed by ELISA

The mIL-10 levels detected in plasma samples are shown in pg/ml. The standard deviation (n=3 per group) is indicated with error bars. Statistical analysis was made with One-way ANOVA and Tukey post-test (**p<0.01; ***p<0.001 ns = not significant).

3.6. Part 6 – Increase in coding capacity of vectors containing the shut-off system

3.6.1. Generation of AAV vectors with increased coding capacity

As the last step, the shut-off system encoded by a single AAV vector should be improved by increasing the coding capacity available. Therefore, the polyA signal (for Rluc) and the second CMV promoter (for CreER^{T2}) of the vectors from part 4 were replaced by the P2A element from Porcine Teschovirus-1. The whole expression cassette (Rluc-P2A-CreER^{T2}) is transcribed as a single mRNA. The small P2A peptide (22 amino acids) is so-called "self-cleaving" which means that the formation of a peptide bond between two distinct amino acids during translation is prevented. The missing bond results in ribosome skipping so that the subsequent protein (CreER^{T2}) gets translated.

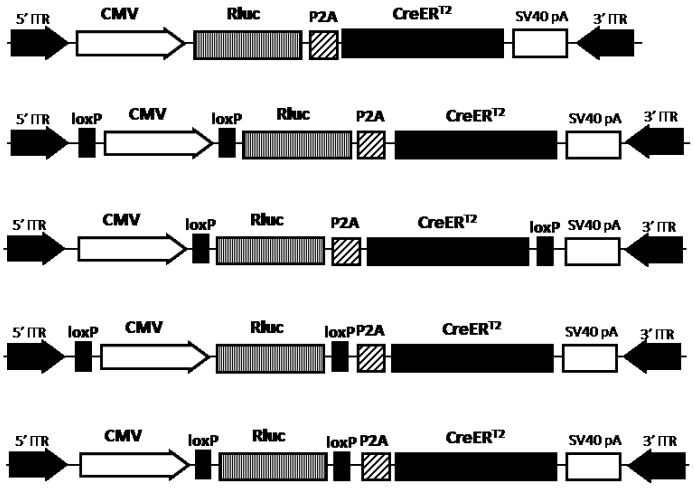

Figure 40: Scheme of AAV vector genomes generated with increased coding capacity
Promoters, transgenes and loxP sequences (in parallel orientation) were cloned into a single-stranded AAV background (pSSV9). The vector without loxP sites served as a control.

3.6.2. In vitro analysis of vectors containing the P2A element

The "self-cleaving" activity of the P2A peptide was first validated by Western blot analysis. Therefore, HEK293T cells were transduced by the control AAV2 vector (without loxP sites) or the vector containing the *floxed* Renilla luciferase gene. Cells not transduced with any vector served as controls. Cells were harvested 72 h after induction with 4-OHT and cell lysates were used for Western blot analysis.

To analyze the cleavage efficacy of the P2A peptide, antibodies against the *Renilla* luciferase and the CreER^{T2} were used simultaneously. The luciferase thereby appeared at a molecular weight of about 36 kDa whereas the CreER^{T2} showed a band at about 74 kDa. If the cleavage of P2A during translation was not complete a protein band at about 110 kDa should be detectable. In case of non-transduced cell lysates, there were no bands at neither of these protein weights visible, independently of the treatment of cells (vehicle vs. 4-OHT). The control vector without loxP sites showed clear bands for the luciferase and the CreER^{T2} as well as a faint band at 110 kDa for the uncleaved polyprotein in both vehicle- and tamoxifen-treated cell lysates. In contrast, the *floxed* Rluc vector only generated a band at the molecular weight of the CreER^{T2} but not for the luciferase, again independently of the treatment. As an internal loading control, the anti-GAPDH antibody was used which appeared at a protein weight of about 37 kDa.

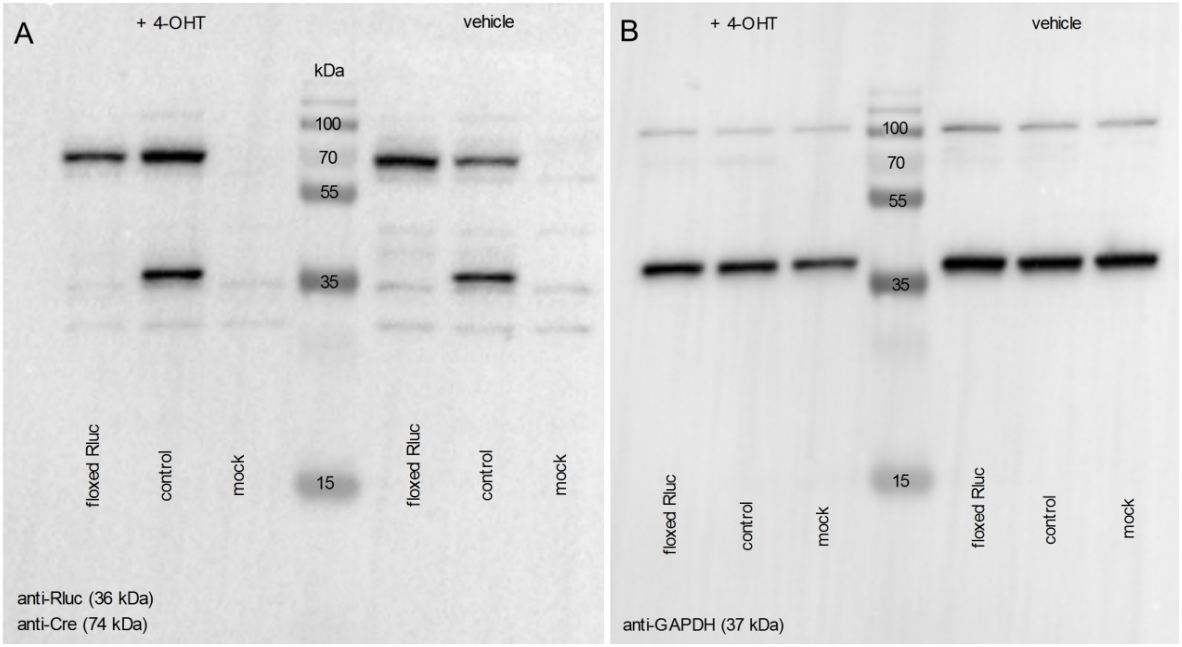

Figure 41: Western blot analysis of P2A-containing AAV2 vectors
HEK293T cells were transduced by AAV2-ss-CMV-Rluc-P2A-CreER^{T2} (control) or AAV2-ss-CMV-lox-Rluc-lox-P2A-CreER^{T2} (floxed Rluc) vectors. Non-transduced cells served as the "mock" control. Western Blot analysis was performed with cell lysates 72 h after induction with 4-OHT. The protein weight marker is indicated by protein weight in kDa. Anti-rabbit-HRP served as the secondary antibody for all primary antibodies used. Dilutions can be found in the material's part. **A)** Western blot membranes were incubated simultaneously with anti-Rluc and anti-Cre antibodies. **B)** Anti-GAPDH antibody was used as an internal control.

The next step was to show that the CreER^{T2} can still be activated by tamoxifen administration in the context of P2A-bearing AAV vectors. Therefore, X-Gal stainings with AAV transduced CV-1 NB cells were performed (figure 42). In cells which were not transduced by any AAV vector, no cells were stained positive for β-galactosidase. The same was true for cells transduced by the *floxed* Rluc-…-CreER^{T2} vector. Only single positive cells could be detected in cells treated with *floxed* CMV and *floxed* CMV-Rluc vectors. The control vector without loxP sites generated some cells which were stained blue but the most positive cells were achieved by applying the *floxed* Rluc vector onto the cells.

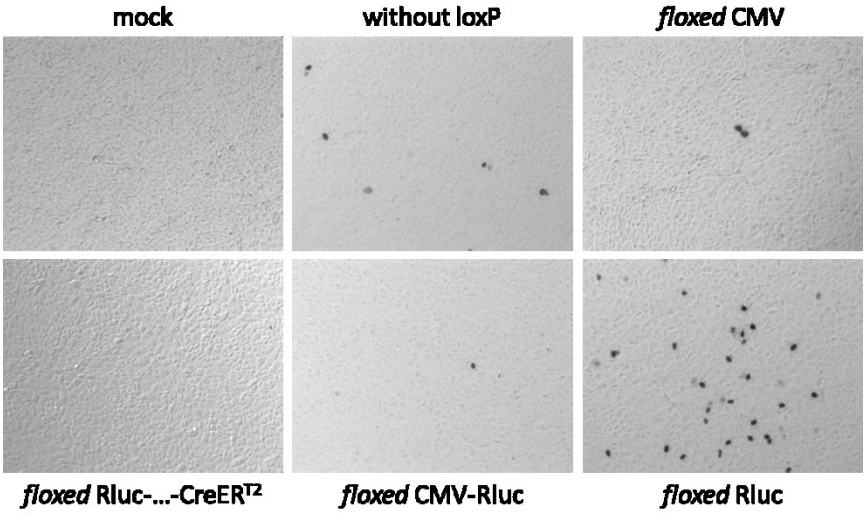

Figure 42: X-Gal staining of CV-1 NB cells transduced with *floxed* AAV2-ss-CMV-Rluc-P2A-CreERT2
Cells were transduced with 10^4 vg/cell. Induction with 1 µM 4-OHT was performed 2 days after transduction. Cells were stained for β-galactosidase expression 72 hours after induction. Images were taken with 10-fold magnification.

To evaluate the efficacy of the shut-off system in context of a P2A-bearing AAV vector, *Renilla* luciferase assays of cell lysates were performed. Therefore, AAV genomes were packaged into AAV capsids of serotype 2 to transduce HEK293T cells. Luciferase assays were carried out at different time points after induction with 4-OHT. A generic experiment is shown in figure 43 which was performed 72 h after induction. As seen with the shut-off systems consisting of two expression cassettes, the control vector without loxP sites yielded the highest luciferase expression of all AAV vectors tested. Also, a significant increase in Rluc expression could be detected by applying 4-OHT onto the cells transduced by the control

vector. In case of all *floxed* AAV vectors used, administration of 4-OHT always led to a significant decrease in luciferase expression.

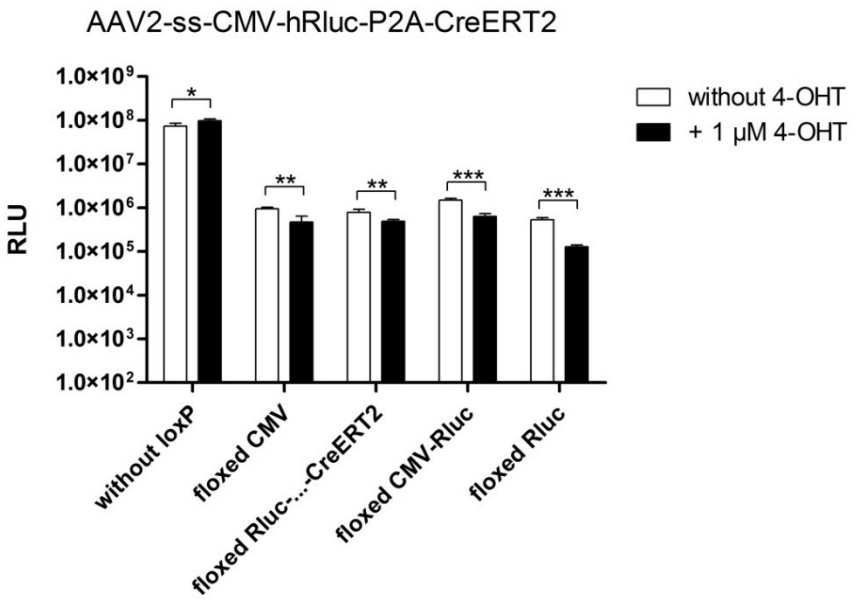

Figure 43: Generic *Renilla* luciferase assay for testing the P2A-bearing AAV vectors *in vitro*
HEK293T cells were transduced with AAV vectors without and with loxP sequences at different positions (10^4 vg/cell). Induction with 4-OHT (black bars) was performed 2 days after transduction. The luciferase assay was carried out 3 days after initial induction. Mean values of relative light units (RLU) with 4 replicates per group are shown. The standard deviation is indicated with error bars. Statistical analysis was made with Student's t-test (*p<0.05; **p<0.01; ***p<0.001).

Three independently performed experiments are summarized in figure 44 by calculating the fold changes between vehicle- and tamoxifen-treated HEK293T cells. Except for the time point 24 h after induction, luciferase expression of all *floxed* vectors used could be down-regulated significantly after administration of 4-OHT. The highest extend of reduction in *Renilla* luciferase expression was thereby achieved by the *floxed* Rluc vector at almost all time points (about 3-fold reduction).

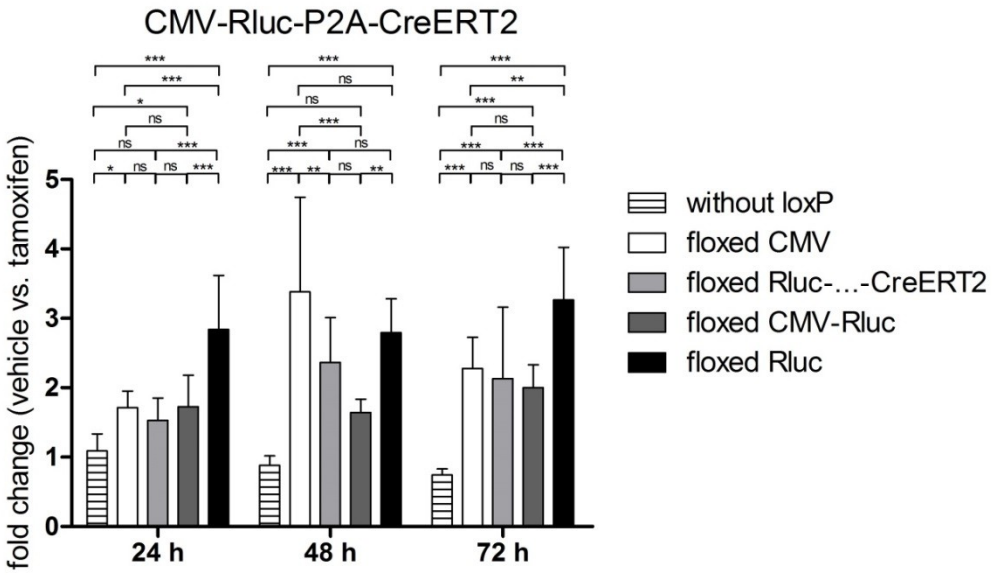

Figure 44: Analysis of fold changes between relative light units of vehicle and 4-OHT treated cells transduced with *floxed* AAV2-ss-CMV-Rluc-P2A-CreERT2 vectors
The summary of 3 independent experiments which were performed as displayed in figure 43 is shown. Fold changes between RLUs of vehicle and tamoxifen treated cells at different time points after initial induction were calculated. The standard deviation is indicated with error bars. Statistical analysis was made with One-way ANOVA and Tukey post-test (*p<0.05; **p<0.01; ***p<0.001; ns = not significant).

The time point of 72 h after induction with 4-OHT was also chosen for the quantification of mRNA levels. Cells were therefore transduced by *floxed* CMV-Rluc and *floxed* Rluc vectors and harvested 72 h after the first 4-OHT administration. Quantitative PCR was performed with specific primers for different parts of the AAV vectors (*Renilla* luciferase, $CreER^{T2}$) and cDNA made from isolated RNA.

Figure 45 shows the results achieved by qPCR where the fold change normalized to non-transduced cells was calculated. In case of the *floxed* CMV-Rluc vector, mRNA levels coding for the *Renilla* luciferase and the $CreER^{T2}$ were down-regulated if the cells were treated with 4-OHT. In cells transduced by the *floxed* Rluc vector, the mRNA levels encoding for the luciferase were reduced significantly whereas the $CreER^{T2}$-bearing mRNAs were increased after 4-OHT administration. In general, transduction by the *floxed* CMV-Rluc vector resulted in higher luciferase mRNA levels compared to cells transduced by the *floxed* Rluc vector.

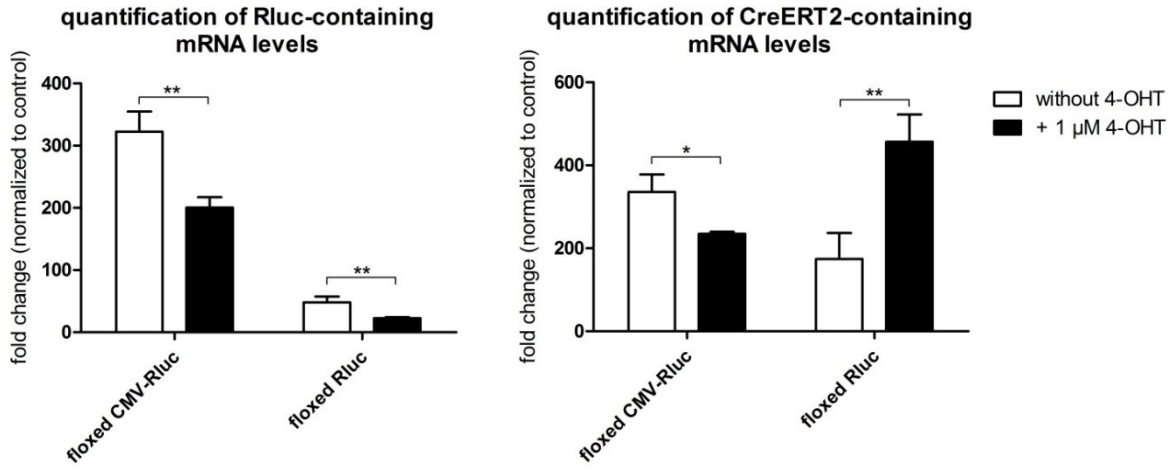

Figure 45: Analysis of mRNA levels in cells transduced with *floxed* AAV2-ss-CMV-Rluc-P2A-CreERT2 vectors

The fold changes of mRNA levels normalized to untreated cells are shown. Primer sets were used to detect mRNAs coding for *Renilla* luciferase or $CreER^{T2}$. Tamoxifen-treated cells are visualized by black bars. Fold changes to non-transduced cells were calculated by the $\Delta\Delta Cq$ method. The standard deviation is indicated with error bars. Statistical analysis was made with Student's t-test (*$p<0.05$; **$p<0.01$; ns=not significant).

3.6.3. Assessment of P2A-bearing AAV vectors in vivo

To assess the performance of the P2A-bearing vectors *in vivo*, 8 week old male C57Bl/6 mice were injected with either control, *floxed* CMV-Rluc, or *floxed* Rluc vectors. After 4 weeks, the first tamoxifen dosing was applied. The second tamoxifen administration round was done 2 weeks after the first application and mice were dissected one week after the last tamoxifen administration.

The *Renilla* luciferase expression from the control and *floxed* AAV vectors was analyzed in homogenized organ samples from C57Bl/6 mice treated with vehicle or tamoxifen. In the control animals, the first tamoxifen administration led to a significant reduction in luciferase levels. After the second tamoxifen dosing, the luciferase activity was significantly higher compared to one tamoxifen application round. In case of the *floxed* CMV-Rluc vector, only the second tamoxifen administration led to a significant decrease in luciferase expression. In contrast, the *floxed* Rluc vector showed a significant shut-off of Rluc levels after tamoxifen application which could not be enhanced by the second tamoxifen dosing.

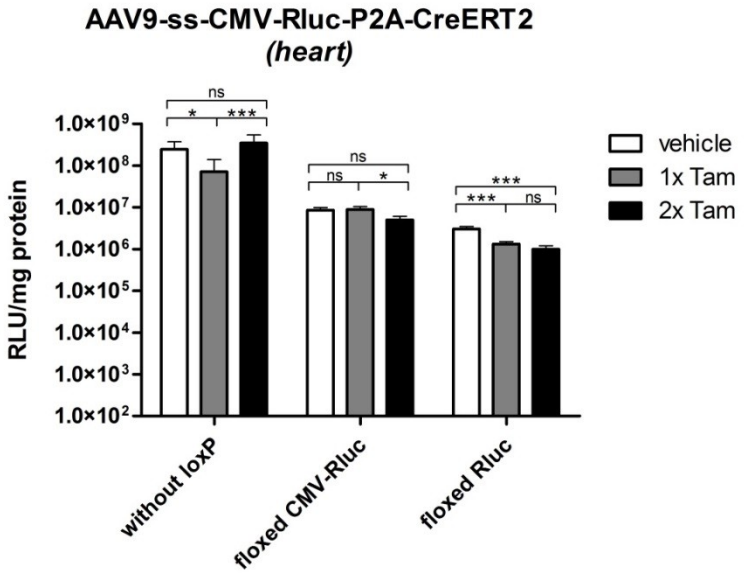

Figure 46: *Renilla* luciferase assay from homogenized heart samples of mice treated with AAV9 vectors containing the P2A element

The rate of relative light units (RLU) to protein amount (in mg) was measured. White bars indicate animals treated with vehicle solution, grey and black bars represent tamoxifen-treated mice (3 animals per group). The standard deviation is shown with error bars. Statistical analysis was made with One-way ANOVA and Tukey post-test (*p<0.05; ***p<0.001; ns = not significant).

In other organs than the heart, there were no significant differences in luciferase expression in the control group, independent on the treatment. The only exception was detectable in the spleen, were the first tamoxifen administration led to a significant reduction in Rluc activity. The *floxed* CMV-Rluc vector showed the same results as the control vector but the overall luciferase expression levels were lower. In case of the *floxed* Rluc vector, a significant decrease in luciferase expression could be shown in every organ but there was no further reduction if a second tamoxifen dosing was applied.

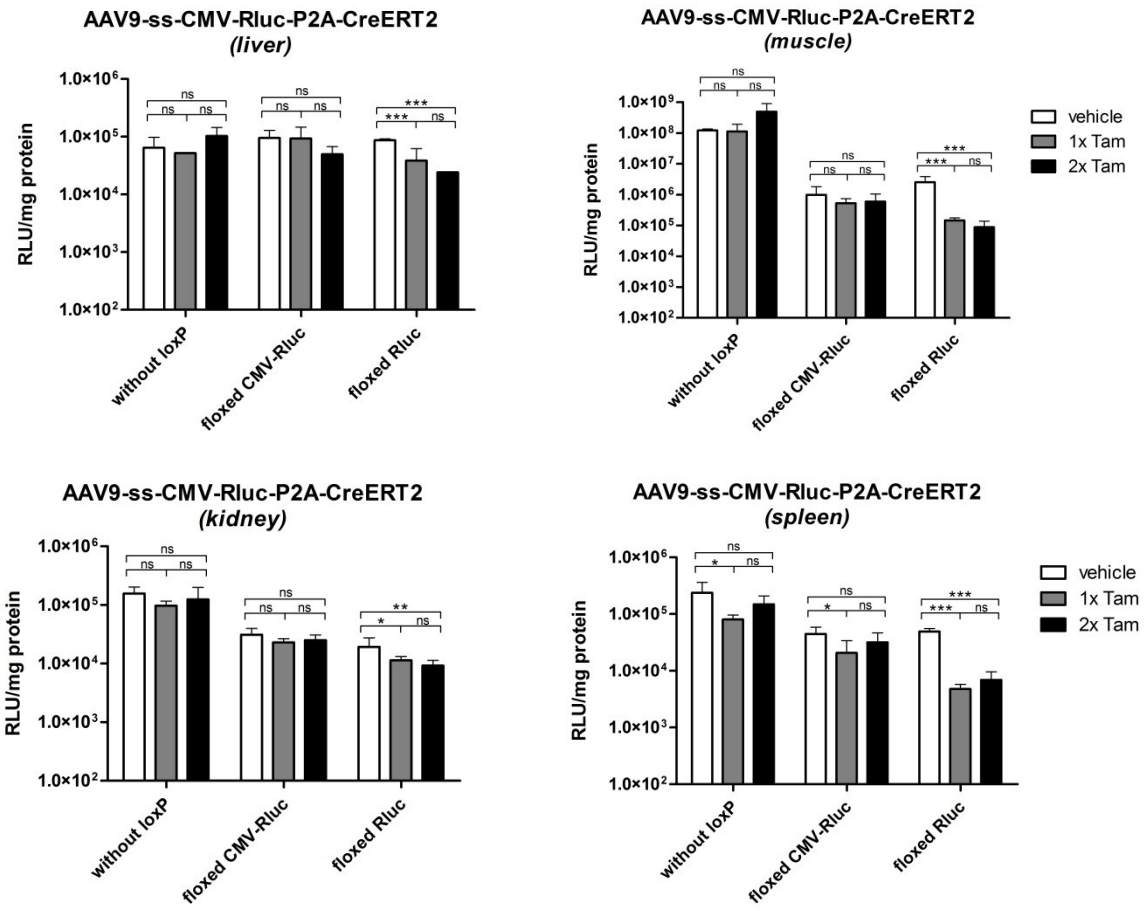

Figure 47: *Renilla* luciferase assay from homogenized organ samples of mice treated with AAV9 vectors containing the P2A element

The rate of relative light units (RLU) to protein amount (in mg) was measured. White bars indicate animals treated with vehicle solution, grey and black bars represent tamoxifen-treated mice (4 animals per group). The standard deviation is shown with error bars. Statistical analysis was made with One-way ANOVA and Tukey post-test (*p<0.05; **p<0.01; ***p<0.001; ns = not significant).

To determine the extent of down-regulation after tamoxifen administration, the ratio between vehicle- and tamoxifen-treated animals was calculated (figure 48). Compared to the control vector without loxP sites, the *floxed* CMV-Rluc AAV vector did not show a significantly higher extent of down-regulation if tamoxifen was applied. However, the *floxed* Rluc vector yielded in a significantly reduction in luciferase activity compared to both the control vector and the *floxed* CMV-Rluc vector. To put these findings into numbers, the control vector achieved a fold change of about 1.19 whereas the *floxed* CMV-Rluc vector was down-regulated about 1.13 to 1.70-fold (first and second tamoxifen administration). The AAV containing the *floxed* Rluc showed a reduction of luciferase levels of about 2.41-fold if a

single tamoxifen dosing was administered. If a second tamoxifen dosing was applied a slightly higher decrease of Rluc was detectable, achieving a fold change of about 3.04-fold.

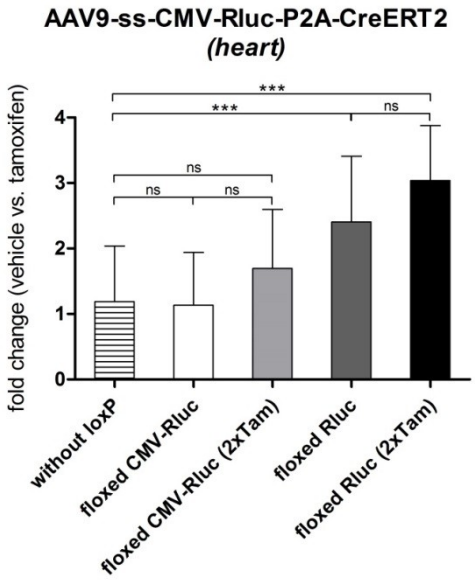

Figure 48: Extent of *Renilla* luciferase down-regulation after tamoxifen administration in heart samples from mice treated with AAV9 vectors containing the P2A element

The fold changes between vehicle- and tamoxifen-treated animals receiving different AAV9 vectors and/or repeated tamoxifen dosing are shown. The standard deviation is indicated with error bars. Statistical analysis was made with One-way ANOVA and Tukey post-test (***$p<0.001$; ns = not significant).

4. DISCUSSION

Although Adeno-associated viral vectors are one of the safest viral gene therapy systems available, many modifications towards increasing the safety are under investigation. On one hand, improvements in terms of efficacy and specificity have to be made, e.g. by designing AAV vectors targeting specifically distinct cell types or tissues. On the other hand, AAV vectors have to be modified to avoid binding to pre-existing neutralizing antibodies which limits the transduction efficacy of the gene transfer and allows only the treatment of patients that are pre-screened for low titer anti-AAV antibodies.

Moreover, a system to eliminate the AAV vectors after administration would be beneficial, e.g. if adverse events arise or if the treatment should be limited to a distinct time period. Possible side-effects may not occur due to the presence of the AAV vector itself but due to the overexpression of the gene of interest. It could be easily conceivable that the expression of the transgene has beneficial therapeutic effects until a distinct threshold is reached and additional expression leads to an imbalance in cellular functions. Therefore, a shut-off system for AAV vectors applicable after administration which can be activated in case of side-effects would be highly desirable. Ideally, the system should work independently on the AAV serotype, promoters and transgenes used. The generation of such system was thus the main focus of the present study.

4.1. Part 1 – Induction of the inducible Cre recombinase from an AAV vector

Before establishing the final shut-off system which is encoded on a single AAV vector, several pre-experiments were performed. First, the expression and background activity of the inducible CreER^{T2} recombinase were investigated. *In vitro*, the induction of the CreER^{T2} was already detectable 24 h after the first 4-OHT administration. Further 4-OHT applications did not lead to an increase of cells positively stained for β-galactosidase. Moreover, recombination did not occur in cells which were not treated with 4-OHT whereas the addition of 4-OHT resulted in cells positively stained for β-galactosidase. However, some background activity of the CreER^{T2} could be detected in vehicle-treated animals *in vivo*. This basal activity in the absence of tamoxifen was indeed as low as described by other groups [153-155]. To further reduce the activity of the CreER^{T2} in the absence of tamoxifen, a

second ER^{T2} domain could be fused to the recombinase [142, 143]. In case of the final shut-off system encoded by a single AAV vector, this $ER^{T2}CreER^{T2}$ recombinase would be too large in size so that no coding capacity for the transgene would be left. Therefore, this low background activity is acceptable and does not lead to any undesired effects.

4.2. Part 2 – Localization and functionality of loxP sites within an AAV vector

Besides the functionality of the inducible $CreER^{T2}$ recombinase, also the localization of the loxP sequences within the AAV vectors as well as the impact on expression levels was analyzed. In this case, the human cardiac-specific promoter TnT (troponin T) driving the expression of the *Firefly* luciferase reporter gene was used. The TnT promoter reduces expression of the transgene in the liver whereas the expression in heart and muscle remains high [112]. The *Firefly* luciferase gene was used to study the recombination events with the help of *in vivo* imaging which is better established than using the *Renilla* luciferase as reporter gene [169]. Moreover, the vector sets used in this part did not possess a limited coding capacity so that the use of the *Firefly* luciferase was possible. In case of the final shut-off system (part 4), the gene for the *Firefly* luciferase was too large for insertion into the single AAV vector.

The AAV vectors with and without loxP sites were first tested in cell culture by co-transduction with an AAV vector expressing the inducible $CreER^{T2}$ recombinase. The expression of the luciferase reporter gene could be down-regulated significantly in case of the *floxed* AAV vectors after 4-OHT was applied to the cells. However, the extent of down-regulation was not very high (about 1.6-fold in case of the *floxed* Fluc vector). One explanation for this faint effect is the co-transduction itself since both AAV vectors have to enter the same cell which then also has to be penetrated by 4-OHT for successful induction. To evaluate the influence of the loxP sites on the expression levels of the reporter gene, a comparison between the control vector and the *floxed* vectors in vehicle-treated cells can be made. The luciferase encoded by the control vector without loxP sites was expressed to a 3.1- to 5.8-fold higher extent than seen with the *floxed* AAV vectors. Therefore, the loxP sequences seem to reduce the expression of the reporter gene which has also been described by Sauer in 1998 [170]. Due to the complementary sequences within the loxP sites, hairpins are formed which are also present in transcripts. If these hairpins are located

upstream of the transgene the expression can be impaired. This is the case of both *floxed* vectors used in this experimental part. A greater distance to the start codon of the gene or the placement of the loxP sites within introns could improve this negative effect on expression levels.

For *in vivo* analysis of the respective AAV vectors, a mouse model expressing the inducible MerCreMer recombinase under the control of the cardio-specific αMHC (myosin heavy chain) promoter was used. Because of time constraints, these mice were used instead of models expressing the $CreER^{T2}$ which were not available on the campus. Already one week after the first tamoxifen administration, almost no light emission catalyzed by *Firefly* luciferase activity could be detected in mice treated with AAV9-ss-TnT-loxP-Fluc-loxP vectors. This indicates that recombination and therefore the excision of the reporter gene is a fast process which may not require daily tamoxifen administrations on 5 consecutive days. In some studies, two tamoxifen administrations were sufficient to achieve the maximal recombination 4 days after induction [158]. By analyzing the *Firefly* activity in homogenized heart samples, a significant reduction in tamoxifen-treated mice could be shown for both *floxed* AAV vectors (*floxed* TnT and *floxed* Fluc) but not for the control vector without loxP sites. For liver samples, a down-regulation of luciferase expression was not seen upon tamoxifen administration since the inducible MerCreMer recombinase is only expressed in heart and to a lower extent also in skeletal muscle. The extent of down-regulation (16- to 43-fold compared to vehicle-treated animals) in the heart was much higher as seen in cell culture which can be explained by the endogenous expression of the inducible Cre that had to be co-transduced in the cell culture experiments. Theoretically, every cardiomyocyte transduced by the *floxed* AAV vector and treated with tamoxifen should show this reduction in luciferase activity. But a complete shut-off of the *floxed* AAV vectors by tamoxifen administration is hardly achievable due to the efficacy of the MerCreMer-mediated recombination which is about 80% [160]. Moreover, every cell transduced by an AAV vector also has to be targeted by tamoxifen to reach a recombination efficacy of 100%.

Another aspect already described for the *in vitro* experiments was the impact of the loxP sites on the transgene expression levels. *In vivo*, this effect was not as pronounced as in cell culture. Here, the luciferase expression level was at maximum 3-fold higher in the control vector compared to the *floxed* TnT vector. In case of the *floxed* Fluc vector, no differences in expression levels compared to the control vector could be detected.

4.3. Part 3 – Co-transduction of CreER^{T2}- and loxP-bearing AAV vectors

Both experimental parts described before were combined for the next step toward the establishment of the final shut-off system encoded by a single AAV vector. Here, one AAV vector expressing the inducible CreER^{T2} recombinase was co-transduced with a second vector containing the *Renilla* luciferase reporter gene and loxP sequences at different positions within the AAV genome.

Again, first analyses were made in cell culture to evaluate the most suitable vectors for *in vivo* approaches. Here, co-transduction combined with the 4-OHT administration resulted in a significant down-regulation of reporter gene expression in case of all *floxed* vectors used. The extent of reduction varied between 4- and 9-fold compared to vehicle-treated cells. The vector achieving the highest down-regulation was the one containing the Rluc gene flanked by loxP sites. Moreover, the control vector achieved about 1.4- to 1.9-fold higher expression levels than the *floxed* vectors in vehicle-treated cells. Compared to the AAV vectors containing the *Firefly* luciferase gene under the control of the TnT promoter (part 2), the vectors used in this experimental part showed higher reductions in reporter gene expression upon 4-OHT addition. In general, the CMV promoter is active in almost all cell types whereas the TnT promoter is specific for cardiac and muscle cells. In the cell culture experiments shown, kidney cells were used so that the TnT promoter only results in low reporter gene expression (10^5 relative light units) whereas the CMV promoter leads to higher expression levels (10^7 relative light units). These differences in the promoters used may explain the differences in the down-regulation *in vitro*.

For *in vivo* experiments, the AAV vector expressing the luciferase flanked by loxP sites was used. Upon tamoxifen administration, the significant down-regulation in *Renilla* luciferase expression seen *in vitro* could be reproduced in the heart and the liver whereas in other organs (muscle, kidney, and spleen) a tendency towards a reduction was detectable. The extent of down-regulation was about 2.8-fold and therefore lower than seen in cell culture. Again, the shut-off of the reporter gene requires a transduction of a single cell by two AAV vectors which can be achieved more easily in cell culture than *in vivo*. *In vitro*, 10^4 vg per cell were used per AAV vector whereas *in vivo* in total 10^{12} vg per vector were injected systemically.

4.4. Part 4 – Generation of the shut-off system encoded within a single AAV vector

The final shut-off system is encoded by a single AAV containing both loxP sites and the CreER^{T2}. The coding capacity of a single-stranded AAV vector is about 4.8 kb including the ITRs. Because of the two expression cassettes used, the AAV genome consisting of the shut-off system reached a size of about 5.2 kb. Although this might exceed the packaging limit of an AAV vector, the production of these vectors was unproblematic resulting in reasonable AAV titers. Therefore, the use of smaller transgenes than the *Renilla* luciferase gene (about 940 bp) should be possible with this vector system. Larger genes could result in a drop of AAV vector titers and a higher probability that not the whole AAV genome gets packaged into an AAV particle.

The AAV vectors shown in figure 19 were first tested *in vitro*. In HEK293T cells, the expression of the luciferase could be down-regulated significantly in almost all *floxed* vectors after 4-OHT administration. The only exception was the vector containing loxP sites before the luciferase gene and after the CreER^{T2} recombinase. This vector did not show any reduction in luciferase activity, independently of the time points analyzed. After recombination in case of this vector, a complete mRNA consisting of the CreER^{T2}, one loxP site, the *Renilla* reporter gene, and the SV40 polyA signal can be transcribed under the control of the CMV promoter left. Therefore, the translation of the CreER^{T2} should still be possible whereas the luciferase should not be translated due to the stop codon of the CreER^{T2} terminating the translation. Conceivable read-through of this stop codon, e.g. by ribosome skipping, could lead to production of luciferase. Moreover, nucleotide motifs in close proximity to the stop codon may facilitate the translational read-through. Such a motif could be displayed by the loxP site between the CreER^{T2} and *Renilla* luciferase genes.

In case of the *floxed* AAV vectors leading to a reduction of luciferase activity upon 4-OHT addition, the extent of down-regulation varied between the vectors. The most efficient was the one containing the *floxed* Rluc gene, resulting in a 3-fold reduction in luciferase expression 72 h after induction. The AAV vectors with *floxed* CMV and *floxed* CMV-Rluc only reached a 1.4-fold down-regulation in cell culture. As seen in the pre-experiments, the overall expression levels of luciferase in vehicle-treated cells were reduced in the AAV vectors containing loxP sites. In comparison to the control vector without loxP sites, the expression of the *floxed* Rluc vector was about 68-fold reduced whereas the *floxed* CMV-Rluc

vector showed only a 16-fold reduction. Again, the secondary structure of the loxP sequences seems to affect the expression of the transgene if they are placed in close proximity to the 5'-end of the gene as seen with the *floxed* Rluc vector. In case of the *floxed* CMV-Rluc, there is no loxP site located between the promoter and the luciferase gene so that the influence of the loxP sequences within the AAV genome seems to be decreased.

In CV-1 cells, the expression and induction of the CreER^{T2} recombinase was analyzed. Cells positive for β-galactosidase expression could be detected with all AAV vectors applied. This experiment should verify that the CreER^{T2} expression is sufficient for successful down-regulation of luciferase activity upon 4-OHT administration. Therefore, a deficient CreER^{T2} expression in case of the *floxed* Rluc-…-CreER^{T2} vector which did not show any reduction in luciferase expression after 4-OHT addition could be excluded.

Another *in vitro* experiment was made by detecting the recombination products generated upon 4-OHT administration. This so-called "mini circles" which consist of the excised DNA fragments were amplified by PCR. In general, this PCR leaded to some unspecific DNA bands but the recombination products could be clearly verified. In case of the *floxed* Rluc-…-CreER^{T2} vector, the respective "mini circle" was not very prominent which confirms the results seen in the luciferase assays performed. Another reason could be the efficacy of the PCR itself since the DNA fragment amplified was the largest (3500 bp).

The expression and induction of the CreER^{T2} was also monitored *in vivo*, at least for the control vector without loxP sites. Here, successful recombination could be detected in animals treated with tamoxifen whereas there were almost no eGFP-positive cells in vehicle-treated Tomato reporter mice. In comparison to the AAV9-CMV-CreER^{T2} vector used in part 1, the extent of positive cells showing successful recombination was much lower. Therefore, the vectors containing the shut-off system seem to be less efficient in terms of transduction and CreER^{T2} expression. The size above the packaging limit of these vectors could be one of the reasons for this effect but also the bicistronic expression cassettes could lead to reduced expression levels of the genes encoded.

The expression of the *Renilla* luciferase was also analyzed *in vivo* with the *floxed* AAV vectors which performed best *in vitro*. In the heart, both *floxed* vectors showed a significant down-regulation of luciferase activity upon tamoxifen administration whereas at least a tendency towards a reduction could be detected in the other organs analyzed. Thereby, a 2.5-fold

down-regulation of luciferase levels could be achieved by the *floxed* CMV-Rluc vector whereas the *floxed* Rluc vector resulted in a 9-fold reduction. This extent of down-regulation was higher than observed in cell culture. In cells, the half-time and stability of the luciferase protein could lead to remaining *Renilla* activity although the recombination was successful. To avoid this effect, the time between induction and harvesting of the cells could be prolonged. As seen in cell culture, the expression levels of the luciferase in vehicle-treated animals were different between the control vector and the *floxed* AAV vectors. Here, the expression of the control vector was 1.5-fold and 2.4-fold higher than the luciferase levels of the *floxed* Rluc vector and *floxed* CMV-Rluc vector, respectively. As described for all other experiments before, this observation of reduced expression levels due to the presence of loxP sites was not as prominent as observed in cell culture.

Another step in analyzing the shut-off system was the validation of the assumption that further tamoxifen administrations would lead to a higher degree in reporter gene down-regulation. Therefore, the most efficient vector containing the *floxed* Rluc gene was used. Indeed, a second round of tamoxifen addition yielded in a further reduction of the luciferase levels which was not significant due to relative high variations between single animals. However, calculation of the extent of down-regulation resulted in significant differences between one tamoxifen dosing (5 days, 1 mg each day) and two administrations (10 days, 1 mg each day). The 9-fold reduction seen with a single tamoxifen dosing could be enhanced to a 26-fold down-regulation in luciferase expression. An explanation for this effect could be that the cells transduced by the corresponding AAV vector also have to be penetrated by tamoxifen to make the shut-off system functional. The more tamoxifen is applied, the higher the probability of targeting the cells transduced by the vector. Therefore, it could be conceivable that further tamoxifen administrations lead to higher shut-off levels. It may not be required that one tamoxifen administration round consists of 5 consecutive days. Also, the concentration of tamoxifen applied could be increased to avoid repeated administrations.

In comparison to the co-transduction of two AAV vectors (see part 3) the shut-off system encoded on a single AAV vector is more efficient in terms of down-regulation of the reporter gene encoded. For example, the *floxed* Rluc vector with the complete shut-off system achieved a 9-fold reduction in luciferase expression whereas the down-regulation in the co-transduction setting was only 2.8-fold. As described before, a co-transduction requires the

delivery of all components into the same cell which is not as efficient as the delivery of all necessary compounds by a single AAV vector. Another aspect that got obvious by comparison of part 3 and part 4 of this thesis was the difference in expression levels of the luciferase encoded by the AAV vectors. In the co-transduction experiment, the measurement of luciferase levels resulted in about 10^8 relative light units whereas the shut-off system on a single AAV vector led to a maximum of 10^7 relative light units. Again, this discrepancy could be explained by the size of AAV genomes used which is slightly too large in case of the AAV vectors encoding the complete shut-off system. The use of a minimal CMV promoter could enable a reduction of the vector genome size below 5.0 kb.

4.5. Part 5 - Efficacy of the shut-off system in case of a side effect-causing gene

In a next step, the shut-off system should be evaluated with a side effect-causing gene replacing the reporter gene used in part 4. Therefore, the murine interleukin-10 (mIL-10) cDNA was used. In humans, IL-10 is an anti-inflammatory cytokine and plays a role in protection of the organism by blocking exaggerating immune reactions [171, 172]. In a study for the treatment of cystic fibrosis using an AAV vector expressing IL-10 (AAV1-IL-10), beneficial effects could be seen in the treatment of allergic reactions [173]. However, in the same study, side effects caused from prolonged overexpression of IL-10 were observed, including thrombocytopenia and splenomegaly. The authors claim that the treatment with IL-10 is effective but caution has to be taken in settings where a long-term secretion of IL-10 is involved. Experiments in our laboratory with systemically applied, cardio-specific AAV9 vectors coding for murine IL-10 (AAV9-mIL-10) confirmed the adverse events seen in the study described above. Animals (C57Bl/6) treated with AAV9-mIL-10 showed a consistent weight loss from day 35 on after AAV injection. After dissection, a severe splenomegaly and inflammations in several organs including liver and pancreas could be detected (unpublished data).

Therefore, the gene coding for murine IL-10 was cloned into the AAV genome consisting of the shut-off system. The AAV vector generated expressing the mIL-10 flanked by loxP sites was then administered to C57Bl/6 mice in two different doses and the body weight was monitored 3 times per week. Since the animals gained body weight until day 37 after AAV injection, three mice per group were sacrificed to validate the mIL-10 expression. In terms of

body weight, heart weight and spleen weight, these animals did not show any significant differences between the groups. Analysis of the mIL-10 expression levels in the heart revealed a slight 2-fold increase in the high dose group which was not significant. In contrast, in the previous study using a cardio-specific promoter driving the mIL-10 expression, a 2000-fold and a 20000-fold overexpression of mIL-10 in the low and high dose groups could be achieved in heart samples. Also the expression levels yielded in liver samples were higher in the previous study (2000-fold in the low dose group, 4000-fold in the high dose group). In this experiment, the low dose group showed a 15-fold overexpression of mIL-10 compared to untreated mice in the liver whereas the high dose group displayed a 77-fold increase in mIL-10 mRNA levels. Due to these differences, an analysis of the mIL-10 mRNA levels generated by transfection of these AAV genomes into HEK293 cells was performed. This showed that the vector used in the previous study achieved about 25-fold higher mIL-10 levels than the vector containing the shut-off system (data not shown). *In vivo*, these variations seemed to be even more prominent than in cell culture. Again, the size of the AAV vector containing the shut-off system and the negative influence of the loxP sites on the transgene expression may explain the effects seen. The expression data analyzed by qRT-PCR were confirmed by the ELISA for the detection of mIL-10 in the plasma. Here, only the high dose group showed significantly higher mIL-10 levels compared to the untreated controls. In the previous study, mIL-10 plasma levels of about 120000 pg/ml were achieved whereas the high dose group in this experiment only reached about 8 pg/ml.

Because of these data, it was decided to leave the remaining animals for a longer time period. The body weight was still monitored 3 times per weeks until day 91. The animals treated with mIL-10 expressing AAV vectors showed a stable body weight since day 65 without gaining as much weight as seen in the control group. Therefore, some animals were treated with tamoxifen for 5 consecutive days from day 92 on. After tamoxifen treatment, these mice gained body weight very quickly whereas the body weight of the vehicle-treated and control animals remained stable. Surprisingly, the spleen weight of mice having received tamoxifen was significantly higher than of vehicle-treated and control animals. Moreover, the plasma ELISA for mIL-10 showed higher mIL-10 levels in animals treated with tamoxifen. Here, plasma levels of about 20 pg/ml were achieved in tamoxifen-treated animals whereas the control groups only reached levels of about 9 pg/ml. On one hand, the detection range of the plasma ELISA is stated from the manufacturer as 15.6 to 1000 pg/ml. Therefore, the

mIL-10 levels measured are beyond the detection level of the ELISA. On the other hand, tamoxifen itself could have an effect on mIL-10 levels in the plasma. To verify this, another experiment to answer this question should be performed where an untreated control group receiving the same amount of tamoxifen is included. The mIL-10 expression levels measured by qRT-PCR in the heart revealed that there were no significant differences between the groups. A slight reduction in the mIL-10 mRNA could be seen in mice to which tamoxifen was applied. Again, these findings were not significant. In contrast, the high dose group showed a significant up-regulation of mIL-10 expression in the liver (15-fold compared to the untreated control animals) which could be reduced to a 4-fold overexpression of mIL-10 upon tamoxifen administration. Therefore, the aim of the shut-off system to reduce the expression from the vector after tamoxifen administration could be verified.

Another finding was that the transcript levels of mIL-10 in the liver decreased over time. On day 37, a 77-fold overexpression could be detected whereas only a 15-fold up-regulation was shown on day 102 after AAV injection. One explanation could be that the background activity of the $CreER^{T2}$ recombinase results in the reduction of mRNA levels. Moreover, the turn-over of cells in the liver is much higher as for example in the heart. If liver cells are renewed the AAV genome gets lost and overall expression levels decrease.

Taken together, the main drawback of the shut-off system containing a side effect-causing gene seems to be the expression levels achieved from the AAV vector. In case of vector coding for the *Renilla* luciferase reporter gene, this was not a severe problem due to the sensitivity of the luciferase quantification assays. But using other genes like mIL-10, the low expression levels achieved may lie beyond the therapeutic levels necessary to induce side effects. Higher doses of these AAV vectors would be necessary to yield comparable levels of the transgene as seen with AAV vectors only encoding the transgene.

4.6. Part 6 – Increase in coding capacity of AAVs containing the shut-off system

Finally, the shut-off system encoded by a single AAV vector should be improved in terms of coding capacity available. Therefore, the polyA signal of the *Renilla* luciferase reporter gene and the CMV promoter driving the CreER^{T2} expression were replaced by the "self-cleaving" P2A peptide from Porcine Teschovirus-1. The size of the AAV genome could be reduced from 5.2 kb to 4.4 kb which is below the limiting capacity for AAV genomes of 4.8 kb. The packaging of these vectors containing the P2A element should be facilitated in comparison to the vectors containing two expression cassettes. The CMV promoter driving the luciferase expression now also controls the expression of the P2A element and the CreER^{T2}. A single mRNA is transcribed and finally a polyprotein is translated. During translation, the P2A element results in a cleavage between the *Renilla* luciferase and the CreER^{T2} recombinase so that two distinct proteins are generated [174]. Besides the P2A peptide from Teschovirus-1, other 2A oligopeptides are available, e.g. from Foot-and-Mouth Disease virus (F2A) or Equine Rhinitis A virus (E2A). All of these 2A peptides were shown to work in eukaryotic systems with P2A achieving the highest cleavage efficacy [175]. The advantage of these 2A peptides over the use of an internal ribosome entry site (IRES) is the small size of these elements (about 66 nt versus about 600 nt of the IRES). Moreover, the expression of the genes up- and downstream of the 2A element is quite similar whereas the gene downstream of the IRES shows decreased expression efficacies.

To verify the cleavage efficacy of the P2A in cell culture, Western blot analysis of HEK293T cells transfected with the corresponding AAV genomes was performed. The control vector without loxP sites showed defined bands at the molecular weights for both the *Renilla* luciferase (36 kDa) and the CreER^{T2} (74 kDa), independently of the treatment applied (vehicle/4-OHT). The cleavage efficacy of the P2A element was indeed high because there was only a very faint band at 110 kDa visible, indicating the uncleaved polyprotein. In case of the AAV genome containing the *Renilla* luciferase flanked by loxP sites, there was only a band for the CreER^{T2} detectable but not for the luciferase. Further experiments were performed to clarify if the expression of the luciferase is reduced due to the presence of loxP sequences (see below).

For all vectors containing the P2A element, independently on the locations of the loxP sequences within the AAV genome, the expression and inducibility of the CreER^{T2} was tested

by X-Gal stainings. Because the P2A elements get cleaved co-translationally, some amino acids from this peptide remain at the C-terminus of the luciferase and the N-terminus of the CreER^{T2}. The X-Gal stainings should exclude that these N-terminal added amino acids have an influence on the CreER^{T2} expression and activation upon tamoxifen administration. Surprisingly, the amount of positively stained cell varied strongly between the different AAV vectors applied. Only few positive cells were detectable in case of the control vector, the *floxed* CMV vector and the *floxed* CMV-Rluc vector. The vector containing the *floxed* Rluc-…-CreER^{T2} cassette did not show any positive cell whereas the *floxed* Rluc vector yielded in by far the most positive cells compared to all other vectors. As an explanation, the CMV promoter gets excised upon 4-OHT addition in case of the *floxed* CMV and CMV-Rluc vectors. Therefore, expression of further CreER^{T2} transcripts and subsequent translation is not possible anymore. The same is true for the *floxed* Rluc-…-CreER^{T2} vector where recombination leads to the excision of the CreER^{T2} itself. In contrast, only the luciferase gene is removed in the *floxed* Rluc vector during recombination. As a result, the CreER^{T2} gets directly under the control of the CMV promoter which leads to increased CreER^{T2} levels. However, the CreER^{T2} expression in case of the control vector was assumed to be higher than detected by X-Gal stainings. Therefore, it cannot be ruled out that the remaining amino acids from the P2A element have an impact on the expression and/or induction of the recombinase.

Next, the *Renilla* luciferase activity of all vectors was analyzed in cell culture. Here, a significant down-regulation of luciferase expression could be shown for all vectors containing loxP sites. The extent of the reduction varied between 2-fold and 3.3-fold with the *floxed* Rluc vector showing the highest down-regulation. These results were comparable to the data achieved with the AAV vectors of part 4 containing two expression cassettes. In general, the AAV vectors containing the P2A element yielded in at least 10-fold higher luciferase levels compared to the vectors from part 4. Another aspect to analyze was the influence of the loxP sites on luciferase expression in the P2A-containing vector set. Here, the luciferase levels were about 50- to 140-fold reduced compared to the control vector. These differences were much higher than seen with the vectors containing two expression cassettes. The reason seems not to be the presence of the P2A element itself since the control vector performed much better than the control vector from part 4.

To correlate the *Renilla* luciferase and the CreER^{T2} expression levels, qRT-PCRs were performed with cells treated with the *floxed* CMV-Rluc and the *floxed* Rluc vectors. In case of both vectors, the *Renilla* luciferase mRNA levels were significantly reduced upon 4-OHT administration due to the excision of the luciferase gene. In vehicle-treated cells, the *floxed* CMV-Rluc vector yielded in about 6.7-fold more luciferase-containing transcripts than the *floxed* Rluc vector. Considering the CreER^{T2} mRNA levels of the *floxed* CMV-Rluc vector, the amount of transcripts was comparable to the luciferase mRNA levels. By addition of 4-OHT, the CreER^{T2} expression was reduced significantly in the *floxed* CMV-Rluc vector due to the loss of the promoter driving the recombinase expression. In contrast, the transcripts of the CreER^{T2} were significantly increased if the *floxed* Rluc vector and 4-OHT were applied. As stated before, the excision of the luciferase upon 4-OHT addition lead to the generation of a remaining AAV vector, comprising the CMV promoter, the P2A element and the CreER^{T2}. Therefore, the recombinase gets directly under the control of the promoter which in turn results in an increase of transcript amounts. As already seen with the luciferase-containing mRNAs in vehicle-treated cells, the CreER^{T2} transcript levels were lower with the *floxed* Rluc vector compared to the *floxed* CMV-Rluc vector. Thus, the position of the loxP sequences within the AAV genome seems to have a greater impact on expression if the loxP sites flank the luciferase gene.

The vectors analyzed via qRT-PCR in cell culture were also chosen for *in vivo* experiments in C57Bl/6 mice. As already seen *in vitro*, the overall luciferase activity reached was about 10-fold higher than achieved by the AAV vectors containing two expression cassettes. However, the extent of down-regulation was much lower compared to the vectors tested in part 4, even if a second tamoxifen dosing was applied. In heart samples, a maximal reduction of 3-fold could be achieved in case of the *floxed* Rluc vector whereas the same vector containing two expression cassettes yielded a 26-fold down-regulation *in vivo*. The reduction in luciferase activity was only significant in case of the *floxed* Rluc vector, with a second tamoxifen administration not leading to a further down-regulation. The difference in luciferase expression between one and two tamoxifen dosing rounds was significant if the *floxed* CMV-Rluc vector was applied. Here, the extent of down-regulation was only 1.8-fold (two tamoxifen administrations). Even the control vector without loxP sites showed differences between the treatment groups which can be explained by the small groups (3 animals per group) and the high variation between single animals. The data from heart

samples were also transferable to the results achieved in other organs (liver, muscle, kidney, and spleen). Taken together, the outcome of the *in vivo* experiments with P2A-containing AAV vectors was not as expected. On one hand, one could assume that the recombination and excision of *floxed* DNA fragments within P2A-bearing AAV vectors is not as effective as seen with the AAV vectors comprising two expression cassettes. The additional amino acids on the N-terminal domain of the CreER^{T2} may impair the activity and efficacy of the recombinase which has also been shown for the Cre recombinase comprising an ER^{T2} domain on each end of the protein [137, 142]. In one of these studies, the Cre activity dropped to 35% of the original Cre recombinase if two ER^{T2} domains were fused to the recombinase. On the other hand, the outcome of the *in vitro* experiments with P2A-bearing vectors was comparable to the AAV vectors containing two expression cassettes. Therefore, the reason for the poor down-regulation upon tamoxifen administration *in vivo* may lie in the tamoxifen batch used for the P2A experiments. A repetition of the experiments, at least with one of the *floxed* AAV vectors, would be helpful to rule out problems with the tamoxifen applied.

4.7. Final remarks

As already described in the introduction, the regulatory systems having been used in the context of AAV vectors so far allow the induction of gene expression from the vector by administration of an inducer drug. The main drawbacks of these systems are size of the components encoded, the origin of single regulatory elements (e.g. of viral origin) and the adverse effects induced by the drug itself. In case of the coding capacity required by the regulation system, it is beneficial if all elements can be expressed from a single AAV vector to increase efficacy of the system applied. This avoids the requirement of two AAV vectors targeting the same cell to deliver all components necessary for regulation. Therefore, the aim of this thesis was the development of a regulatory system fitting into one AAV genome and using the Cre/loxP technology. Another safety aspect of regulation system is the origin of single regulatory elements encoded by the vector. For example, the Tet- and RU486-inducible systems use the viral transactivator domain (VP16) from Herpes Simplex virus which may induce immune responses. Thus, systems delivering only mammalian components for efficient regulation would be highly beneficial. By applying the regulatory system using the inducible Cre recombinase, elements from bacteriophage P1 (loxP sites, Cre

recombinase) are also not of mammalian origin. It was shown, that the expression of the CreER^{T2} did not lead to any toxicities, independently of the induction status (active/inactive) [153]. Besides the components of the regulatory system, the inducer drug itself has to be evaluated for the clinical use, e.g. in humans [115]. Tetracycline and doxycycline were shown to induce photosensitivity and immune responses if applied for long time periods. Rapamycin acts as an immunosuppressant agent and too high doses would be required in humans to fully induce the regulation system. RU486 has been used in the clinical setting for terminating pregnancy but even if the doses needed for induction are lower than to terminate pregnancy, side effects may arise. All of these regulatory systems require the application of the drug to induce expression from the gene therapy vector. If the effects of the transgene overexpression should be achieved over a longer period the inducer agents need to be applied for the same interval to maintain expression. Thus, this long-term administration of drugs may lead to adverse effects, impairment of health or even changes in phenotypes [176]. The transgene expression of the regulation system described in this thesis is constantly switched on until tamoxifen is administered. Therefore, the application of the inducer drug is only required if side effects occur or if the treatment should be terminated. This avoids long-term administration of tamoxifen which in turn could result in adverse effects. In several studies it was shown that tamoxifen only has to be applied for 2-5 days to achieve high induction rates for the Cre recombinase, at least in mouse models. Other studies reported that also lower tamoxifen doses applied are sufficient for effective recombination. Tamoxifen itself has been in clinical use for a long time to treat breast cancer patients. The treatment is limited to 5 years to avoid side effects which include hot flashes, weight gain, joint aches, mood disturbances, thromboembolic disease or endometrial cancer [177, 178]. These adverse events may result only after long-term administration of tamoxifen on a daily basis which would not be required to switch-off the regulatory system described in this thesis. Moreover, the use of the active metabolite of tamoxifen, 4-hydroxytamoxifen (4-OHT), would prevent the application of high tamoxifen doses due to its 30- to 100-fold more potent activity compared to the prodrug tamoxifen [179]. As a drawback, the commercially available 4-OHT is more expensive than tamoxifen.

Taken together, the shut-off system developed in this thesis can be applied if transgene expression should be switched off due to side effects arising or if the treatment should be limited to a certain time period. The system can be adapted to individual requirements, e.g.

by using cell- or tissue-specific promoters instead of the CMV promoter. Moreover, all AAV serotypes can be applied so that targeting of various tissues and cell types is possible. The only limitation of the system is the coding capacity for the transgene which is limited to 1 kb in case of the vectors containing two expression cassettes and the CMV promoter. If other promoters should be used the cloning capacity has to be evaluated again.

As seen in several experiments, the loxP sequences decrease the expression level of the transgene encoded, dependent on the position of the sites within the AAV genome. For functional studies using therapeutic genes, this drawback has to be taken into account. Therefore, dose finding studies should be performed to evaluate the therapeutic range of the AAV vector applied. Improvements of the AAV vector itself could also lead to higher expression levels, e.g. by inserting spacer regions between the loxP sites and the transgene. Furthermore, the extent of down-regulation achievable by tamoxifen administration has to be considered for therapeutic studies. If a complete shut-off of the transgene expression is required the tamoxifen doses and treatment intervals have to be adapted. It is assumed that not the Cre expression levels are the limiting factor for efficient recombination but the intracellular amount of tamoxifen [140]. Thus, doses of the AAV vector and tamoxifen have to be validated before the functional study.

Besides the optimization of the expression levels of the transgene in context of loxP-bearing AAV vectors, another improvement could be implemented to the shut-off system. Instead of using two homotypic loxP sites, heterotypic sequences could be applied to avoid the reversible recombination reaction. In case of the excision of the DNA fragment, this reversible reaction is not a major problem since intramolecular excisions are the most efficient and stable recombination reactions and therefore favored over integrations or inversions [130]. Moreover, the excised DNA from the shut-off system is relatively small and elements required for productive DNA replication are lacking. Thus, these small circular DNA molecules get rapidly lost *in vivo* [129].

In conclusion, the delivery of an inducible $CreER^{T2}$ recombinase in combination with AAV genomes flanked by loxP sites allows efficient (self)-inactivation of AAV-mediated gene expression upon tamoxifen administration. These findings contribute to the generation of a novel shut-off system for AAV-based gene transfer vectors applicable for the use of various promoters, transgenes and AAV serotypes.

5. REFERENCES

1. Wirth, T., N. Parker, and S. Yla-Herttuala, *History of gene therapy.* Gene, 2013. **525**(2).
2. Rogers, S., et al., *Induction of arginase activity with the Shope papilloma virus in tissue culture cells from an argininemic patient.* J. Exp. Med., 1973. **137**.
3. Terheggen, H.G., et al., *Unsuccessful Trial of Gene Replacement in Arginase Deficiency.* Z. Kinderheilk., 1975. **119**.
4. Rosenberg, S.A., et al., *Gene transfer into humans - Immunotherapy of patients with advanced melanoma, using tumor-infiltrating lymphocytes modified by retroviral gene transduction.* New england journal of medicine, 1990. **323**(9).
5. Blaese, R.M., et al., *T Lymphocyte-Directed Gene Therapy for ADASCID: Initial Trial Results After 4 Years.* Science, 1995. **270**.
6. Stolberg, S.G., *The Biotech Death of Jesse Gelsinger.* N.Y. Times Mag., 1999.
7. Peng, Z., *Current status of Gendicine in China: Recombinant human Ad-p53 agent for treatment of cancers.* Hum Gene Ther, 2005. **16**.
8. Robbins, P.D. and S.C. Ghivizzani, *Viral Vectors for Gene Therapy.* Pharmacol. Ther., 1998. **80**(1).
9. Young, L.S., et al., *Viral gene therapy strategies: from basic science to clinical application.* Journal of Pathology, 2006. **208**.
10. Toscano, M.G., et al., *Physiological and tissue-specific vectors for treatment of inherited diseases.* Gene Ther, 2011. **18**.
11. Atchison, R.W., B.C. Casto, and W.M. Hammon, *Adenovirus-Associated Defective Virus Particles.* Science, 1965. **149**.
12. Hoggan, M.D., N.R. Blacklow, and W.P. Rowe, *Studies of small DNA viruses found in various Adenovirus preparations: physical, biological, and immunological characteristics.* PNAS, 1966. **55**.
13. Buller, R.M., et al., *Herpes Simplex Virus Types 1 and 2 Completely Help Adenovirus-Associated Virus Replication.* Journal of Virology, 1981. **40**(1).
14. McPherson, R.A., L.J. Rosenthal, and J.A. Rose, *Human Cytomegalovirus Completely Helps Adeno-Associated Virus Replication.* Virology, 1985. **147**.
15. Schlehofer, J., M. Ehrbar, and H. zur Hausen, *Vaccinia Virus, Herpes Simplex Virus, and Carcinogens Induce DNA Amplification in a Human Cell Line and Support Replication of a Helpervirus Dependent Parvovirus.* Virology, 1986. **152**.
16. Meyers, C., et al., *Altered biology of adeno-associated virus type 2 and human papillomavirus during dual infection of natural host tissue.* Virology, 2001. **287**(1).
17. Berns, K.I., et al., *Detection of Adeno-Associated Virus (AAV)-Specific Nucleotide Sequences in DNA Isolated from Latently Infected Detroit 6 Cells.* Virology, 1975. **68**.
18. Kotin, R.M., et al., *Site-specific integration by adeno-associated virus.* Proc Natl Acad Sci U S A, 1990. **87**.
19. Samulski, R.J., et al., *Targeted integration of adeno-associated virus (AAV) into human chromosome 19.* The EMBO Journal, 1991. **10**(12).
20. Huser, D., et al., *Integration preferences of wildtype AAV-2 for consensus rep-binding sites at numerous loci in the human genome.* PLoS Pathog, 2010. **6**(7): p. e1000985.
21. Cheung, A.K.M., et al., *Integration of the Adeno-Associated Virus Genome into Cellular DNA in Latently Infected Human Detroit 6 Cells.* Journal of Virology, 1980. **33**(2).

22. Grieger, J.C. and R.J. Samulski, *Adeno-associated virus vectorology, manufacturing, and clinical applications.* Methods Enzymol, 2012. **507**.
23. Forsayeth, J.R. and K.S. Bankiewicz, *AAV9: over the fence and into the woods.* Mol Ther, 2011. **19**(6).
24. Pacak, C.A., et al., *Recombinant adeno-associated virus serotype 9 leads to preferential cardiac transduction in vivo.* Circ Res, 2006. **99**(4).
25. Inagaki, K., et al., *Robust systemic transduction with AAV9 vectors in mice: efficient global cardiac gene transfer superior to that of AAV8.* Mol Ther, 2006. **14**(1).
26. Qi, Y., et al., *Selective tropism of the recombinant adeno-associated virus 9 serotype for rat cardiac tissue.* J Gene Med, 2010. **12**(1).
27. Xiao, W., et al., *Gene Therapy Vectors Based on Adeno-Associated Virus Type 1.* Journal of Virology, 1999. **73**(5).
28. Wu, Z., et al., *Alpha2,3 and alpha2,6 N-linked sialic acids facilitate efficient binding and transduction by adeno-associated virus types 1 and 6.* J Virol, 2006. **80**(18).
29. Srivastava, A., E.W. Lusby, and K.I. Berns, *Nucleotide Sequence and Organization of the Adeno-Associated Virus 2 Genome.* Journal of Virology, 1983. **45**(2).
30. Summerford, C. and R.J. Samulski, *Membrane-Associated Heparan Sulfate Proteoglycan Is a Receptor for Adeno-Associated Virus Type 2 Virions.* Journal of Virology, 1998. **72**(2).
31. Kashiwakura, Y., et al., *Hepatocyte growth factor receptor is a coreceptor for adeno-associated virus type 2 infection.* J Virol, 2005. **79**(1).
32. Qing, K., et al., *Human fibroblast growth factor receptor 1 is a co-receptor for infection by adeno-associated virus 2.* Nature Medicine, 1999. **5**(1).
33. Akache, B., et al., *The 37/67-kilodalton laminin receptor is a receptor for adeno-associated virus serotypes 8, 2, 3, and 9.* J Virol, 2006. **80**(19).
34. Kurzeder, C., et al., *CD9 promotes adeno-associated virus type 2 infection of mammary carcinoma cells with low cell surface expression of heparan sulphate proteoglycans.* Int J Mol Med, 2007. **19**.
35. Muramatsu, S.-I., et al., *Nucleotide Sequencing and Generation of an Infectious Clone of Adeno-Associated Virus 3.* Virology, 1996. **221**.
36. Ling, C., et al., *Human hepatocyte growth factor receptor is a cellular coreceptor for adeno-associated virus serotype 3.* Hum Gene Ther, 2010. **21**(12).
37. Blackburn, S.D., R.A. Steadman, and F.B. Johnson, *Attachment of adeno-associated virus type 3H to fibroblast growth factor receptor 1.* Arch Virol, 2006. **151**(3).
38. Chiorini, J.A., et al., *Cloning of Adeno-Associated Virus Type 4 (AAV4) and Generation of Recombinant AAV4 Particles.* Journal of Virology, 1997. **71**(9).
39. Chiorini, J.A., et al., *Cloning and Characterization of Adeno-Associated Virus Type 5.* Journal of Virology, 1999. **73**(2).
40. Kaludov, N., et al., *Adeno-associated virus serotype 4 (AAV4) and AAV5 both require sialic acid binding for hemagglutination and efficient transduction but differ in sialic acid linkage specificity.* J Virol, 2001. **75**(15).
41. Di Pasquale, G., et al., *Identification of PDGFR as a receptor for AAV-5 transduction.* Nat Med, 2003. **9**(10).
42. Rutledge, E.A., C.L. Halbert, and D.W. Russell, *Infectious Clones and Vectors Derived from Adeno-Associated Virus (AAV) Serotypes Other Than AAV Type 2.* Journal of Virology, 1998. **72**(1).
43. Gao, G.P., et al., *Novel adeno-associated viruses from rhesus monkeys as vectors for human gene therapy.* Proc Natl Acad Sci U S A, 2002. **99**(18).

44. Gao, G., et al., *Clades of Adeno-associated viruses are widely disseminated in human tissues.* J Virol, 2004. **78**(12).
45. Bell, C.L., et al., *The AAV9 receptor and its modification to improve in vivo lung gene transfer in mice.* J Clin Invest, 2011. **121**(6).
46. Mori, S., et al., *Two novel adeno-associated viruses from cynomolgus monkey: pseudotyping characterization of capsid protein.* Virology, 2004. **330**(2).
47. Schmidt, M., et al., *Adeno-associated virus type 12 (AAV12): a novel AAV serotype with sialic acid- and heparan sulfate proteoglycan-independent transduction activity.* J Virol, 2008. **82**(3).
48. Mayor, H.D., et al., *Plus and Minus Single-Stranded DNA Separately Encapsidated in Adeno-Associated Satellite Virions.* Science, 1969. **166**.
49. Hermonat, P.L., et al., *Genetics of Adeno-Associated Virus: Isolation and Preliminary Characterization of Adeno-Associated Virus Type 2 Mutants.* Journal of Virology, 1984. **51**(2).
50. Zhou, X., et al., *Biochemical Characterization of Adeno-Associated Virus Rep68 DNA Helicase and ATPase Activities.* Journal of Virology, 1999. **73**(2).
51. King, J.A., et al., *DNA helicase-mediated packacking of adeno-associated virus type 2 genomes into preformed capsids.* The EMBO Journal, 2001. **20**(12).
52. Johnson, F.B., H.L. Ozer, and M.D. Hoggan, *Structural Proteins of Adenovirus-Associated Virus Type 3.* Journal of Virology, 1971. **8**(6).
53. Rose, J.A., et al., *Structural Proteins of Adenovirus-Associated Viruses.* Journal of Virology, 1971. **8**(5).
54. Laughlin, C.A., H. Westphal, and B.J. Carter, *Spliced adenovirus-associated virus RNA.* PNAS, 1979. **76**(11).
55. Cassinotti, P., M. Weitz, and J.-D. Tratschin, *Organization of the Adeno-Associated Virus (AAV) Capsid Gene: Mapping of a Minor Spliced mRNA Coding for Virus Capsid Protein 1.* Virology, 1988. **167**.
56. Trempe, J.P. and B.J. Carter, *Alternate mRNA Splicing Is Required for Synthesis of Adeno-Associated Virus VP1 Capsid Protein.* Journal of Virology, 1998. **62**(9).
57. Kern, A., et al., *Identification of a Heparin-Binding Motif on Adeno-Associated Virus Type 2 Capsids.* Journal of Virology, 2003. **77**(20).
58. Opie, S.R., et al., *Identification of Amino Acid Residues in the Capsid Proteins of Adeno-Associated Virus Type 2 That Contribute to Heparan Sulfate Proteoglycan Binding.* Journal of Virology, 2003. **77**(12).
59. Bleker, S., F. Sonntag, and J.A. Kleinschmidt, *Mutational analysis of narrow pores at the fivefold symmetry axes of adeno-associated virus type 2 capsids reveals a dual role in genome packaging and activation of phospholipase A2 activity.* J Virol, 2005. **79**(4).
60. Girod, A., et al., *The VP1 capsid protein of adeno-associated virus type 2 is carrying a phospholipase A2 domain required for virus infectivity.* Journal of General Virology, 2002. **83**.
61. Zadori, Z., et al., *A Viral Phospholipase A2 Is Required for Parvovirus Infectivity.* Developmental Cell, 2001. **1**.
62. Sonntag, F., K. Schmidt, and J.A. Kleinschmidt, *A viral assembly factor promotes AAV2 capsid formation in the nucleolus.* PNAS, 2010. **107**(22).
63. Lusby, E.W., R. Bohenzky, and K.I. Berns, *Inverted Terminal Repetition in Adeno-Associated Virus DNA: Independence of the Orientation at Either End of the Genome.* Journal of Virology, 1981. **37**(3).

64. Im, D.-S. and N. Muzyczka, *The AAV Origin Binding Protein Rep68 Is an ATP-Dependent Site-Specific Endonuclease with DNA Helicase Activity.* Cell, 1990. **61**.
65. Snyder, R.O., D.-S. Im, and N. Muzyczka, *Evidence for Covalent Attachment of the Adeno-Associated Virus (AAV) Rep Protein to the Ends of the AAV Genome.* Journal of Virology, 1990. **64**(12).
66. Ryan, J.H., S. Zolotukhin, and N. Muzyczka, *Sequence Requirements for Binding of Rep68 to the Adeno-Associated Virus Terminal Repeats.* Journal of Virology, 1996. **70**(3).
67. Wang, X.-S., S. Ponnazhagan, and A. Srivastava, *Rescue and Replication Signals of the Adeno-associated Virus 2 Genome.* J. Mol. Biol., 1995. **250**.
68. Wang, X.-S., et al., *Adeno-Associated Virus Type 2 DNA Replication In Vivo: Mutation Analyses of the D Sequence in Viral Inverted Terminal Repeats.* Journal of Virology, 1997. **71**(4).
69. Wang, X.-S., S. Ponnazhagan, and A. Srivastava, *Rescue and Replication of Adeno-Associated Virus Type 2 as well as Vector DNA Sequences from Recombinant Plasmids Containing Deletions in the Viral Inverted Terminal Repeats: Selective Encapsidation of Viral Genomes in Progeny Virions.* Journal of Virology, 1996. **70**(3).
70. Gonçalves, M., *Adeno-associated virus: from defective virus to effective vector.* Virology Journal, 2005. **2**(43).
71. Balague, C., M. Kalla, and W.-W. Zhang, *Adeno-Associated Virus Rep78 Protein and Terminal Repeats Enhance Integration of DNA Sequences into the Cellular Genome.* Journal of Virology, 1997. **71**(4).
72. McLaughlin, S.K., et al., *Adeno-Associated Virus General Transduction Vectors: Analysis of Proviral Structures.* Journal of Virology, 1988. **62**(6).
73. Samulski, R.J., L.-S. Chang, and T. Shenk, *Helper-Free Stocks of Recombinant Adeno-Associated Viruses: Normal Integration Does Not Require Viral Gene Expression.* Journal of Virology, 1989. **63**(9).
74. Mitchell, A.M., et al., *AAV's Anatomy: Roadmap for Optimizing Vectors for Translational Success.* Curr Gene Ther, 2010. **10**(5).
75. Kronenberg, S., J.A. Kleinschmidt, and B. Böttcher, *Electron cryo-microscopy and image reconstruction of adeno-associated virus type 2 empty capsids.* EMBO Reports, 2001. **21**(11).
76. Xie, Q., et al., *The atomic structure of adeno-associated virus (AAV-2), a vector for human gene therapy.* Proc Natl Acad Sci U S A, 2002. **99**(16).
77. Duan, D., et al., *Dynamin Is Required for Recombinant Adeno-Associated Virus Type 2 Infection.* Journal of Virology, 1999. **73**(12).
78. Sanlioglu, S., et al., *Endocytosis and Nuclear Trafficking of Adeno-Associated Virus Type 2 Are Controlled by Rac1 and Phosphatidylinositol-3 Kinase Activation.* Journal of Virology, 2000. **74**(19).
79. Nonnenmacher, M. and T. Weber, *Adeno-associated virus 2 infection requires endocytosis through the CLIC/GEEC pathway.* Cell Host Microbe, 2011. **10**(6).
80. Bartlett, J.S., R. Wilcher, and R.J. Samulski, *Infectious Entry Pathway of Adeno-Associated Virus and Adeno-Associated Virus Vectors.* Journal of Virology, 2000. **74**(6).
81. Douar, A.M., et al., *Intracellular trafficking of adeno-associated virus vectors: routing to the late endosomal compartment and proteasome degradation.* J Virol, 2001. **75**(4).

82. Akache, B., et al., *A two-hybrid screen identifies cathepsins B and L as uncoating factors for adeno-associated virus 2 and 8.* Mol Ther, 2007. **15**(2).
83. Xiao, W., et al., *Adenovirus-Facilitated Nuclear Translocation of Adeno-Associated Virus Type 2.* Journal of Virology, 2002. **76**(22).
84. Johnson, J.S. and R.J. Samulski, *Enhancement of adeno-associated virus infection by mobilizing capsids into and out of the nucleolus.* J Virol, 2009. **83**(6).
85. Ferrari, F.K., et al., *Second-Strand Synthesis Is a Rate-Limiting Step for Efficient Transduction by Recombinant Adeno-Associated Virus Vectors.* Journal of Virology, 1996. **70**(5).
86. Fisher, K.J., et al., *Transduction with Recombinant Adeno-Associated Virus for Gene Therapy Is Limited by Leading-Strand Synthesis.* Journal of Virology, 1996. **70**(1).
87. Schnepp, B.C., et al., *Characterization of adeno-associated virus genomes isolated from human tissues.* J Virol, 2005. **79**(23).
88. Wistuba, A., et al., *Subcellular Compartmentalization of Adeno-Associated Virus Type 2 Assembly.* Journal of Virology, 1997. **71**(2).
89. Prasad, K.-M.R. and J.P. Trempe, *The Adeno-Associated Virus Rep78 Protein Is Covalently Linked to Viral DNA in a Preformed Virion.* Virology, 1995. **214**.
90. Dubielzig, R., et al., *Adeno-Associated Virus Type 2 Protein Interactions: Formation of Pre-Encapsidation Complexes.* Journal of Virology, 1999. **73**(11).
91. Calcedo, R., et al., *Worldwide epidemiology of neutralizing antibodies to adeno-associated viruses.* J Infect Dis, 2009. **199**(3).
92. Zaiss, A.K. and D.A. Muruve, *Immunity to adeno-associated virus vectors in animals and humans: a continued challenge.* Gene Ther, 2008. **15**(11).
93. Nayak, S. and R.W. Herzog, *Progress and prospects: immune responses to viral vectors.* Gene Ther, 2010. **17**(3).
94. Zaiss, A.K., et al., *Differential Activation of Innate Immune Responses by Adenovirus and Adeno-Associated Virus Vectors.* Journal of Virology, 2002. **76**(9).
95. McCaffrey, A.P., et al., *The host response to adenovirus, helper-dependent adenovirus, and adeno-associated virus in mouse liver.* Mol Ther, 2008. **16**(5).
96. Calcedo, R. and J.M. Wilson, *Humoral immune response to AAV.* Frontiers in Immunology, 2013. **4**(341).
97. Zhu, J., X. Huang, and Y. Yang, *The TLR9-MyD88 pathway is critical for adaptive immune responses to adenoassociated virus gene therapy vectors in mice.* The Journal of Clinical Investigation, 2009. **119**(8).
98. Murphy, S.L., et al., *Diverse IgG subclass responses to adeno-associated virus infection and vector administration.* J Med Virol, 2009. **81**(1).
99. Mingozzi, F., et al., *CD8(+) T-cell responses to adeno-associated virus capsid in humans.* Nat Med, 2007. **13**(4).
100. Wobus, C.E., et al., *Monoclonal Antibodies against the Adeno-Associated Virus Type 2 (AAV-2) Capsid: Epitope Mapping and Identification of Capsid Domains Involved in AAV-2–Cell Interaction and Neutralization of AAV-2 Infection.* Journal of Virology, 2000. **74**(19).
101. Huttner, N.A., et al., *Genetic modifications of the adeno-associated virus type 2 capsid reduce the affinity and the neutralizing effects of human serum antibodies.* Gene Ther, 2003. **10**.
102. Monahan, P.E. and R.J. Samulski, *Adeno-associated virus vectors for gene therapy: more pros than cons?* Molecular Medicine Today, 2000. **6**.

103. McCarty, D.M., S.M. Young, Jr., and R.J. Samulski, *Integration of adeno-associated virus (AAV) and recombinant AAV vectors.* Annu Rev Genet, 2004. **38**.
104. Schaffer, D.V., J.T. Koerber, and K.I. Lim, *Molecular engineering of viral gene delivery vehicles.* Annu Rev Biomed Eng, 2008. **10**.
105. Zincarelli, C., et al., *Analysis of AAV serotypes 1-9 mediated gene expression and tropism in mice after systemic injection.* Mol Ther, 2008. **16**(6).
106. Muller, O.J., et al., *Improved cardiac gene transfer by transcriptional and transductional targeting of adeno-associated viral vectors.* Cardiovasc Res, 2006. **70**(1).
107. Rabinowitz, J.E., et al., *Cross-Packaging of a Single Adeno-Associated Virus (AAV) Type 2 Vector Genome into Multiple AAV Serotypes Enables Transduction with Broad Specificity.* Journal of Virology, 2002. **76**(2).
108. Buning, H., et al., *Receptor targeting of adeno-associated virus vectors.* Gene Ther, 2003. **10**(14).
109. Muller, O.J., et al., *Random peptide libraries displayed on adeno-associated virus to select for targeted gene therapy vectors.* Nat Biotechnol, 2003. **21**(9).
110. Varadi, K., et al., *Novel random peptide libraries displayed on AAV serotype 9 for selection of endothelial cell-directed gene transfer vectors.* Gene Ther, 2012. **19**(8).
111. Brooks, A.R., et al., *Transcriptional silencing is associated with extensive methylation of the CMV promoter following adenoviral gene delivery to muscle.* J Gene Med, 2004. **6**(4).
112. Werfel, S., et al., *Rapid and highly efficient inducible cardiac gene knockout in adult mice using AAV-mediated expression of Cre recombinase.* Cardiovasc Res, 2014. **104**(1).
113. Geisler, A., et al., *microRNA122-regulated transgene expression increases specificity of cardiac gene transfer upon intravenous delivery of AAV9 vectors.* Gene Ther, 2011. **18**(2).
114. Naidoo, J. and D. Young, *Gene regulation systems for gene therapy applications in the central nervous system.* Neurol Res Int, 2012. **2012**.
115. Toniatti, C., et al., *Gene therapy progress and prospects: transcription regulatory systems.* Gene Ther, 2004. **11**(8).
116. Gossen, M. and H. Bujard, *Tight control of gene expression in mammalian cells by tetracycline-responsive promoters.* Proc Natl Acad Sci U S A, 1992. **89**: p. 5547-5551.
117. Jazwa, A., et al., *Gene therapy on demand: site specific regulation of gene therapy.* Gene, 2013. **525**(2).
118. Vanrell, L., et al., *Development of a liver-specific Tet-on inducible system for AAV vectors and its application in the treatment of liver cancer.* Mol Ther, 2011. **19**(7).
119. Tafuro, S., et al., *Inducible adeno-associated virus vectors promote functional angiogenesis in adult organisms via regulated vascular endothelial growth factor expression.* Cardiovasc Res, 2009. **83**(4).
120. Haberman, R.P. and T.J. McCown, *Regulation of gene expression in adeno-associated virus vectors in the brain.* Methods, 2002. **28**.
121. Maddalena, A., et al., *Adeno-associated Virus-mediated, Mifepristone-regulated Transgene Expression in the Brain.* Mol Ther Nucleic Acids, 2013. **2**.
122. Karzenowski, D., D.W. Potter, and M. Padidam, *Inducible control of transgene expression with ecdysone receptor: gene switches with high sensitivity, robust expression, and reduced size.* BioTechniques, 2005. **39**.

123. Sternberg, K. and D. Hamilton, *Bacteriophage P1 Site-specific Recombination: Recombination Between loxP Sites.* J. Mol. Biol., 1981. **150**.
124. Abremski, K., R. Hoess, and N. Sternberg, *Studies on the Properties of PI Site-Specific Recombination: Evidence for Topologically Unlinked Products following Recombination.* Cell, 1983. **32**.
125. Hoess, R.H., M. Ziese, and N. Sternberg, *P1 site-specific recombination: Nucleotide sequence of the recombining sites.* Proc. NatL Acad. Sci. USA, 1982. **79**.
126. Hamilton, D. and K. Abremski, *Site-specific Recombination by the Bacteriophage Pl lox-Cre system: Cre-mediated Synapsis of Two lox Sites.* J. Mol. Biol., 1984. **178**(481-486).
127. Hoess, R., A. Wierzbicki, and K. Abremski, *Formation of small circular DNA molecules via an in vitro site-specific recombination system.* Gene, 1985. **40**.
128. Nagy, A., *Cre Recombinase: The Universal Reagent for Genome Tailoring.* Genesis, 2000. **26**.
129. Kilby, N.J., M.R. Snaith, and J.A.H. Murray, *Site-specific recombinases: tools for genome engineering.* TIG, 1993. **9**(12).
130. Metzger, D. and R. Feil, *Engineering the mouse genome by site-specific recombination.* Current Opinion in Biotechnology, 1999. **10**.
131. Hoess, R.H. and K. Abremski, *Mechanism of Strand Cleavage and Exchange in the Cre-lox Site-specific Recombination System.* J. Mol. Biol., 1985. **181**.
132. Guo, F., D.N. Gopaul, and G.D. Van Duyne, *Structure of Cre recombinase complexed with DNA in a sitespecific recombination synapse.* Nature, 1997. **389**.
133. Ghosh, K. and G.D. Van Duyne, *Cre–loxP biochemistry.* Methods, 2002. **28**.
134. Van Duyne, G.D., *A structural viel of Cre-loxP site-specific recombination.* Annu. Rev. Biophys. Biomol. Struct., 2001. **30**.
135. Abremski, K. and R. Hoess, *Bacteriophage P1 Site-specific Recombination: Purification and properties of the Cre recombinase protein.* Journal of Biological Chemistry, 1984. **259**(3).
136. Gorski, J.A. and K.R. Jones, *Efficient bicistronic expression of cre in mammalian cells.* Nucleic Acids Res, 1999. **27**(9).
137. Shimshek, D.R., et al., *Codon-improved Cre recombinase (iCre) expression in the mouse.* Genesis, 2002. **32**(1).
138. Metzger, D., et al., *Conditional site-specific recombination in mammalian cells using a ligand-dependent chimeric Cre recombinase.* Proc. Natl. Acad. Sci. USA, 1995. **92**.
139. Feil, R., et al., *Ligand-activated site-specific recombination in mice.* Proc. Natl. Acad. Sci. USA, 1996. **93**.
140. Brocard, J., et al., *Spatio-temporally controlled site-specific somatic mutagenesis in the mouse.* Proc. Natl. Acad. Sci. USA, 1997. **94**.
141. Feil, R., et al., *Regulation of Cre Recombinase Activity by Mutated Estrogen Receptor Ligand-Binding Domains.* Biochemical and Biophysical Research Communications, 1997. **237**.
142. Casanova, E., et al., *ER-based double iCre fusion protein allows partial recombination in forebrain.* Genesis, 2002. **34**(3).
143. Jullien, N., et al., *Use of ERT2-iCre-ERT2 for conditional transgenesis.* Genesis, 2008. **46**(4).
144. Zhang, Y., et al., *Inducible site-directed recombination in mouse embryonic stem cells.* Nucleic Acids Res, 1996. **24**(4).

145. Verrou, C., et al., *Comparison of the Tamoxifen Regulated Chimeric Cre Recombinases MerCreMer and CreMer.* Biol Chem, 1999. **380**.
146. Kühn, R., et al., *Inducible Gene Targeting in Mice.* Science, 1995. **269**.
147. Kellendonk, C., et al., *Regulation of Cre recombinase activity by the synthetic steroid RU 486.* Nucleic Acids Res, 1996. **24**(8).
148. Sauer, B. and N. Henderson, *Cre-stimulated recombination at /arP-containing DNA sequences placed into the mammalian genome.* Nucleic Acids Res, 1989. **17**(1).
149. Rajewsky, K., et al., *Conditional gene targeting.* J Clin Invest, 1996. **98**(3).
150. Schwenk, F., et al., *Temporally and spatially regulated somatic mutagenesis in mice.* Nucleic Acids Research, 1998. **26**(6).
151. Seibler, J., et al., *Rapid generation of inducible mouse mutants.* Nucleic Acids Research, 2003. **31**(4).
152. Doetschman, T. and M. Azhar, *Cardiac-specific inducible and conditional gene targeting in mice.* Circ Res, 2012. **110**(11).
153. Hameyer, D., et al., *Toxicity of ligand-dependent Cre recombinases and generation of a conditional Cre deleter mouse allowing mosaic recombination in peripheral tissues.* Physiol Genomics, 2007. **31**.
154. Forde, A., et al., *Temporal Cre-mediated recombination exclusively in endothelial cells using Tie2 regulatory elements.* Genesis, 2002. **33**(4).
155. Kuehbandner, S., et al., *Temporally Controlled Somatic Mutagenesis in Smooth Muscle.* Genesis, 2000. **28**.
156. Sohal, D.S., et al., *Temporally Regulated and Tissue-Specific Gene Manipulations in the Adult and Embryonic Heart Using a Tamoxifen-Inducible Cre Protein.* Circulation Research, 2001. **89**.
157. Koitabashi, N., et al., *Avoidance of transient cardiomyopathy in cardiomyocyte-targeted tamoxifen-induced MerCreMer gene deletion models.* Circ Res, 2009. **105**(1).
158. Andersson, K.B., et al., *Tamoxifen administration routes and dosage for inducible Cre-mediated gene disruption in mouse hearts.* Transgenic Res, 2010. **19**(4).
159. Hall, M.E., et al., *Systolic dysfunction in cardiac-specific ligand-inducible MerCreMer transgenic mice.* Am J Physiol Heart Circ Physiol, 2011. **301**.
160. Bersell, K., et al., *Moderate and high amounts of tamoxifen in alpha-MHC-MerCreMer mice induce a DNA damage response, leading to heart failure and death.* Dis Model Mech, 2013.
161. Akagi, K., et al., *Cre-mediated somatic site-specific recombination in mice.* Nucleic Acids Res, 1997. **25**(9).
162. Atasoy, D., et al., *A FLEX switch targets Channelrhodopsin-2 to multiple cell types for imaging and long-range circuit mapping.* J Neurosci, 2008. **28**.
163. Betley, J.N. and S.M. Sternson, *Adeno-associated viral vectors for mapping, monitoring, and manipulating neural circuits.* Hum Gene Ther, 2011. **22**(6).
164. Sohal, V.S., et al., *Parvalbumin neurons and gamma rhythms enhance cortical circuit performance.* Nature, 2009. **459**.
165. Saunders, A., C.A. Johnson, and B.L. Sabatini, *Novel recombinant adeno-associated viruses for Cre activated and inactivated transgene expression in neurons.* Front Neural Circuits, 2012. **6**.
166. Saunders, A. and B.L. Sabatini, *Cre Activated and Inactivated Recombinant Adeno-Associated Viral Vectors for Neuronal Anatomical Tracing or Activity Manipulation.* Curr Protoc Neurosci, 2015. **72**.

167. Kuhlman, S.J. and Z.J. Huang, *High-Resolution Labeling and Functional Manipulation of Specific Neuron Types in Mouse Brain by Cre-Activated Viral Gene Expression.* PLOS one, 2008. **3**(4).
168. Li, X.G., et al., *Viral-mediated temporally controlled dopamine production in a rat model of Parkinson disease.* Mol Ther, 2006. **13**(1).
169. Close, D.M., et al., *In Vivo Bioluminescent Imaging (BLI): Noninvasive Visualization and Interrogation of Biological Processes in Living Animals.* Sensors, 2011. **11**(180-206).
170. Sauer, B., *Inducible Gene Targeting in Mice Using the Cre/lox System.* Methods in Enzymology, 1998. **14**.
171. Moore, K.W., et al., *Interleukin-10 and the interleukin-10 receptor.* Annu. Rev. Immunol., 2001. **19**.
172. Trifunovic, J., et al., *Pathologic patterns of interleukin 10 expression--a review.* Biochem Med (Zagreb), 2015. **25**(1).
173. Mueller, C., et al., *The pros and cons of immunomodulatory IL-10 gene therapy with recombinant AAV in a Cftr-/- -dependent allergy mouse model.* Gene Ther, 2009. **16**(2).
174. de Felipe, P., et al., *E unum pluribus: multiple proteins from a self-processing polyprotein.* Trends Biotechnol, 2006. **24**(2).
175. Kim, J.H., et al., *High cleavage efficiency of a 2A peptide derived from porcine teschovirus-1 in human cell lines, zebrafish and mice.* PLoS One, 2011. **6**(4).
176. Guo, C., W. Yang, and C.G. Lobe, *A Cre recombinase transgene with mosaic, widespread tamoxifen-inducible action.* Genesis, 2002. **32**(1).
177. Perez, E.A., *Safety profiles of tamoxifen and the aromatase inhibitors in adjuvant therapy of hormone-responsive early breast cancer.* Ann Oncol, 2007. **18 Suppl 8**.
178. Garreau, J.R., et al., *Side effects of aromatase inhibitors versus tamoxifen: the patients' perspective.* Am J Surg, 2006. **192**(4).
179. Goetz, M.P., et al., *The impact of cytochrome P450 2D6 metabolism in women receiving adjuvant tamoxifen.* Breast Cancer Res Treat, 2007. **101**(1).

6. ACKNOWLEDGEMENTS

First of all, I want to thank everyone who was directly or indirectly supporting me during the last three years working on this thesis.

I would like to express my gratitude towards my supervisor Prof. Dr. Oliver Müller who gave me the opportunity to work in his lab on this project and financial support over all these years.

Moreover, I would like to thank Prof. Dr. Martin Müller to accept being the first supervisor of my thesis and helpful discussions during my TAC meetings. Also, my thank goes to Dr. Dirk Grimm for being part of the TAC meeting and supporting this work with material and scientific input.

Many thanks go to the Müller lab for scientific support, especially to Dr. Andreas Jungmann, Daniela Zimmermann and Dr. Karl Varadi for their support during experiments, helpful scientific input and making my day in and outside the lab. Also, my gratitude goes to Kerstin Mühlburger and Franziska Jung for AAV production and their technical assistance. Of course, thanks to all the other members of the Müller lab, the Raake lab and the Most lab for their support during the three years.

I would also like to thank HBIGS for accepting me as a graduate student and its excellent program for scientific and personal development.

Last but not least, I want to express my deep gratitude towards my parents, Martina and Carsten Westphal, and my brother, Dr. Robert Westphal, for their lovely support during all these years in all situations. Finally, I want to thank my husband, Kai Rohwedder, for always being with me and giving me the strength to accomplish this part of my life.